

EVALUATION OF TWO SIMPLIFIED FLOOD ROUTING METHODS USING HEC-RAS MODEL

A DISSERTATION

*Submitted in partial fulfillment of the
requirements for the award of the degree
of
MASTER OF TECHNOLOGY
in
HYDROLOGY*

By

VAANI DUBEY



DEPARTMENT OF HYDROLOGY
INDIAN INSTITUTE OF TECHNOLOGY ROORKEE
ROORKEE - 247 667 (INDIA)

JUNE, 2008

CANDIDATE'S DECLARATION

I hereby certify that the work which is being presented in this dissertation entitled "**Evaluation of Two Simplified Flood-Routing Methods Using HEC-RAS Model**" in partial fulfillment of the requirement for the award of the degree of **Master of Technology in Hydrology**, submitted in the Department of Hydrology of Indian Institute of Technology Roorkee, India, is an authentic record of my work carried out during the period from August, 2007 to June, 2008 under the supervision of **Dr. M. Perumal**, Associate Professor, Department of Hydrology , I.I.T. Roorkee.

The matter embodied in this dissertation has not been submitted by me for the award of any other degree.

I.I.T.Roorkee

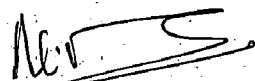
Date: 30/06/2008



(VAANI DUBEY)

Candidate's Signature

This is to certify that the above statement made by the candidate is correct to the best of my knowledge.



(M. PERUMAL)

Associate Professor

Department Of Hydrology

Indian Institute of Technology, Roorkee

Roorkee-247667

ACKNOWLEDGEMENTS

First and foremost I must express my sincere appreciation to my supervisor, Dr. M.Perumal for his guidance, encouragement and continuous support throughout this research work. His extensive knowledge, vision and creative thinking have been the source of inspiration for me to accomplish the work. Without his help I would not have had the opportunity to work on such a challenging and creative project.

I am also grateful to Dr. N.K. Goel, Professor and Head, Department of Hydrology, Indian Institute of Technology, Roorkee for his encouragements and moral support during the study. I also take this opportunity to express my sincere thanks to all the faculty members of Department of Hydrology for their excellent teachings of the concepts and fundamentals which have been used in the studies and inspiration throughout the course.

I would like to express my thanks to Mr. N. N. Rai, Mr. M. Rao, and Mr. Mohanty for their invaluable cooperation, to finalize this dissertation successfully.

My gratefulness to my parents, my family and especially to my husband Mr. Nikhilesh Vyas, who has been a perennial source of inspiration and beacon light of faith and hope for me, is infinite and inexpressible.

Lastly, I would like to thank all the staff members of the Department of Hydrology, my friends Yogesh Dadheech, Shailja Chaturvedi and Sunil Bagde for their invaluable help in my dissertation.

June 2008

I.I.T. Roorkee

(VAANI DUBEY)

ABSTRACT

This study was taken up on the premise that in any real-time flood forecasting model it is desirable to employ a physically based basic model to describe the physical behavior of the system from the remaining part which describe the structure of the residuals; and the parameters of the ‘physical’ part of the model should be estimated independently of those of the residual component model over the basic model. This concept is more amenable for incorporation in a hydrometric data based flood forecasting models, mainly dealing with flood routing process only. Accordingly the study was on the use of such a physically based routing model *viz.* the Variable Parameter Muskingum Discharge routing method as a replacement of the well known linear theory based routing method, *viz.*, the Kalinin-Miliyukov method in state-space formulation, which is widely used in East European countries for flood forecasting in rivers. On this consideration, a strategy was formulated for evaluating the performance of these two methods by routing hypothetical inflow hydrographs in hypothetical uniform rectangular channel reach for a routing reach of 40 km and the solutions obtained by these routing methods were compared with the corresponding solutions. A total of 120 hypothetical test runs were made in similarly the HEC-RAS model routed solutions by these two routing methods. Based on these simulation results, it is concluded that the VPMD routing method is able to reproduce the benchmark solutions more closely than the Kalinin-Miliyukov method based on state-space analysis approach in all aspects of reproduction such as variance explained, peak discharge reproduction and time-to-peak discharge reproduction. Based on this study it is recommended that one may prefer the VPMD method over the K-M method for employing as a basic model of hydrometric data based flood forecasting model.

TABLE OF CONTENTS

CANDIDATE'S DECLARATION	II
ACKNOWLEDGEMENTS	III
ABSTRACT	IV
TABLE OF CONTENTS	V
LIST OF TABLES	VIII
LIST OF FIGURES	VIII
NOTATIONS	IX

CHAPTER 1: INTRODUCTION

1.1 General	1
1.2 Flood Forecasting models	1
1.3 Classification of the Forecasting models	3
1.4 Routing models as components of Flood Forecasting models	5
1.5 Data availability	7
1.6 Objective of the study	8
1.7 Organization of the Thesis	8

CHAPTER 2: REVIEW OF LITRETURE

2.1 General	10
2.2 Classification Of Flood Routing Methods	11
2.2.1 Empirical Regression Or Black-Box Flood Routing Methods	11
2.2.2 Hydrologic Flood Routing Methods	12
2.2.3 Hydraulic Flood Routing Methods	16
2.3 Simplified Hydraulic Flood Routing Methods	18
2.3.1 Directly Derived Simplified Flood Routing Methods	18
2.3.2 Indirectly Derived Simplified Flood Routing Methods (Storage Routing Methods)	21
2.4 Kalinin-Miliyukov Routing Methods	23

2.4.1 Application to Water Resources Systems	27
2.4.2 Continuous State Variable Model for the K-M Method (Nash Cascade Model)	29
2.4.3 Discrete Formulation of The Continuous Nash Cascade	34
2.5 Muskingum Routing Methods	38
2.5.1 Classical Muskingum Method	38
2.5.2 Physically Based Muskingum Routing Methods	39
2.6 Variable Parameter Discharge Routing Method	42
2.6.1 Variable Parameter Discharge Routing Method With Stage Computation Feature	43
2.6.2 Theoretical Background Of The VPMD Method	44
2.7 HEC-RAS Model	50
2.8 Conclusion	53
CHAPTER 3: STATEMENT OF THE PROBLEM	55
CHAPTER 4: STRATEGY ADOPTED FOR EVALUATION OF THE METHODS	
4.1 General	56
4.2 Development of computer code for K-M method based on state-space analysis approach	58
4.2.1 Computation Procedure	60
4.3 Variable Parameter Muskingum Discharge Routing Method	61
4.3.1 Computation Procedure	64
4.4 Routing Using the HEC-RAS Model	64
4.5 Comparison of the Results of the K-M and VPMD methods with the HEC-RAS Results	72
4.6 Evaluation Criteria	72
4.6.1 Variance Explained Criterion	73
4.6.2 Reproduction of Routed Hydrograph Peak Criterion	73
4.6.3 Reproduction of Time to Peak Criterion	74
4.6.4 Volume Error Criterion	74

4.7 Conclusion	75
CHAPTER 5: RESULTS AND DISCUSSION	
5.1 General	76
5.2 Results Obtained	76
5.3 Discussion of results	81
5.4 Conclusion	92
CHAPTER 6: CONCLUSIONS AND RECOMMENDATIONS	
6.1 General	93
6.2 Conclusions	94
6.3 Recommendations For The Further Study	94
CHAPTER 7: REFERENCES	95
APPENDIX 1: FORTRAN Program Used for VPMD Method	xi
APPENDIX 2: MATLAB Program Developed for Moment-Matching Method	xvii
APPENDIX 3: MATLAB Program Developed for K-M Method	xix
APPENDIX 4: MATLAB Program Developed for Nash-Sutcliffe Criterion	xx

LIST OF TABLES

Table 5.1	Pertinent Inflow Hydrograph Characteristics	77
Table 5.2	Test Run details	78
Table 5.3	Results Obtained	84

LIST OF FIGURE

Figure 2.1	Modern approach to dynamic system	27
Figure 2.2	Schematic diagram of state variable model	28
Figure 2.3	State variable representation of the Nash Method	31
Figure 2.4	Definition sketch of the variable parameter Muskingum computational reach	45
Figure 4.1	Typical Routing Results using the K-M method	61
Figure 4.2	Definition Sketch of the Muskingum Reach	62
Figure 4.3	Typical Routing results using the VPMD method	64
Figure 4.4	New Project Window	65
Figure 4.5	Geometric Data Window	66
Figure 4.6	Cross-Section Data Window	67
Figure 4.7	Unsteady Flow Data Window	68
Figure 4.8	Flow Hydrograph Window (for boundary condition)	69
Figure 4.9	Unsteady Flow Data Window (Initial Condition)	70
Figure 4.10	Unsteady Flow Analysis Window	71
Figure 4.11	Flood Routing using HEC-RAS model	71
Figure 4.12	Comparison of both of the methods using HEC-RAS	72
Figure 5.1	Routing Results of Test Run No. 81	89
Figure 5.2	Routing Results of Test Run No. 55	89
Figure 5.3	Routing Results of Test Run No. 79	90
Figure 5.4	Routing Results of Test Run No. 118	90
Figure 5.5	Routing Results of Test Run No. 25	91
Figure 5.6	Routing Results of Test Run No. 78	91

NOTATIONS

- A = area of cross-section;
- B = channel top width;
- b_f = base width of the floodplain channel;
- b_m = base width of the main channel;
- c = wave celerity;
- EVOL = error in volume;
- g = acceleration due to gravity;
- $G(t)$ = input matrix;
- h = depth of flow;
- $h(t)$ = output matrix;
- I = inflow to reach;
- I_p = peak flow;
- K = storage coefficient;
- n = Manning's roughness coefficient;
- N = total number of discharge hydrograph ordinates to be simulated;
- P = wetted parameter;
- Q = discharge;
- Q_{ci} = i^{th} ordinate of the calculated discharge hydrograph;
- Q_{per} = percentage error in attenuation;
- R = mean hydraulic radius;
- S = storage in the reach;
- S_f = friction slope;

- S_0 = bed slope;
 Δt = routing time interval;
 t = time;
 t_p = time to peak;
 t_{per} = error in the time of peak discharge;
 v = average velocity over cross-section;
 x = distance along the reach;
 y = stage;
 γ = skewness factor;
 $\Phi(t)$ = state transition matrix;
 $\Gamma(t)$ = input transition matrix;
 $\underline{F}(t)$ = state matrix;

CHAPTER 1

INTRODUCTION

1.1 GENERAL

Flooding is a global problem that has been increasing at a worrisome pace in recent years. It is as old as human civilization. However natural flooding of large area did not create more dangerous situation in a prehistoric world. But the expansion of human activity and the aggregation of people in larger and larger urbanized areas have resulted in increase in loss of lives and economic damages due to floods.

Early efforts to reduce flood related deaths and damages, however were primarily devoted to flood control measures such as levees, dams and storage reservoirs which fall under the category of structural measures to control flood problems. However, structural measures can not eliminate completely the risk, given the impossibility of building larger and larger structures, to cope with extremely low probability events. Therefore, an important role is left to non-structural measures to be compared, evaluated and actuated in real-time, which implies the need for accurate flood forecasts with a sufficient lead time to allow for their implementation. This is why flood forecasting with sufficient lead time has become an important non-structural measures for flood damages reduction and for minimizing flood related deaths. Therefore, it is essential that flood forecasting methods should be physically based, less data intensive and over and above, should be easily understood by the field engineers.

1.2 FLOOD FORECASTING MODELS

Flood forecasting models enable to simulate the watershed response to a given input at a given location under the existing catchment conditions. Every forecasting model

operates on two modes, viz. a) the calibration mode (off-line mode), and b) the operation mode (on-line mode).

A flood forecasting model in the calibration mode, attempts to produce the watershed response for the past recorded precipitation or upstream flow input. The response of the model is compared with the recorded response at the point of forecasting interest, and if both do not match, either the model structure is changed or the parameters are modified till the matching is done satisfactorily. Once the structure of the model and its parameters are identified using the calibration mode, the model can be used for forecasting and the model is said to be used in the operational mode. While the basic structure of the model is not changed in the operational mode, the parameters of the model need to be changed considering the current catchment conditions due to the variation of the input and subsequent change in other components of the rainfall-runoff process.

Every forecasting model has two components for flow forecasting: 1) deterministic flow components and 2) stochastic flow component. While the former is determined by the hydrologic/hydraulic model, the latter is determined based on the residual (error) series of the difference between the forecasted flow for a specified lead time and the corresponding observed flow. The residual series reflect both the model error, due to the inability of the model used in the forecasting model to correctly model the flow process, and the observational error while measuring the flow. It is imperative therefore, to use an appropriate model to reduce model error. The study focuses on this specific aspect highlighting the relevance of using appropriate model to reduce the model error, by studying the simulation capability of a widely used linear model, the Kalinin-Miliukov routing model, in state-space formulation and a physically based simplified variable parameter

model, the Variable Parameter Muskingum Discharge (VPMD) routing method proposed by Perumal(1994 a) for modelling the same flood wave movement process in a given channel by accounting the non-linearity in the routing process.

As the emphasis of the study is on the use of appropriate model for forecasting purposes specifically focusing on the river routing models, it is necessary to bring out the general background on the type of forecasting models employed in the field.

1.3 CLASSIFICATION OF THE FORECASTING MODELS

It is necessary to stress that the classification of models for hydrological forecasting purposes is not necessarily identical to the classification of models in general or for other purposes, such as for design, estimation of missing data etc. Some models which are based on stochastic principles or statistical approaches may function as the deterministic models, when used for real-time forecasting. Hence, any model which is used for the real-time forecast, by definition, is a deterministic model. The classification of the forecasting models proposed by Nemec(1985) is as follows:

A. Purely deterministic forecasting models:

(1) Hydrometric data-based (involving only stream flow process)

- (i) Correlation of stages and/or volumes (discharge)
- (ii) Systems approach to stream flow (hydrologic routing)
- (iii) Hydraulic/Simplified hydraulic routing using
 - Dynamic wave model
 - Diffusion analogy model and
 - Kinematic wave model

(2) Hydrometeorological and hydrometric data-based models(involving rainfall-runoff and streamflow processes)

- (i) Correlations using physical variables and parameters or indices (such as antecedent precipitation index (API))
- (ii) Systems approach to the basin response to rain fall,
- (iii) Distributed parameter approaches (hydrological and hydraulic routing)
- (iv) Conceptual moisture accounting using
 - a) Soil moisture indices
 - b) Implicit moisture accounting
 - c) Explicit moisture accounting

B. Hybrid—Stochastic-Deterministic forecasting models

- 1. Using only time series stochastic parameterization
- 2. Using systems approach to the basin response and time series stochastic parameterization.

The current development in computer software, coupled with advances in telemetry systems for automatic data acquisition not only allows the improved forecasting of any magnitude of flow at any point in a watershed but also enables the automatic operation of the hydro-systems affected by the forecasted flow. While the improved data acquisition and data transmission systems may help to increase the lead time of forecast their utility would be negated if a poor forecasting model is employed in the forecasting system.

It is essential to employ a hydrologic model, which mimics the hydrological behavior of the catchments, taking care of the spatial variability of the catchment response.

Furthermore, a more mathematically involved hydrological model may be suitable for design purposes, and it may not be suitable for operational forecasting purposes due to the reasons of intensive real-time data requirements and, above all, the understanding of the model by the practicing engineers using the model for forecasting purposes.

While there are so many data driven models ranging from the traditional correlation based models to the recent neural network models, it is required to employ a forecasting model that is physically based *albeit* in a simplified form than using a sophisticated black box model such as that of a neural network model. The relevance of this statement would be recognized when significant changes take place in the catchments or when the upstream data collection station is washed away in flood or when the recorded flood is far exceeding the past floods based on which the parameters of the data driven model have been estimated. Further in a physically based flood forecasting model, all the model components are not simple as far as their estimation is concerned particularly in large catchments. However the use of a data-driven rainfall-runoff transformation process in the headwater catchments along with a simplified hydraulic model based channel routing can solve the forecasting purpose in an elongated catchments such as the Yamuna River basin.

1.4 ROUTING MODELS AS COMPONENTS OF FLOOD FORECASTING MODELS

The focus of this thesis is the study of simplified flood routing models suitable for use in the flood forecasting models. One of the routing models widely used in Eastern European countries especially for flood forecasting of the Danube River, the Kalinin-Miliyukov method proposed by the Russian hydraulic engineers Kalinin and Miliyukov

(1958) based on the state-space analysis (Szollosi-Nagy, 1976, 1982; Jozsef Szilagyi, 2005) is considered for the study. However, this method is a linear theory based method in which the parameters n (the number of linear reservoirs) and K (the storage coefficient of the linear reservoir) remain constant when the model is used for simulating a past recorded event (i.e. in off-line mode). But while applying this method for real-time forecasting, the parameters n and K are modified at every forecasting time level using the updating algorithms such as Kalman Filter which is used for minimizing the forecasting errors for estimating the improved forecast. Kalman filters widely used in control system theory involve tedious mathematical equations and are suitable for application in processes which involve high randomness. Since flows of main river varies smoothly exhibiting more dependence among the flows, the use of simple error updating algorithm may be appropriate rather than using mathematically involved Kalman filter. However, to follow this strategy in real-time flood forecasting it is necessary to use a routing model which is capable of accounting the non-linearity in the routing process. This implies that the routing parameters vary while routing the flow at every time interval unlike them, remain constant in linear theory based models. Therefore, if one can employ a realistic physically based model, then the forecast error may only involve the observation error and the error due to unaccounted lateral flow between the upstream gauging station, where the inflow hydrograph is recorded, and the downstream gauging station of forecast interest.

A routing model which has the required physically based characteristics and is capable of accounting non-linear behavior of flood wave movement has been introduced by Perumal(1994 a). This model directly derived from the Saint-Venant equations with the main assumption of approximately linearly varying water surface at any time, is known as

the Variable Parameter Muskingum Discharge method (VPMD). The parameters of this Muskingum method vary at every routing time level based on the established relationships between the flow and the channel characteristics. The field applications of this routing method have been demonstrated using the data of U.K., Australian and Italian rivers (Perumal et al., 2001; Sahoo, 2007).

1.5 DATA AVAILABILITY

While evaluating the performance of such models in simulating the past recorded events, it may be appropriate to use hypothetical inflow and outflow hydrograph simulated in a hypothetical channel rather than using real field data which may be tainted by unaccounted changes in flow characteristics resulting from processes unrelated to flood - routing, such as lateral flow, seepage or measurement errors etc. Hence, in this study, given hypothetical flood hydrographs are routed in hypothetical channels to arrive at routed hypothetical outflow hydrographs using a standard benchmark model. In this study, the U.S. Hydrologic Engineering Center's HEC-RAS model (2006) is employed as the benchmark model and the hypothetical routing is carried out in the uniform rectangular channels of different widths. The performance of the two models i.e. the Kalinin-Miliyukov method (K-M method) based on state-space analysis approach and the Variable Parameter Muskingum Discharge routing method (VPMD method) are evaluated by reproducing the benchmark solutions, obtained using the HEC-RAS model by these models. It is surmised that the model which is able to reproduce the benchmark solution closely may be considered as the best model for application in a hydrometric data-based flood forecasting model.

1.6 OBJECTIVE OF THE STUDY

With the preceding background information, the objective of the study may be stated as follows:

To investigate the performance of two river routing models, *viz.*, the Kalinin-Miliyukov model based on state-space analysis approach and the Variable Parameter Muskingum-Discharge routing method for their suitability for using in a hydrometric data based flood forecasting models, by evaluating their capability in simulating the benchmark model routing solutions obtained using the HEC-RAS model.

1.7 ORGANIZATION OF THE THESIS

The details of the study reported in this thesis are presented in the following manner:

Chapter 1 introduces the flood routing, the significance of flood routing in hydrological analysis, and objective of this study. Chapter 2 presents a review of existing literature on flood routing including its theory, classification of flood routing methods and a detail discussion on the two flood routing methods which are to be evaluated. Chapter 3 describes the statement of the problem to be studied in the thesis. Chapter 4 discusses the strategy adopted for the evaluation of the two methods *viz.*, 1) Kalinin-Miliyukov method and 2) Variable Parameter Muskingum Discharge routing methods using the HEC-RAS model which is used as the benchmark model.. This chapter gives a brief introduction about the various steps adopted to perform the flood routing using all the three methods including the VPMD method, the K-M method and the HEC-RAS model. In chapter 6, the results obtained for all the three methods and discussion corresponding to the obtained results is given. This chapter also discusses the significance of the VPMD method by showing its

superiority over the well-known K-M method in reproducing the HEC-RAS results. Chapter 6 discusses the conclusions and recommendation for future study.

CHAPTER 2

REVIEW OF LITERATURE

2.1 GENERAL

Many communities owe much of their prosperity to advantages offered by adjacent and nearby streams, the more important being adequate commercial and municipal water supplies, navigation, power development and recreation. Adverse effects however are experienced when high flows occur in the form of floods causing loss of lives and damage to properties. Then economically feasible measures must be taken to eliminate the loss of lives and damage to properties by providing levees and flood walls; channel improvement etc. Procedures for evaluating these measures both in the design and operation phases and method of predicting flood crest are economically very important. These procedures and methods generally require the knowledge in the subject of flood routing. As flood-wave is an unsteady flow, the fundamental law of unsteady flow is applicable for flood-wave also. The fundamental law of unsteady flow is based on the principles of conservation of mass and conservation of momentum. It may be expressed by the following two partial differential equations, assuming no lateral flow as:

$$\frac{\partial Q}{\partial x} + \frac{\partial A}{\partial t} = 0 \quad (2.1)$$

$$S_f = S_0 - \frac{\partial y}{\partial x} - \frac{v}{g} \frac{\partial v}{\partial x} - \frac{1}{g} \frac{\partial v}{\partial t} \quad (2.2)$$

where Q is the discharge, A is the flow area, S_0 is the bed slope, S_f is the energy slope, g is the acceleration due to gravity, v is the average velocity over cross section, y is the depth of flow, and the notations x and t denote the space and time variables, respectively.

The gradients in the momentum equation (2.2): $\partial y/\partial x$, $(v/g)(\partial v/\partial x)$, and $(1/g)(\partial v/\partial t)$ denote the longitudinal water surface gradient, the convective and local acceleration gradients, respectively [Chow V.T., 1959]. There are many flood routing methods available in the literature, which can be broadly classified as [Fread, 1981]: 1) empirical, 2) hydrologic, and 3) hydraulic methods. A brief discussion on the classification of these routing methods is given below.

2.2 CLASSIFICATION OF FLOOD ROUTING METHODS

2.2.1 Empirical, Regression or Black-box Flood Routing Methods

The empirical flood routing methods were developed based on the intuitive relationship between the dependent (output) and independent (input) variables involved in the process of flood hydrology without considering the physical processes involved in the routing mechanism [USACE, 1960]. In practice, these routing methods were applied to long channel/river reaches. Some of the empirical methods which are found useful in real world flood routing are the successive average lag method and the progressive lag method [Linsley et al., 1949]. In recent years, the black-box flood routing methods, viz., the artificial neural networks (ANN) [Muttiah et al., 1997; Dawson and Wilby, 1998; Fernando and Jayawardena, 1998; Thirumalaiah and Deo, 1998a, 1998b; Liong et al., 2000; Birikundavyi et al., 2002; Chau and Cheng, 2002; Chang and Chen, 2003; Abebe and Price, 2004; Sahoo and Ray, 2006; Tayfur et al., 2007], fuzzy logic (FL) [Yu and Yang, 2000; Xiong et al., 2001; Yu and Chen, 2005; Gopakumar and Mujumdar, 2007], genetic algorithm (GA) [Mohan, 1997; Chau, 2002], ANN-FL-GA hybrid methods [Bazartseren et al., 2003], and the entropy theory-based methods [Singh, 1998;

Moramarco and Singh, 2001] which can be categorized as the empirical methods have found their place in the literature. Since these soft computing tools are not based on the physical process of flood routing, these tools can only be used in a prognostic mode. Basically, the empirical methods are considered as the interpolation formulas and their use for extrapolation outside the range of the underlying data sets used for calibration of the parameters involves the risk of large errors [Klemeš, 1982]. Hence, the empirical flood routing methods which do not consider the physical characteristics of the river channel and propagating flood wave are of limited use for the diagnosis of the flood routing mechanism in the meso- and macro-scale basin models, especially when used for predictions in ungauged basins.

2.2.2 Hydrologic Flood Routing Methods:-

Hydrologic-methods employ essentially the equation of continuity. The hydrologic flood routing methods are the data-driven techniques that are based on a spatially lumped form of the continuity equation, often called water balance, and a flux relation expressing storage as a function of inflow and outflow [Singh, 1988]. These methods assume the channel reach as a lumped system, and use the lumped continuity equation and a storage equation as a substitute for the one-dimensional Saint-Venant's momentum equation [Barré de Saint-Venant's, 1871a, 1871b]. In channel routing the storage is a function of both outflow and inflow discharges. The flow in a river during a flood belongs to the category of gradually varied unsteady flow. The water surface in a channel reach is not only not-parallel to the channel bottom but also varies with time. Considering a channel reach having a flood flow, the total volume in storage can be considered under two categories as: Prism storage and Wedge storage.

Prism storage is the volume that would exist if uniform flow occurred at the downstream depth, i.e. the volume formed by an imaginary plane parallel to the channel bottom drawn at the outflow section water surface. Wedge Storage is the wedge like volume formed between the actual water surface profile and the top surface of the prism storage. [USACE, 1960]

For calibration, such routing methods require only data from the past flood events at the upstream and downstream boundary sections of the conceptual channel reach. These methods can be used for simulating the flood dynamics in a channel even when no information on the topographical or roughness characteristics of the intermediate channel sections is available [Dooge, 1986]. However, the Saint-Venant's equations are capable of modeling the flood routing mechanism in a physically distributed manner. Note that since the solution procedures of the full Saint-Venant's equations require the use of numerical methods which could not be attempted till the mid-fifties [Stoker, 1957], these hydrologic routing methods were developed as a simple alternative to the full Saint-Venant's equations for field applications. On the basis of the type of storage equation used in the model framework, the hydrologic routing methods can be classified as linear or nonlinear. To account for the flood wave propagation dynamics in natural rivers characterized by uniform translation and reservoir or pondage action [Langbein, 1942], a class of lumped hydrologic methods were evolved by employing, generally, two routing parameters in the model structure to deal with the convection and diffusion characteristics of a propagating flood wave. The widely used classical Muskingum routing method [McCarthy, 1938], which is based on a linear storage routing concept, employs two routing parameters, viz., the travel time, accounting for the convection dynamics of the

flood wave, and the weighting parameter, accounting for the diffusion characteristics of the flood wave. Similarly, the Nash model [Nash, 1960] that is based on a linear reservoir routing concept and applied for flood routing in channels [Dooge, 1973], accounts for the convection and diffusion characteristics of the flood wave through the parameters of reservoir coefficient and the number of linear reservoirs in series, respectively. The use of linear storage equation in the classical hydrologic routing methods presumes that all the discharges of different magnitudes in a flood wave travel at the same wave speed which is, however, in contradiction with the nonlinear dynamics of the flood wave propagation. To circumvent this deficiency in the linear methods, hydrologic methods with nonlinear storage equations were proposed by various researchers [e.g., Rockwood, 1958; Laurenson, 1962, 1964; Mein et al., 1974]. Note that the routing parameters of the linear or nonlinear storage equations of the hydrologic methods were estimated using only the inflow, outflow, and the corresponding channel storage information pertaining to a particular flood event without directly involving the physically measurable channel characteristics, viz., the channel geometry and roughness. This limits the applicability and predictive capability of the hydrologic routing methods only to those flood events which are within the range of the events used in the calibration of the parameters. The fact that most of the hydrologic routing methods are able to closely reproduce the flood events used in the calibration of the model led to the inference that the storage equation may be considered as a substitute for the Saint-Venant's momentum equation [Apolov et al., 1964; Koussis and Osborne, 1986]. Since the hydrologic methods may be linked to the hydrodynamics-based methods [Weinmann and Laurenson, 1979; Zoppou and O'Neill, 1982], the classification of routing methods as hydrologic or hydraulic has

become more synthetic. For instance, when the Nash model [Nash, 1960] parameter denoting the number of linear reservoirs in a reach is an integer, the Nash model conceptually represents the Kalinin–Milyukov method that is derived indirectly from the Saint-Venant's equations [Dooge, 1973]. Similarly, the Muskingum method, conventionally considered as a storage routing method, can be linked to the hydrodynamics-based methods as investigated by Apollov et al. [1964], Cunge [1969], Dooge [1973], and Dooge et al., [1982]. Further, through the moment matching technique, Dooge [1973] showed that most of the linear storage routing methods may be linked to the hydrodynamics-based methods when the routing parameters can be related to the channel and flow characteristics as described by the linearized Saint-Venant's equations. These typical examples reveal that some of the storage routing methods are also derivable as a simplification of the physically based hydrodynamics methods. Consequently, the real distinction between the hydrologic and hydraulic methods should be on the basis of the estimation of the routing parameters of the method. If the parameters of the storage routing method are estimated using the inflow, outflow, and the corresponding storage information only, then it may be categorized as the hydrologic method; and if they are estimated using the established relationships based on the channel and flow characteristics, then it may be categorized as the hydraulic routing method [Perumal, 1995] or the physically based hydrologic routing method [Kundzewicz, 1986]. A brief description on the hydraulic routing method and its different simplifications are given below.

2.2.3 Hydraulic Flood Routing Method

Hydraulic methods, on the other hand, employ the continuity equation together with the equation of motion of unsteady flow. The basic differential equations used in the hydraulic routing, known as Saint-Venant's equations afford a better description of unsteady flow than hydrologic methods.[Subramanya K., 2006] Hydraulic method of flood routing is essentially a solution of the basic St. Venant equations. These equations are simultaneous, quasi-linear, first-order partial differential equations of the hyperbolic type and are not amenable to general analytical solutions. Only for highly simplified cases can one obtain the analytical solutions of these equations. The development of modern, high speed digital computers during the past two decades has given rise to the evolutions of many sophisticated numerical techniques. The hydraulic methods of flood routing are based on the full Saint-Venant's equations or their simplifications.

Dynamic wave method

This method is based on the solution of the full Saint-Venant's equations. In the dynamic wave method, all the terms in the Saint-Venant's momentum equation are used. The dynamic wave routing method comprises of the full Saint-Venant's equations of continuity and momentum governing the one-dimensional unsteady flow in channels and rivers. In the past, several studies were carried out to ascertain the magnitude of different terms in the Saint-Venant's momentum equation denoting the longitudinal water surface gradient, the convective and local acceleration gradients; thereby, to comprehend their effects on the propagation dynamics of the flood wave. While studying the characteristics of a flood wave, Ferrick [1985] showed that the magnitude of these terms

are widely varying. Further, considering a very fast rising flood wave in a steep natural alluvial river, Henderson [1966] showed that the magnitudes of these terms are very small when compared with the bed slope, S_0 . Similarly, Kuchment [1972] showed that the magnitude of the water surface slope, $\partial y/\partial x$, and the bed slope, S_0 , are of the same order, but the slopes due to the convective and local accelerations are several orders smaller than the bed slope [vide Dooge, 1980]. In a hypothetical inflow hydrograph routing study using the numerical solution approach of the full Saint-Venant's equations in two typical prismatic channels with identical cross sections and frictional properties but different bed slopes, Weinmann and Laurenson [1979] computed the magnitudes of various terms in the momentum equation at a point about midway on the rising limb of the inflow hydrograph. Their study reveals that the simplification of the Saint-Venant's momentum equation by ignoring the inertial terms do not significantly affect the accuracy of the routing results. However, in a very flat channel reach with/without steep hydrographs, the pressure term is of the same magnitude as the bed slope and, hence, its elimination from the momentum equation is not desirable. This conclusion by Kuchment [1972] and Weinmann and Laurenson [1979] was reconfirmed by Zoppou and O'Neill [1982]. It may be surmised from the above findings on the magnitudes of different terms of the Saint-Venant's momentum equation that for many practical cases of flood routing, some of these terms may be truncated or approximated resulting in the simplified momentum equation. Further, when the magnitudes of different terms in the momentum equation are widely varying, the dynamic wave equations become stiff leading to numerical problems and, in such a case, use of the simplified momentum equation is inevitable [Ferrick, 1985]. Woolhiser and Liggett [1967] and Ranga Raju et al. [1993]

also found numerical difficulties in their studies that resulted from modeling the predominantly kinematic waves (e.g., dam break flood waves) using the dynamic wave equations. Ferrick [1985] questioned the relevance of assessing the stability of explicit numerical methods using the dynamic wave celerity criterion, even for the routing cases where the inertia terms are negligible. Consequently, for obtaining accurate routing solutions for all situations without encountering numerical problems, the use of appropriate wave type equations are desirable [Ferrick, 1985]. On the basis of the success of application of the simplified methods for routing floods in the British rivers, the British Flood Studies Report [NERC, 1975] emphasized the need to focus future research on the simplified flood routing methods. The present study focuses only on the simplified flood routing methods and, therefore, the revisit of the flood routing methods is restricted only to those methods.

2.3 Simplified Hydraulic Flood Routing Methods

The simplified hydraulic flood routing methods may be classified into two major groups [Perumal, 1995] as: 1) directly derived simplified methods, and 2) indirectly derived simplified methods.

2.3.1 Directly Derived Simplified Flood Routing Methods: This class of simplified methods is derived directly from the full Saint-Venant's equations after truncating or linearizing or approximating some of the terms in the Saint-Venant's momentum equation. On the basis of the predominance of different terms in the Saint-Venant's momentum equation (as discussed in Section 2.2.3), the flood waves in rivers and channels which are the translatory waves [Linsley et al., 1949] can be classified as [Ferrick, 1985]: 1) bulk waves, 2) dynamic waves, and 3) gravity waves. The bulk waves

are the flood waves in the free flowing rivers which propagate at the kinematic wave (KW) celerity [Seddon, 1900; Lighthill and Whitham, 1955; Iwagaki, 1955; Ferrick et al., 1984]. A detailed review on the kinematic wave theory [Lighthill and Whitham, 1955; Iwagaki, 1955] applied to flood routing studies is given by Moramarco and Singh [2000] and Singh [2002]. Bates and Sivapalan [1990], Sivapalan et al. [1997], Singh and Aravamuthan [1997], and Singh et al. [1997, 2000] used the diffusion wave equation for flood routing studies. Several researchers [e.g., Stoker, 1957; Cunge et al., 1980; Fread, 1981; Lai, 1986] argued in favor of using the numerical solution of the full Saint-Venant's equations for flood routing studies.

Hence, river wave studies based on the gravity, diffusion, and kinematic wave equations, derived as a simplification of the dynamic wave equations, are perceived as inherently less accurate. However, Ferrick [1985] brought out the limitations of the universal application of the dynamic wave equations (as discussed in Section 2.2.3) and suggested the alternate approach of using physical insight to identify an appropriate river wave type. The dynamic waves are of primary importance in river flow mechanics only when inertia is significant, and their role diminishes with the relative importance of inertia. Consequently, the dynamic wave equations cannot be applied to floods in mountainous streams. In the process of flood wave propagation in rivers, the dynamic wave behavior of a flood wave rapidly becomes negligible leading to predominance of the kinematic waves [Lighthill and Whitham, 1955; Ponce and Simons, 1977; Ponce, 1992]. Hence, the storage routing methods which replicate the behavior of diffusion and kinematic waves are successful in practice, except under situations where there is a significant downstream effect of flow.

The convection-diffusion equations [Hayami, 1951; Price, 1973], the approximate convection-diffusion (ACD) equations [Perumal and Ranga Raju, 1999], the kinematic wave equations [Lighthill and Whitham, 1955], and the linearized Saint-Venant's equations of Dooge and Harley [1967] are some of the specific examples of the directly derived simplified methods. The convection-diffusion equation is considered as linear or nonlinear depending on whether the celerity, c , and diffusion, D , in this equation remain constant or vary over the entire routing process. The convection-diffusion equations in linear and nonlinear formulations may be solved by numerical techniques [Thomas and Wormleaton, 1970, 1971; Price, 1973; NERC, 1975; Akan and Yen, 1977; Katopodes, 1982]; and in linear formulation they may also be solved by analytical techniques [Hayami, 1951; Dooge, 1973]. Unlike the full Saint-Venant's equations, the solution of the convection-diffusion equations, depending on the formulation adopted, would either yield a discharge or stage hydrograph but not both. Dooge and Napiorkowski [1987] introduced an improved form of the diffusion equation wherein the convective and local acceleration terms were also retained in an approximate manner by using the kinematic wave equation. According to the prevailing concept, when $D = 0$, the kinematic wave equation becomes a particular case of the convection-diffusion equation that describes a one-to-one relationship between the stage and the discharge at any location of the river or channel reach during unsteady flow and, therefore, there is no diffusion of the flood wave.

Using the perturbation analysis, Dooge and Harley [1967] simplified the Saint-Venant's equations by linearizing them and presented the linearized solution in the form of impulse response for a Dirac-delta function [Dooge, 1973, 1986]. However, Keefer and

McQuivey [1974] argued that, although, the linearized Saint-Venant's solution is more elegant mathematically, it is more difficult to apply in the field condition and its mathematical elegance is lost when converting from instantaneous to hourly or daily response functions.

2.3.2 Indirectly Derived Simplified Flood Routing Methods (Storage routing methods)

The indirectly derived simplified methods are not directly derived from the Saint-Venant's equations, but use a lumped continuity equation in place of the Saint-Venant's distributed continuity equation, and a linear or nonlinear storage equation (usually in linear form). The storage equation expresses storage as a function of inflow and outflow in a channel reach, however, without describing how the storage is distributed within the reach [Kulandaiswamy, 1964]. The single linear reservoir (SLR) model of Zoch [1934], which expresses storage as a linear function of outflow, is not suitable for modeling the flood wave movement in channels except in the case of short reach channels, as it accounts only for the attenuation effect and not for the translation effect of a flood wave. However, a series of SLRs can account for the attenuation as well as translation effects [Nash, 1960]. Dooge [1973] pointed out that Nash's conceptualization of a number of linear reservoirs is used by the Kalinin–Milyukov method [Kalinin and Milyukov, 1958] for modeling flood wave movement in a river reach which is derived using the hydrodynamics principles. The linear storage equation proposed by McCarthy [1938], which expresses the storage as a linear

weighted function of the inflow and the outflow, forms the basis for the development of the classical Muskingum method. However, in this classical Muskingum equation, the routing parameters remain constant over the entire duration of routing process.

Since the flood waves are inherently nonlinear in nature as different discharges travel at varied magnitudes of celerity, the linear storage routing methods were perceived to be of limited use for flood routing studies. To surmount this deficiency in the linear lumped methods/models, the nonlinear black-box models were proposed by Rockwood [1958], Laurenson [1962, 1964], and Mein et al. [1974] for channel routing that expresses storage as a power function of outflow discharge. Subsequently, the nonlinear state-space models and the Volterra series models have also been suggested for modeling flood wave propagation in channels. A detailed review of such nonlinear storage routing models is given by Kundzewicz and Napiorkowski [1986] and Napiorkowski and Kundzewicz [1986].

Subsequently, Gill [1978], Tung [1984], and Yoon and Padmanabhan [1993] proposed the nonlinear Muskingum equations. Almost all forms of the nonlinear models, whether based on the storage equation, or the full Saint-Venant's equations or its simplifications such as the kinematic wave, involve a power function type of relation with an increase in the average velocity as the discharge increases [Pilgrim, 1986]. However, Kulandaiswamy and Subramamian [1967] and Bates and Pilgrim [1983] showed that the power function-type of nonlinear relationship is not accurate for many river basins and that, although, small floods are abhorrently nonlinear, linearity is often applicable at the higher flows of interest. This finding is reconfirmed by Price [1973] and Wong and Laurenson [1983, 1984] while establishing the wave speed-discharge relationships for the

UK and Australian rivers, respectively, and they surmised that the use of power function-type relationship between storage and discharge is not appropriate for field use. Moreover, from the computational viewpoint, the nonlinear models are more difficult to apply than the linear models, and a nonlinear model need not always perform better than a linear model. Napiorkowski and Strupczewski [1981] showed that a mathematically involved nonlinear estimation of diffusion offers little improvement over the results obtained using the linear theory. While comparing the results of the linear versus nonlinear Muskingum methods, Singh and Scarlatos [1987] concluded that the nonlinear Muskingum methods are less accurate than the linear Muskingum method. Furthermore, when input errors are sufficiently large, the linear models may perform better than the nonlinear models because the linear models do not magnify the input errors [Singh and Woolhiser, 1976]. Consequently, the linear storage routing methods were widely used in practice over the nonlinear storage routing methods. In a subsequent development, the linear storage equations of the Kalinin–Milyukov and Muskingum methods were linked with the hydrodynamic equations. Hence, quite a detailed description of these two routing methods is given in the next Sections.

2.4 KALININ–MILYUKOV ROUTING METHOD

The Kalinin–Milyukov routing method [Kalinin and Milyukov, 1958; Apolov et al., 1964] is a conceptual linear storage routing method derived from the hydrodynamics principles in which a given prismatic channel reach is subdivided into a number of sub reaches (characteristic reaches) wherein the storage is a linear function of the outflow discharge. This method is based on the assumption of a one-to-one relationship between the stage and the discharge during unsteady flow condition in which the discharge at any

instant of time at the outlet of the reach is related to the stage at the middle of the reach. Hence, the discharge at any instant of time is a function of the depth of flow and the slope of the water surface at that section. During unsteady flow condition, it is assumed that the slope of the water surface remains constant over the length of the characteristic reach. Further, during the transformation of a steady flow to unsteady flow, the discharge at the outflow section of the reach does not change. The number of characteristic reaches, N_c , required for routing a discharge hydrograph using the Kalinin–Milyukov method in a given reach of length Δx is given by [Miller and Cunge, 1975]

$$N_c = \frac{S_0 B_0 c_0 \Delta x}{Q_0} \quad (2.3)$$

and the reservoir coefficient, K , of each characteristic reach is

$$K = \frac{Q_0}{S_0 B_0 c_0^2} \quad (2.4)$$

where Q_0 is the reference discharge corresponding to the reference stage y_0 , B_0 is the water surface width corresponding to y_0 , and c_0 is the wave celerity corresponding to Q_0 .

Using the moment matching technique, Dooge [1973] linked the first and second moments of the Nash model instantaneous unit hydrograph (IUH) with the corresponding moments of the linearized Saint-Venant equations, when the Froude number, $F = 0$; and arrived at the same relationships for the number of linear reservoirs in series and the reservoir coefficient as given by equations (2.3) and (2.4), respectively. Note that when the Nash model parameter representing the number of linear reservoirs in a reach is an integer, the Nash model becomes a conceptual representation of the Kalinin–Milyukov method.

In order to enable the use of Kalinin-Miliyukov (K-M) method for flood forecasting, the K-M method has been formulated using state-space analysis (Szolloso Nagy, 1976). State-space analysis of K-M method enables the easy use of error updating algorithms such as Kalman filter to improve the forecasting of floods by minimizing the errors between the forecasted floods and the corresponding observed floods. Therefore it is pertinent to describe the K-M method in the context of state-space analysis. Before the application of the K-M method in the context of state-space analysis, it is pertinent to give the state-space analysis description.

State-Space Analysis

For real-time hydrological forecasting so many methods have been developed. Many of them are based upon the principle of state-space analysis. This notion was born in the early 1960's in control engineering. The reason for the application of state-space techniques in hydrology lies in the fact that parameter state updating required in real-time hydrological forecasting control can be quite easily done within this framework. Provided that one possesses the appropriate state model, or internal description of a dynamic hydrologic system, the modern filtering techniques, notably the celebrated Kalman filter can easily be used to perform the real-time updating--prediction-control tasks, using small-sized computers, or even in some cases, micro-processors. But to apply this methodology one has to always keep in mind that the model of the process should be discrete only.

State and State-space: A *state* of the dynamic system is the smallest collection of numbers which must be specified at time $t = t_0$ in order to be able to predict uniquely the behavior of the system for any time $t \geq t_0$ for any input belonging to the given input set,

provided that every element of the input set is known for $t \geq t_0$. Such numbers are called **state variables**. The **input set** here is defined as the set of all possible inputs that can be applied to the system. The state of a system at time t is uniquely determined by the state at time t_0 and the known input for $t \geq t_0$ and is independent of values of the state and input before t_0 .

Suppose that at least n state variables x_1, x_2, \dots, x_n are needed to describe completely the behavior of a given system. Then the set of n state variables can be considered as n components of a vector \mathbf{x} . Such a vector \mathbf{x} is called a **state vector**. A **state space** is defined as an n -dimensional space in which x_1, x_2, \dots, x_n are coordinates. The state at time t of a system defined by n first-order differential equations can then be represented by a point in an n -dimensional state space. Note that in the state space approach of analysis and synthesis of control systems we deal with a set of n first-order differential equations rather than a single n th-order differential equation. A point in a state space at time t is called a **representative point**. The locus of representative points for a time interval $t_0 \leq t \leq t_1$ is called a trajectory for this time interval.

State Variable Modelling Concept

The concept of state variable modeling was developed primarily to analyze automatic control systems in the field of electrical engineering. It is capable of describing systems which are linear or non linear, time-variant or time-invariant, deterministic or stochastic, while having multiple inputs and outputs at the same time. For a system to be solvable by the state variable modeling analysis, it must be lumped.

In other words, a system must be represented in only one dimension such as time or space and must be describable by ordinary differential or differential equations.

Water resources systems are usually distributed, but they can be approximated by dividing the entire system into subsystems, (see the Fig.1) which may be individually treated as lumped system. Also, water resources systems are dynamic in nature with the inputs, outputs, and throughputs varying with respect to time.

Dynamic System Modelling:

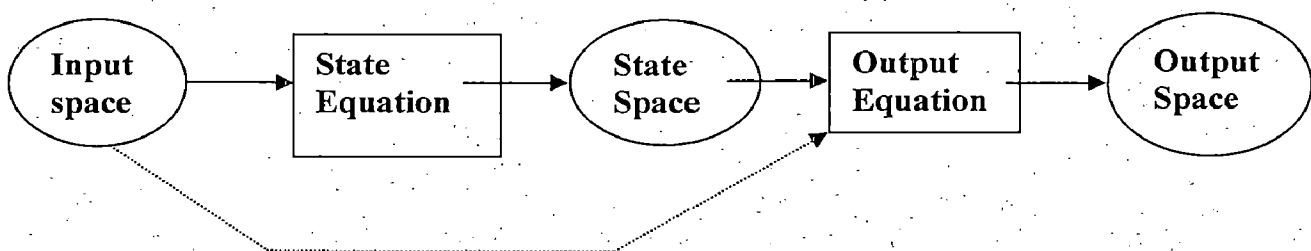


Fig 2.1 Modern approach to dynamic system

2.4.1 Application to water resources systems

In water resources systems, the state variables are usually expressed in volumetric or mass units and can represent, e.g., the volume of water or the amounts of pollutant contained in various parts of the system. The input and output variables commonly correspond to volume or mass flow rates, which may be rainfall intensity or rate of discharge pollutant. The state of the system is a measure of the level of the

activity in each of its components and can be thought of as the interface between the past and the future of the state of the system.

General description of state-space model

In general the very first step in the analytical study of systems is to setup mathematical equations to describe the systems. Because of different analytical methods used, we may often setup different mathematical models to describe the same system. When for any reason, the analysis in the time domain is to be preferred, the use of so called state space approach will offer a great deal of convenience conceptually, notationally and some times analytically. The adoption of state space representation to the numerical solution is an added advantage particularly when the system to be investigated contains time varying and non linear elements.

The state variable model for continuous time can formulated as follows, see Fig.1

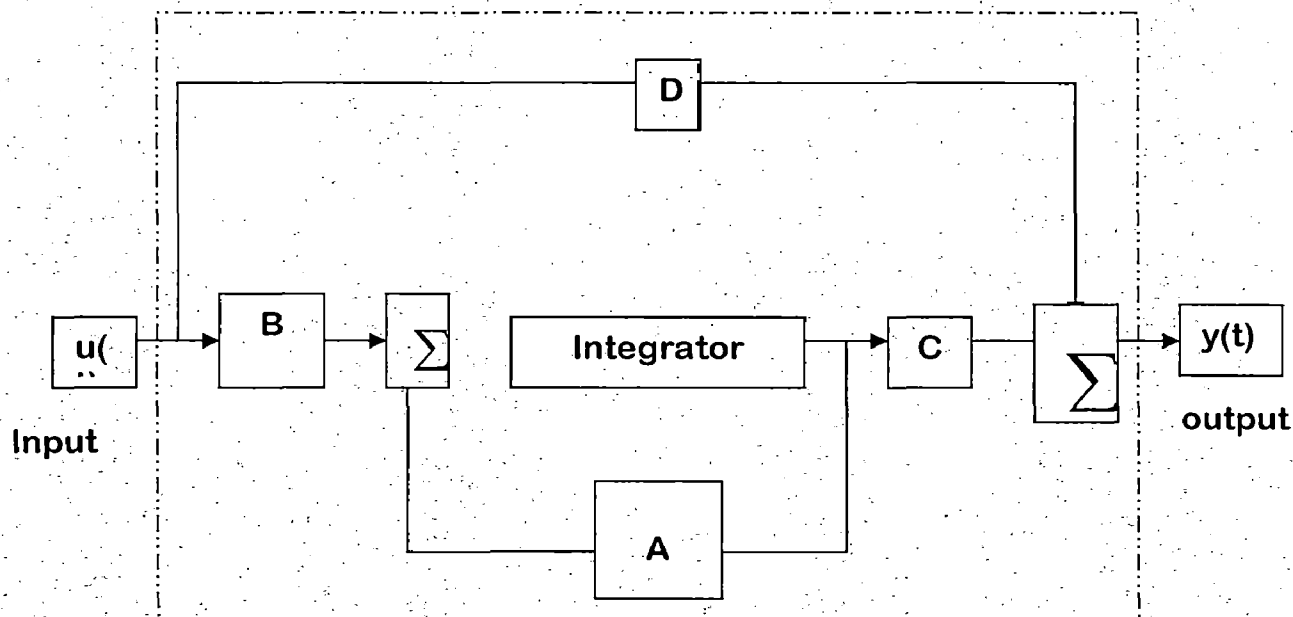


Figure 2.2 Schematic diagram of state variable model

$$\dot{\underline{x}}(t) = \underline{A}\underline{x}(t) + \underline{B}\underline{u}(t) \text{ and} \quad (2.5)$$

$$\underline{y}(t) = \underline{C}\underline{x}(t) + \underline{D}\underline{u}(t) \quad (2.6)$$

in which equation (2.5) and (2.6) are the state equation and output equation, respectively;

$\dot{\underline{x}}(t) = \frac{d}{dx} \underline{x}(t)$ = the time rate of change of the state vector

$\underline{u}(t)$ = input vector

$\underline{y}(t)$ = output vector

and $\underline{A}, \underline{B}, \underline{C}$ and \underline{D} = matrices that can be constant or function of time or space, or both.

The system representation given by eq.(2.5) and(2.6) is shown schematically in Fig.2. The time rate of change of the system state , $\dot{\underline{x}}(t)$, is formed as the sum of modified inputs , $\underline{B}\underline{u}(t)$ and the modified current state; $\underline{A}\underline{x}(t)$. Also the state feed back has a major role in determining the future behavior of the system. The rate of change of the state vector, $\dot{\underline{x}}(t)$, is continuously integrated with the current state to produce the new state.

The output $\underline{y}(t)$ is formed by summing the new state which has been scaled by matrix \underline{C} with a direct contribution from modified input, $\underline{D}\underline{u}(t)$. These features of the state variable modelling make it particularly attractive because, once the system parameters are identified; the only requirements for a solution are the initial conditions of the system and the input to the system.

2.4.2 Continuous State Variable Model for the K-M method (Nash Cascade Model)

Nash model (Nash, 1957) well known in literature for representing rain fall runoff process of the catchment, assuming that the catchment is made of n identical linear

reservoirs in series may also be used for flood routing in rivers. Nash model in conceptual form is same as the K-M method derived using hydraulic principles.

Single linear reservoir:

Let us consider a single reservoir with inflow $u(t)$ and outflow $y(t)$, respectively.

Then, using continuity equation change of the stored water $x(t)$ can be expressed by the storage equation:

$$\frac{dx(t)}{dt} = -y(t) + u(t) \quad (2.7)$$

The momentum equation for the flow is usually replaced in catchment and flood-routing hydrology by a simplified relation that relates outflow and storage. This relation is usually in the form of:

$$x(t) = K(t)y^m(t) \quad (2.8)$$

where $K(t)$ is the storage coefficient with the dimension of time, the average delay time imposed on the inflow by the reservoir, while m is a discharge coefficient. In the case when $K(t) = K = \text{constant}$ and $m = 1$ the storage is a linear function:

$$x(t) = K y(t) \quad (2.9)$$

of the outflow. With these assumptions we have a linear time-invariant reservoir whose state equation then is:

$$\frac{dx(t)}{dt} = -K^{-1}x(t) + u(t) \quad (2.10)$$

where now the state variable $x(t)$ has a distinct physical meaning, i.e. storage. The corresponding output equation is given by:

$$y(t) = K^{-1}x(t) \quad (2.11)$$

Linear reservoirs in series:

Kalinin and Milyukov's (1957) flow routing method assumes that a river section with no lateral inflow can be conceptualized as a series of characteristic reaches where the out flow $y(t)$ is a linear function of water stored $x(t)$ with in the reach. Assuming that a given stream section can be separated as a series of n characteristic reaches (where n is an integer number) with identical storage coefficients, Kalinin and Milyukov (1958) derived that the impulse response h , a continuous function of time t , of n such equal characteristic reaches can be expressed as

$$h(t) = k \frac{(kt)^{n-1}}{(n-1)!} e^{-kt} \quad (2.12)$$

The linearity condition ensures that the outflow of the characteristic reach through time can be calculated by the convolution integral of the inflow and the impulse response function (h) [which in hydrology is called the Instantaneous Unit Hydrograph (IUH)]

$$y(t) = \int_0^t h(\tau) u(t-\tau) d\tau = \int_0^t h(t-\tau) u(\tau) d\tau \quad (2.13)$$

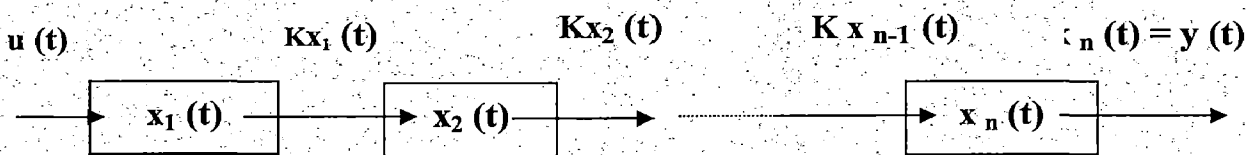


Fig. 2.3 State variable representation of the Nash cascade model

By definition of the characteristic reach one can call such a reach a linear reservoir where stored water in the reservoir is directly proportional to the outflow from it. Noticing that

the output of the i^{th} reservoir is the input to the $(i+1)^{\text{th}}$ reservoir, (see Fig.2). Eq. (2.10) can be written in matrix form for a cascade of order n as (e.g., Szollosi-Nagy 1982)

$$\begin{bmatrix} \dot{x}_1(t) \\ \dot{x}_2(t) \\ \dot{x}_3(t) \\ \vdots \\ \dot{x}_n(t) \end{bmatrix} = \begin{bmatrix} -k & 0 & & & \\ k & -k & & & \\ & k & -k & & \\ & & & \ddots & \\ 0 & & & k & -k \end{bmatrix} \begin{bmatrix} x_1(t) \\ x_2(t) \\ x_3(t) \\ \vdots \\ x_n(t) \end{bmatrix} + \begin{bmatrix} 1 \\ 0 \\ 0 \\ \vdots \\ 0 \end{bmatrix} u(t) \quad (2.14)$$

Where the dot denotes the temporal rate of change in the variable and the subscripts denote the place of the reservoir in the line of cascade. Eq. (2.14) is the state equation of the continuous KMN cascade, and can be written in a more clearly as:

$$\dot{x}(t) = \underline{F}x(t) + \underline{G}u(t) \quad (2.15)$$

where, \underline{F} is an $n \times n$ Toeplitz type system matrix.

Since the out flow from the last reservoir in the output of the whole system the output equation becomes:

$$y(t) = [0 \ 0 \ \dots \ k] \begin{bmatrix} x_1(t) \\ x_2(t) \\ x_3(t) \\ \vdots \\ x_n(t) \end{bmatrix} = \underline{H}x(t) \quad (2.16)$$

The solution of the state equation (2.15) is given by (Szollosi-Nagy 1982)

$$x(t) = \underline{\Phi}(t, t_0) \underline{x}(t_0) + \int_{t_0}^t \underline{\Phi}(t, \tau) \underline{G}(\tau)u(\tau) d\tau \quad (2.17)$$

where ,for the KMN-cascade the input (\underline{G}) = $[1, 0, 0, \dots, 0]^T$ and output (\underline{H}) = $[0, 0, 0, \dots, k]$

vectors are constant vectors, so is the system matrix, \underline{F} which causes the $n \times n$ state

transition matrix, $\underline{\Phi}$ depend only on the time-lag between t and t_0 . $\underline{\Phi}$ is the matrix exponential of \underline{F} such as

$$\underline{\Phi}(t, t_0) = e^{\underline{F}(t-t_0)} \quad (2.18)$$

is the $n \times n$ State -transition matrix.

The elements of the $\underline{\Phi}$ are the following

$$\underline{\Phi}(t, t_0) = \begin{bmatrix} e^{-k(t-t_0)} & 0 & 0 & \dots & 0 \\ k(t-t_0)e^{-k(t-t_0)} & e^{-k(t-t_0)} & 0 & \dots & 0 \\ \frac{(k(t-t_0))^2 e^{-k(t-t_0)}}{2!} & k(t-t_0)e^{-k(t-t_0)} & e^{-k(t-t_0)} & \dots & 0 \\ \vdots & \vdots & \vdots & \ddots & \vdots \\ \frac{(k(t-t_0))^{n-1} e^{-k(t-t_0)}}{(n-1)!} & \frac{(k(t-t_0))^{n-2} e^{-k(t-t_0)}}{(n-2)!} & \frac{(k(t-t_0))^{n-3} e^{-k(t-t_0)}}{(n-3)!} & \dots & e^{-k(t-t_0)} \end{bmatrix} \quad (2.19)$$

Combining Eqs. (2.16) and (2.17) and assuming that the system is initially relaxed

$\underline{x}(t_0) = 0$ at $t_0 = 0$, i.e., the reservoirs are empty, one obtains

$$\underline{y}(t) = \int_0^t \underline{H} \underline{\Phi}(t, \tau) \underline{G}(\tau) u(\tau) d\tau = \int_0^t h(t-\tau) u(\tau) d\tau \quad (2.20)$$

which is the convolution Eq.2.13 in the matrix form. Note that the left-multiplication of $\underline{\Phi}$, by \underline{H} in Eq. 2.20 produces the last line of $\underline{\Phi}$ as a row vector multiplied by k , and which upon further multiplication from right by \underline{G} results in the bottom left-most element of $\underline{\Phi}$ (multiplied by k), thus recovering eq. (2.12) for the IUH of the KMN-cascade. In

other wards, the IUH of Eq.(2.12) for an integer value of n is recaptured as k times the last element of the first column of $\underline{\Phi}$, provided $t_0 = 0$ is chosen.

2.4.3 Discrete Formulation of the Continuous Nash-Cascade:

When the instantaneous values of $u(t)$ is available at discrete time intervals ($t = \Delta t, 2\Delta t, 3\Delta t, \dots$) of equal length , and the state variables \underline{x} is known at time t then by virtue of eq.(2.17) \underline{x} at time $t + \Delta t$ can be calculated as (Szollosi- Nagy 1989)

$$\underline{x}(t + \Delta t) = \underline{\Phi}(t + \Delta t, t)\underline{x}(t) + \left[\int_t^{t + \Delta t} \underline{\Phi}(t + \Delta t, \tau) \underline{G}(\tau) d\tau \right] \underline{u}(\tau) \quad (2.21)$$

Which transforms into the following simpler form provided that $u(t) = \text{constant}$ at the value, it obtains at time t in the $(t, t + \Delta t)$ interval. (Szollosi- Nagy 1982)

$$\underline{x}(t + \Delta t) = \underline{\Phi}(\Delta t)\underline{x}(t) + \underline{\Gamma}(\Delta t)\underline{u}(t) \quad (2.22)$$

The STM that corresponds to Δt can be obtained from eq. (2.19), the STM of the continuous Nash Cascade, as

$$\underline{\Phi}(\Delta t) = \begin{bmatrix} e^{-k\Delta t} & 0 & 0 & \dots & 0 \\ k\Delta t e^{-k\Delta t} & e^{-k\Delta t} & \cdot & \cdot & 0 \\ \frac{(k\Delta t)^2 e^{-k\Delta t}}{2!} & k\Delta t e^{-k\Delta t} & e^{-k\Delta t} & \cdot & 0 \\ \vdots & \vdots & \vdots & \ddots & \vdots \\ \frac{(k\Delta t)^{n-1} e^{-k\Delta t}}{(n-1)!} & \frac{(k\Delta t)^{n-2} e^{-k\Delta t}}{(n-2)!} & \frac{(k\Delta t)^{n-3} e^{-k\Delta t}}{(n-3)!} & \ddots & e^{-k\Delta t} \end{bmatrix} \quad (2.23)$$

where again the time invariance of the \underline{F} system matrix was utilized. The $\underline{\Gamma}$ vector results from eq. (2.21) if the inflow value $u(t)$, which is assumed to be constant between the integral bounds i.e. $[t, t + \Delta t] \ni \tau$, $u(\tau) = \text{constant}$ is brought outside the integral

$$\underline{\Gamma}_r(\Delta t) = \int_t^{t+\Delta t} \underline{\Phi}(t + \Delta t - \tau) \underline{G} d\tau \quad (2.24)$$

The $n \times 1$ $\underline{\Gamma}$ vector, which is a more general approach is indeed a matrix, called the input transition matrix in system engineering.

The i^{th} element or row of $\underline{\Gamma}$ can be expressed as

$$\underline{\Gamma}(i)_r(\Delta t) = \int_t^{t+\Delta t} \frac{k(t + \Delta t - \tau)^{i-1}}{(i-1)!} e^{-k(t+\Delta t-\tau)} d\tau \quad (2.25)$$

and the j^{th} order takes the Poisson distribution with parameter $k\Delta t$, the column vector of the input transition in eq.(2.22) is obtained in the form of

$$\underline{\Gamma}_r(\Delta t) = \begin{bmatrix} (1 - e^{-k\Delta t}) / k \\ (1 - e^{-k\Delta t} (1 + k\Delta t)) / k \\ \vdots \\ \vdots \\ \left[1 - e^{-k\Delta t} \sum_{j=0}^{n-1} \frac{(k\Delta t)^j}{j!} \right] / k \end{bmatrix} \quad (2.26)$$

This complete the discrete state equation for the Nash Cascade derived from its continuous model. The corresponding discrete output equation remains structurally unchanged.

$$y(t) = Hx(t) \quad (2.27)$$

Once the state variable model is formulated, the output from the system can be obtained by solving the state equation and the output equation recursively. Although water resources system actually operates continuously in time, the data are usually analyzed using discrete time intervals.

The solution procedure for the discrete time state variable continuous Nash cascade involves the following steps:

Step 1: The inflow hydrograph to the channel reach is discretized into several time stages where time intervals need to be equal.

Step 2: From the initial stage of the system storage x_1 , and initial inflow rate to the channel reach u_1 , the time rate of change of storage volume in the channel reach at the initial stage \dot{x}_1 , can be evaluated by the state equation, (Eq.2.22)

Step3: The state of the system, i.e., channel storage, at the next time stage x_2 , is estimated or approximated as $x_2 = x_1 + \dot{x}_1 \Delta t$, (Eq.2.27)

Step4: The magnitude of the outflow rate at the current stage can then be calculated by solving the output Eq.2.27 , using the current values of inflow rate and channel storage at the same stage.

Step5: Using current information on inflow and channel storage, steps 2 - 4 are repeated recursively until the stage is reached.

State-space approximation for a non-integer n-cascade of linear storage elements:

In practical applications number of reservoirs is not always in integer numbers. But the method which we have discussed above is valid only for integer value of n. To make this method applicable for non-integer value of n, Jozsef Szilagyi (2006) revised it and suggested that storage coefficient K for the fractional reservoir should be:

$$k_x = \frac{k}{x} \quad (2.28)$$

Where k_x = is the storage coefficient of the fractional reservoir and $x = [n - \text{int}(n)]$ where int designates the integer part of n. Since the mean storage time is k^{-1} , which is expected to be smaller for a fractional storage element than for full one (i.e. when $n=1$). With this constant coefficient approximation a fractional storage element will behave as a full one with magnified k value. For simplification, the fractional storage element must always be the last one in the cascade, ensuring that only the last row of the system matrices is different from the case of a uniform cascade.

Thus due to last fractional reservoir we will get a new system matrix \underline{F} of $n^* \times n^*$ where, [$n^* = \text{int}(n+1)$] dimension, which will remain unchanged in it's $\text{int}(n) \times \text{int}(n)$ dimension but it's last row/ column will be changed.

$$\underline{F} = \begin{bmatrix} -k & & & & 0 \\ k & -k & & & \\ & k & -k & & \\ & & \ddots & \ddots & \\ & & & \ddots & \\ 0 & & & k & -\frac{k}{x} \end{bmatrix} \quad (2.29)$$

Determination of the new state-transition matrix $\underline{\Phi}$ can be achieved by successive convolution. Note that unlike the system matrix case, each element of the last row of $\underline{\Phi}$ will be different. Performing the matrix exponential in Eq.2.18 for small values of n^* with trial and error one can deduce that the last row will contain the IUH's (divided by k_x) of non-integer cascade.

2.5 MUSKINGUM ROUTING METHOD

2.5.1 Classical Muskingum method

The classical Muskingum method [McCarthy, 1938], which is coined after its first application to the Muskingum River, a tributary of the Ohio River in the USA, is a linear storage routing method being widely used in practice [Singh, 1988]. This method combines the lumped continuity equation

$$\frac{dS}{dt} = I - O \quad (2.30)$$

with the linear storage equation

$$S = K[\theta I + (1-\theta)O] \quad (2.31)$$

to arrive at the difference equation which on simplification leads to the Muskingum routing equation as

$$O_{j+1} = C_1 I_{j+1} + C_2 I_j + C_3 O_j \quad (2.32)$$

where S is the storage volume, I is the inflow discharge, O is the outflow discharge, K is the travel time, θ is the weighting parameter, the suffix j denotes the ordinate at time $j\Delta t$, Δt is the routing time step, and the coefficients C_1 , C_2 , and C_3 are expressed as

$$C_1 = \frac{-K\theta + 0.5\Delta t}{K(1-\theta) + 0.5\Delta t} \quad (2.33a)$$

$$C_2 = \frac{K\theta + 0.5\Delta t}{K(1-\theta) + 0.5\Delta t} \quad (2.33b)$$

$$C_3 = \frac{K(1-\theta) - 0.5\Delta t}{K(1-\theta) + 0.5\Delta t} \quad (2.33c)$$

The condition $C_1 + C_2 + C_3 = 1.0$, shows the mass conserving ability of the classical Muskingum method. The routing parameters K and θ of this method are computed by

using the historical flood events by the trial and error approach. To calculate the value of θ , the storage S is plotted against the corresponding weighted discharge value $[0 I + (1-\theta)O]$ in equation (2.31) for different trial values of θ resulting in various sizes of loops; and the value of θ which gives the narrowest loop of this plot is considered as the appropriate one for its use in the model. The solution of these equations (2.30) and (2.31) is given by Nash [1959], Diskin [1967], and Dooge [1973].

Subsequently, several attempts have been made by various researchers [Dooge and Harley, 1967; Cunge, 1969; Dooge et al., 1982] to link the routing parameters K and θ of the classical Muskingum method with the flow and channel characteristics using the hydrodynamics principles to transform it into a physically based method. Apart from the simplicity and wide applicability, the Muskingum method produces unrealistic initial routed outflow, namely, “negative flow” or “reduced flow” or “dip” which is well documented in the literature [Dooge, 1973; Weinmann and Laurenson, 1979; Perumal, 1992c, 1993b]. This defect is also inherent with the different variants of the classical Muskingum method wherein the parameters are estimated based on the channel and flow characteristics.

However, the classical Muskingum method is still popular in the present-day literature [e.g., Neitsch et al., 2005; Arnold and Fohrer, 2005; Gassman, 2007] for the simplicity in its model framework.

2.5.2 Physically based Muskingum routing methods:

Since the early sixties, various attempts have been made for the physical interpretation of the classical Muskingum method which may be categorized as [Kundzewicz, 1986; Perumal, 1995]: i) direct interpretation [Strupczewski and Kundzewicz, 1980], ii)

matching the impulse response of the Muskingum method with that of the linearized Saint-Venant's equation using the method of moments approach [Dooge, 1973], iii) matching difference schemes [Cunge, 1969; Koussis, 1976; Dooge et al., 1982], and iv) the method based on the extension of the Kalinin–Milyukov method [Apollov et al., 1964; Perumal, 1992c]. The salient features of each of these approaches are described below.

i) **Direct interpretation:** Strupczewski and Kundzewicz [1980] attempted the interpretation of the Muskingum method directly from the Saint-Venant's equations, but they could not express the flood storage within the reach as a linear function of the weighted discharge due to their interpretation of a one-to-one relationship between the stage and the discharge for depicting the storage equation of the Muskingum method. However, this interpretation is not appropriate for describing flood waves when the one-to-one relationship between the stage and the discharge is not valid. Further, Strupczewski and Kundzewicz [1980] could not express the parameters K and θ explicitly in terms of channel and flow characteristics. Hence, their approach for interpreting the physical basis of the Muskingum method is not appropriate.

ii) **Method based on the moment matching approach:** By matching the first and second moments of the IUH of the linearized Saint-Venant's equation with the corresponding moments of the Muskingum IUH, and using the Chezy's friction law in wide rectangular channels, Dooge [1973] arrived at the following expressions for the routing parameters K and θ of the Muskingum method, respectively, as

$$K = \frac{\Delta x}{c_0} \quad (2.34)$$

$$\theta = \frac{1}{2} - \frac{Q_0 \bar{y}_r}{2S_0 A_0 c_0 \Delta x} [1 - (m-1) F_0^2] \quad (2.35)$$

where y_r is the average hydraulic mean depth, A_0 is the area of cross section corresponding to Q_0 , and $m = 3/2$ or $5/3$ for the Chezy's or Manning's friction law used, respectively.

iii) Methods based on the matching difference schemes:

Although, Dooge and Harley [1967] presented the Muskingum parameter relationships with the wide rectangular channel and flow characteristics through the moment matching technique [Nash, 1960], and Dooge et al. [1982] later arrived at the same for any shape of prismatic channel and for any type of friction law, it is the Cunge's [1969] matched diffusivity approach which has become more popular as the "Muskingum–Cunge (MC) method." It was Price [1973] who first coined the term "Muskingum–Cunge method." By matching the numerical diffusivity of the approximate linear kinematic wave equation, derived from the classical Muskingum difference equation with the physical diffusivity of the linear convection–diffusion equation, Cunge [1969] arrived at the relationship for K as given in equation (2.34) and θ for wide rectangular channels as

$$\theta = \frac{1}{2} - \frac{Q_0}{2S_0 B_0 c_0 \Delta x} \quad (2.36)$$

Using a more refined difference scheme to represent the Muskingum routing equation and based on the matched diffusivity concept, Koussis [1976, 1978, 1980, 1983] arrived at an alternate relationship for θ different from that given by equation (2.36). However, a comparison between the Cunge's and Koussis' approaches shows that both the approaches lead to the same coefficients of the Muskingum routing equation and the differences in the form of the weighting parameter of both the schemes are only apparent

[Perumal, 1989]. On the basis of the state trajectory variation method applied to the Saint-Venant's equations, Dooge et al. [1982] established the generalized relationships for K and θ for

prismatic channels having any shape of cross sections, in which the relationship for K is same as equation (2.34) and the relationship for θ expressed as given in equation (2.35). Note that when the Froude number, $Fo = 0$, Dooge et al.'s [1982] expression (2.35) for θ reduces to Cunge's [1969] expression (2.36). Perumal [1992a] studied the differences in the routing results obtained using equations (2.35) and (2.36) for varying Froude number cases and showed that the use of latter equation makes a very insignificant improvement on the estimated numerical value of θ over that using the former equation. However, the use of equation (2.35) is advantageous as it retains the Vedernikov number [Jolly and Yevjevich, 1971; Ponce, 1991; e.g., Perumal, 1992a] which gives the amplification criterion of a flood wave while it moves downstream of a channel.

iv) Method based on the extension of the Kalinin–Milyukov method: On the basis of the extension of the Kalinin–Milyukov method described by Apollov et al. [1964] for the interpretation of the Muskingum method, Perumal [1992c] brought out that only this method enables one to establish the reason behind the formation of negative or reduced outflow at the beginning of the Muskingum method solution. The parameter relationships for K and θ as established by this approach are the same as given by equations (2.34) and (2.36). Wong [1984] also independently made the interpretation of the Muskingum storage equation on the lines of Apollov et al. [1964].

2.6 VARIABLE PARAMETER DISCHARGE ROUTING METHODS

2.6.1 Variable Parameter Muskingum Discharge Routing Methods with Stage Computation Feature

The Saint-Venant's equations have the capability to route a discharge hydrograph and to estimate the corresponding stage hydrograph along a channel or river reach. However, the simplified discharge routing methods with the stage computation feature are difficult to arrive at and the results are, generally, characterized by poor accuracy [NERC, 1975]. For modeling flows in tail water reaches of hydroelectric plants, Ferrick et al. [1984] first developed an improved variable parameter Muskingum method accounting for the water surface slope, which is capable of computing the stage values simultaneously. However, this routing method is not familiar among the researchers as the procedure of computing wave celerity in this method by using the "Jone's formula" [Henderson, 1966] was not convincing. Similarly, an iterative flood routing method for estimating the flow depth was developed by Koussis [1975] which resulted in the numerical instabilities of the solution [vide Weinnann, 1977]. To circumvent this problem in the earlier methods, Perumal [1994a, 1994b] developed a physically based variable parameter Muskingum discharge hydrograph (VPMD) routing method directly derived from the Saint-Venant's equations which is capable to compute the stage corresponding to the routed discharge at any river cross section. This method is found more adaptable to the field conditions [Perumal et al., 2001]. Since, the VPMD method is basically used in this thesis for comparison with the K-M method, a detailed theoretical background of this method is given below.

2.6.2 Theoretical background of the VPMD method

The VPMD routing method [Perumal, 1994a, 1994b] is directly derived from the full Saint-Venant's equations (2.1) and (2.2) describing the continuity and momentum of one dimensional unsteady flow, respectively. The parameters of the VPMD method vary at every routing time interval, and they are related to channel and flow characteristics by the same relationships as established for the physically based Muskingum method [Apolov et al., 1964; Cunge, 1969; Dooge et al., 1982]. The VPMD method is based on the hypothesis that during steady flow in a river reach having any shape of prismatic cross section, the stage and, hence, the cross sectional area of flow at any point of the reach is uniquely related to the discharge at the same location defining the steady flow rating curve. However, this situation is altered during unsteady flow, as conceptualized in the definition sketch of Figure 2.1 of the VPMD routing reach of length Δx , in which the same unique relationship is maintained between the stage and the corresponding steady discharge at any given instant of time, recorded not at the same section, but at a dynamic downstream section (section 3 in Figure 2.1) preceding the corresponding steady stage section (midsection in Figure 2.1). For the sake of better understanding of the VPMD routing method, a brief description of it is presented herein.

The VPMD routing method is derived from the Saint-Venant's equations (2.1) and (2.2), which govern the propagation of one-dimensional unsteady flow in channels and rivers, without considering lateral flow. The derivation of the routing method involves some assumptions which facilitate the simplification of the unsteady flow dynamics by assuming the channel reach to be prismatic and the longitudinal water surface gradient,

$\partial y / \partial x$, the convective acceleration gradient, $(v/g)(\partial v / \partial x)$, and the local acceleration gradient, $(1/g)(\partial v / \partial t)$, all remain approximately constant at any instant of time in a given computational routing reach. The latter assumption implies that the friction slope S_f is approximately constant over the computational reach length and, hence, the variation of discharge is approximately linear (i.e., $\partial^2 Q / \partial x^2 \approx 0$). It has been shown by Perumal [1994a] and Perumal and Ranga Raju [1999] that the use of approximately constant S_f and the Manning's or Chezy's friction law governing the unsteady flow enable to arrive at the simplified momentum equation expressed

$$\frac{\partial Q}{\partial x} = v \left[\frac{\partial A}{\partial y} + m P \frac{\partial R}{\partial y} \right] \left[\frac{\partial y}{\partial x} \right] \quad (2.37)$$

where R is the hydraulic radius ($= A/P$), P is the wetted perimeter, and m is an exponent which depends on the friction law used ($m = \frac{2}{3}$ for the Manning's friction law; $m = \frac{1}{2}$ for the Chezy's friction law).

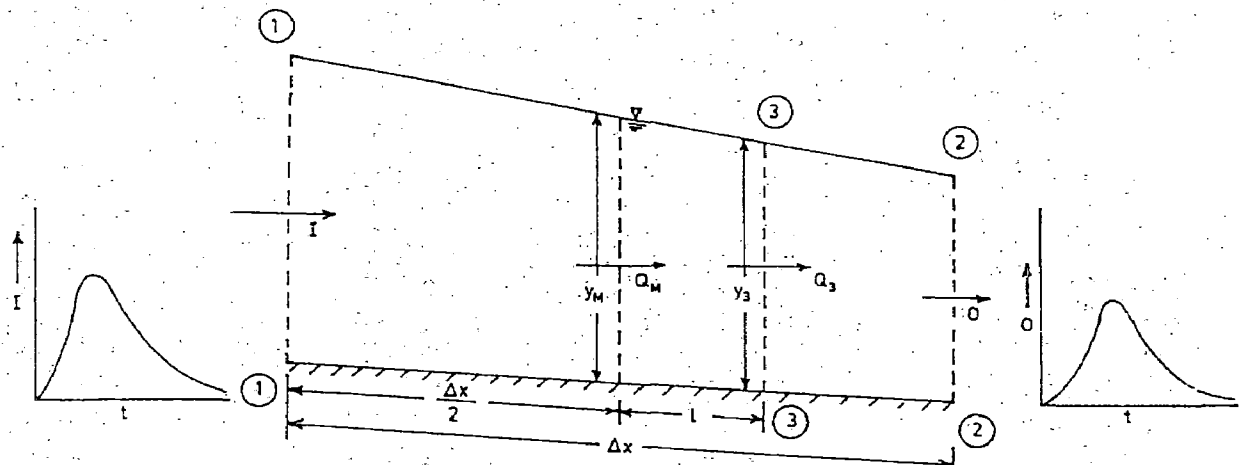


Figure 2.4 Definition sketch of the variable parameter Muskingum computational reach

Using equation (2.37), the celerity, c , of the flood wave can be estimated as [e.g., NERC, 1975]

$$c = \frac{\partial Q}{\partial A} = \left[1 + m \left(\frac{P \partial R / \partial y}{\partial A / \partial y} \right) \right] v \quad (2.38)$$

Q_u , Q_M , Q_3 , and Q_d are the discharges at sections 1, M, 3, and 2, respectively; and the corresponding stage variables are y_u , y_M , y_3 , and y_d , respectively.

Using the full Saint-Venant's equations of continuity (2.1) and momentum (2.2), equation (2.38), and the expression of discharge using the Manning's friction law, S_f can be expressed as [Perumal, 1994a]

$$S_f = S_0 \left[1 - \frac{1}{S_0} \frac{\partial y}{\partial x} \left\{ 1 - \left[m F \left(\frac{P \partial R / \partial y}{\partial A / \partial y} \right) \right]^2 \right\} \right] \quad (2.39)$$

where the Froude number, F , is expressed as

$$F = \left(\frac{v^2 \partial A / \partial y}{gA} \right)^{1/2} \quad (2.40)$$

Using equation (2.39) in the expression for discharge Q_M at the middle of the computational channel reach (i.e., section M in Figure 2.1), with the Manning's friction law, and its simplification based on binomial series expansion leads to the simplified expression for Q_M as

$$Q_M = Q_3 - \frac{Q_3 \left[1 - m^2 F_M^{-2} \left(\frac{P \partial R / \partial y}{\partial A / \partial y} \right)_M^2 \right]}{2 S_0 \left(\frac{\partial A}{\partial y} \right)_3 3 \left[1 + m \left(\frac{P \partial R / \partial y}{\partial A / \partial y} \right)_3 \right] v_3} \quad (2.41)$$

Equation (2.41) expresses the discharge Q_M in terms of discharge Q_3 , which is the normal discharge corresponding to the flow depth y_M at the middle of the reach. Since

the discharge also varies approximately linearly, the term adjunct to $(\partial Q / \partial x)_3$ in equation (2.41) represents the distance L between the midsection M and the downstream section 3 where the normal discharge Q_3 passes, as shown in Figure 2.1. Hence, the distance L is expressed as

$$L = \frac{Q_3 \left[1 - m^2 F_M^{-2} \left(\frac{P \partial R / \partial y}{\partial A / \partial y} \right)_M^2 \right]}{2 S_0 \left(\frac{\partial A}{\partial y} \right)_3 \left[1 + m \left(\frac{P \partial R / \partial y}{\partial A / \partial y} \right)_3 \right] v_3} \quad (2.42)$$

where the subscripts M and 3 attached with different variables denote these variables at sections M and 3, respectively.

Further, Perumal and Ranga Raju [1999] proposed a new wave type equation, known as the ACD equation in discharge form as

$$\frac{\partial Q}{\partial t} + c \frac{\partial Q}{\partial x} = 0 \quad (2.43)$$

Note that equation (2.25) is a special case of the diffusive wave equation

$$\frac{\partial Q}{\partial t} + c \frac{\partial Q}{\partial x} = D \frac{\partial^2 Q}{\partial x^2} \quad (2.44)$$

Perumal and Ranga Raju [1999] have clarified that although the form of the ACD equation (2.43) is similar to that of the well-known kinematic wave equation [Lighthill and Whitham, 1955], it is capable of approximately modeling a flood wave in the transition range between the zero-inertia wave, governed by Hayami's [1951] convection-diffusion equation and the kinematic wave, including the latter. The basis behind this inference is that the right hand side of equation (2.43) is zero because of the assumption $\partial^2 Q / \partial x^2 \approx 0$, and the diffusivity coefficient associated with this term $D \neq 0$.

This enables the application of equation (2.43) for modeling lower order diffusive flood waves, including the kinematic wave. This inference, however, contradicts the conventional perception that equation (2.43) is strictly applicable for modeling kinematic flood waves only. Applying equations (2.38) and (2.43) at section 3 of Figure 2.1 and its simplification leads to [Perumal, 1994a, 1994b] the governing differential equation of the Muskingum type routing, using discharge as the operating variable, and it is expressed as

$$Q_u - Q_d = \frac{\Delta x}{\left[1 + m \left(\frac{P \partial R / \partial y}{\partial A / \partial y} \right)_3 \right] v_3} \times \frac{\partial}{\partial t} \left[Q_d + \left(\frac{1}{2} - \frac{L}{\Delta x} \right) (Q_u - Q_d) \right] \quad (2.45)$$

where Q_u and Q_d denote the discharges at the upstream and downstream of the Muskingum reach, respectively. Using the analogy between the governing differential equation of the Muskingum method in discharge formulation:

$$Q_u - Q_d = \frac{\partial S}{\partial t} = \frac{\partial}{\partial t} \left[K (Q_u + (1-\theta) Q_d) \right] \quad (2.46)$$

and the equation (2.45), it is inferred that the travel time, K , of the Muskingum-type discharge routing method can be expressed as

$$K = \frac{\Delta x}{\left[1 + m \left(\frac{P \partial R / \partial y}{\partial A / \partial y} \right)_3 \right] v_3} \quad (2.47)$$

and the weighting parameter, θ , after substituting for L from equation (2.42), can be obtained as

$$\theta = \frac{1}{2} - \frac{Q_3 \left[1 - m^2 F_M^2 \left(\frac{P \partial R / \partial y}{\partial A / \partial y} \right)_M^2 \right]}{2S_0 \left(\frac{\partial A}{\partial y} \right)_3 \left[1 + m \left(\frac{P \partial R / \partial y}{\partial A / \partial y} \right)_3 \right] v_3 \Delta x} \quad (2.48)$$

Assuming the magnitude of the inertial terms to be negligible in natural flood waves [Henderson, 1966; Price, 1985], equation (2.48) can be modified using $F_M \approx 0$ as

$$\theta = \frac{1}{2} - \frac{Q_3}{2S_0 \left(\frac{\partial A}{\partial y} \right)_3 \left[1 + m \left(\frac{P \partial R / \partial y}{\partial A / \partial y} \right)_3 \right] v_3 \Delta x} \quad (2.49)$$

Substituting equations (2.47) and (2.49) in (2.45) and using the classical Muskingum difference scheme [McCarthy, 1938], the differential equation (2.45) is converted to a difference equation which on algebraic operation reduces to the Muskingum routing equation expressed as

$$Q_{d,j+1} = C_1 Q_{u,j+1} + C_2 Q_{u,j} + C_3 Q_{d,j} \quad (2.50)$$

where $Q_{u,j+1}$ and $Q_{d,j+1}$, denote the upstream and downstream discharges at time step $(j+1)\Delta t$, respectively; $Q_{u,j}$, and $Q_{d,j}$, denote the upstream and downstream discharges at time step $j\Delta t$, respectively, and the coefficients C_1 , C_2 , and C_3 are expressed as given by equations (2.33a)–(2.33c).

For estimating the stage hydrograph corresponding to the routed discharge hydrograph, the flow depth y_d corresponding to the routed discharge Q_d can be estimated using equation (2.37) as

$$y_d = y_M + \frac{Q_d - Q_M}{\left(\frac{\partial A}{\partial y} \right)_M \left[1 + m \left(\frac{P \partial R / \partial y}{\partial A / \partial y} \right)_M \right] v_M} \quad (2.51)$$

in which y_M is estimated iteratively using the Manning's equation:

$$Q_3 = \frac{1}{n} A_M R^{2/3} S_0^{1/2} \quad (2.52)$$

Using the computed flow depths y_d and y_M in the first sub-reach, the upstream flow depth corresponding to the inflow discharge can be estimated using the assumption of approximately linear variation of water surface. The above simplified hydraulic VPMD method, which is directly derived from the Saint-Venant's equations for routing floods in channels having any shape of prismatic cross-section, allows the simultaneous computation of discharge hydrograph as well as the corresponding stage hydrograph. Hence, the relationship (2.51) between y_d and Q_d can be used for establishing the looped rating curve in a downstream river section.

2.7 HEC-RAS MODEL

HEC-RAS is an integrated system of software, designed for interactive use in a multi-tasking environment. The system is comprised of a graphical user interface (GUI), separate analysis components, data storage and management capabilities, graphics and reporting facilities.

The HEC-RAS system contains four one-dimensional river analysis components for: 1) steady flow water surface profile computations; 2) unsteady flow simulation; 3) movable

boundary sediment transport computations; and 4) water quality analysis. A key element is that all four components use a common geometric data representation and common geometric and hydraulic computation routines. In addition to the four river analysis components, the system contains several hydraulic design features that can be invoked once the basic water surface profiles are computed. The current version of HEC-RAS supports steady and unsteady flow water surface profile calculations; sediment transport/mobile bed computations; and water temperature analysis. In the study we have taken HEC-RAS as a benchmark model.

Procedure adopted by the HEC-RAS model for solving the one-dimensional unsteady flow equations is the four-point implicit scheme, also known as box scheme. Under this scheme, space derivatives and function values are evaluated at an interior point, $(n+\gamma)\Delta t$. Thus values at $(n+1)\Delta t$ enter into all terms in the equations. The simultaneous solution is an important aspect of this scheme because it allows information from the entire reach to influence the solution at any one point. Consequently, the time step can be significantly larger than with explicit numerical schemes. Von Neumann stability analysis performed by Fread(1974), and Liggett and Cunge (1975), show the implicit scheme to be unconditionally stable (theoretically) for $0.5 < \gamma \leq 1.0$, conditionally stable for $\gamma = 0.5$, and unstable for $\gamma < 0.5$. In a convergence analysis performed by the same authors, it was shown that the numerical damping increased as the ratio $\lambda/\Delta x$ decreased, where λ the length of a wave is in the hydraulic system. For streamflow routing problems where the wave lengths are long with respect to spatial distances, convergence is not a serious problem.

The general implicit finite difference forms are:

Time derivative

$$\frac{\partial f}{\partial t} \approx \frac{\Delta f}{\Delta t} = \frac{0.5(\Delta f_{j+1} - \Delta f_j)}{\Delta t} \quad (2.53)$$

Space derivative

$$\frac{\partial f}{\partial x} \approx \frac{\Delta f}{\Delta x} = \frac{(f_{j+1} - f_j) + \gamma(\Delta f_{j+1} - \Delta f_j)}{\Delta x} \quad (2.54)$$

Function value

$$f \approx \bar{f} = 0.5(f_j + f_{j+1}) + 0.5\gamma(\Delta f_j + \Delta f_{j+1}) \quad (2.55)$$

Continuity equation

The continuity equation describes conservation of mass for the one-dimensional system.

The continuity equation for the system can be written as:

$$\frac{\partial A}{\partial t} + \frac{\partial S}{\partial t} + \frac{\partial Q}{\partial x} - q_1 = 0 \quad (2.56)$$

- Where:
- x = distance along the channel
 - t = time
 - Q = flow,
 - A = cross-sectional area,
 - S = storage from non conveying portion of cross-section
 - q_1 = lateral inflow per unit distance.

as in our study we are not considering the lateral inflow so $q_1=0$ in our case.

Momentum equation

The momentum equation states that the rate of change in momentum is equal to the external forces acting on the system. Thus for a single channel:

$$\frac{\partial Q}{\partial t} + \frac{\partial(VQ)}{\partial x} + gA \left(\frac{\partial z}{\partial x} + S_f \right) = 0 \quad (2.57)$$

Where: g = acceleration of gravity

S_f = friction slope

V = velocity

2.8 CONCLUSION

This Chapter presented an overview of vast literature available on flood routing methods in general and Kalinin-Milyukov routing method in particular, which is widely used in Eastern European countries as the basic model of a flood forecasting model based on the use of hydrometric data only. The K-M method in linear form, when used as the basic model of a flood forecasting model, enables the adoption of linear filters in the forecasting models, such as the well known Kalman filters, which offers the easy feature of updating the parameters of the K-M method in real time, by minimizing the errors between the observed and forecasted series till the time of forecast. However it is recognized that the parameters of the K-M method updated in this manner are not based on the physics of the flood wave movement process considering the nonlinear characteristics of the flood wave movement and estimated merely based on the minimization of errors between the observed and forecasted flow series at the time of forecasting. It is argued that the parameters of the physical part of the basic routing

method should be estimated independently of those of the noise component consisting of the model and observation errors, thus reducing the domination of the noise model over the basic model. [Excerpts from the conclusion speech given by professor J. E. Nash in the Oxford Symposium on Hydrological forecasting, April 1980 (News reported in the Hydrological Sciences-Bulletin, 25(4), 1980.)]

When a basic model having the same simplicity of the linear model is used, but with a capability of incorporating the nonlinear feature of the flood wave moment, then the use of complicated filters such as the Kalman filters in a real time forecasting model may not be required and the use of simple updating model such as the auto regressive model may be adequate. The VPMD routing method which offers such a feature is discussed in detail in this chapter. Therefore, the K-M method as used in the flood forecasting model of the East European countries, and the VPMD method need to be investigated for their suitability in adopting them as basic models in flood forecasting models. Such an investigation of these two models is presented in the subsequent chapters of this thesis.

CHAPTER 3

STATEMENT OF THE PROBLEM

It is proposed to investigate the performance of two available river routing methods viz., 1) the well known Kalinin-Miliyukov method based on state-space formulation as advocated by Szollosi-Nagy (1976 and 1982), and 2) the recently introduced Variable Parameter Muskingum Discharge routing method (Perumal, 1996a)by routing hypothetical flood hydrographs in hypothetical channels for arriving at routed hydrographs and to evaluate the ability of one method over the other in closely reproducing the corresponding routed solutions of a benchmark model.

CHAPTER 4

STRATEGY ADOPTED FOR EVALUATION OF THE METHODS

4.1 GENERAL

The K-M method in state-space formulation was advocated by Szollosi-Nagy (1976) as basic model in the hydrometric data based real-time flood forecasting models. However, it was pointed out in Chapter-2 that the two parameters of the K-M model remain constant when the past recorded outflow hydrograph events are simulated using the corresponding inflow hydrographs, implying that the K-M model is operated in linear mode and is not capable of reproducing the non-linear characteristics of flood wave movement in rivers in off-line mode. To overcome this deficiency of the K-M method, but maintaining the same recursive nature of the solution algorithm of the K-M method, the use of VPMD method was advocated in Chapter-2.

In order to verify the capability of the VPMD method over that of the K-M method the same past recorded outflow event should be simulated by both these methods for the corresponding recorded inflow hydrograph, and the VPMD method should be able to reproduce the recorded outflow hydrograph closely than the K-M method. To thoroughly verify the better capabilities of the VPMD method over that of the K-M method, many past events recorded under various possible channel and flow conditions should be used. However, this requirement is not easy to achieve due to practical reasons and, therefore, it is considered appropriate to use different hypothetical inflow hydrographs for routing in hypothetical uniform rectangular channels to arrive at corresponding outflow hydrographs, at specified downstream site.

The flood routing phenomenon is considered for all practical purposes, as one dimensional flow event governed by Saint-Venant's equations, a standard, well-tested benchmark model which employ the full Saint-Venant's equations may be used to serve this purpose. Accordingly, the U.S. Army Corps of Engineer's HEC-RAS model (2006) is used herein as the benchmark model. The comparison of the performances of the K-M and VPMD methods in reproducing the benchmark solutions are made using various performance criteria. The entire exercise is taken up under the consideration that the method which is capable of reproducing the benchmark solutions closely may be considered as the appropriate basic model to be employed in a hydrometric data based flood forecasting model.

This chapter describes the development of computer codes using MATLAB for the programming of the K-M routing method based on state-space formulation as advocated by Szollosi-Nagy(1976 and 1982). A brief description of the steps involved in the development of already available computer code of the VPMD method (Perumal, 1995) is also presented. A typical routing example is presented for each of these methods using the computer program. Details of test runs describing channel configurations and inflow hydrographs used and performance criteria adopted to evaluate these methods are also presented in this chapter.

4.2 DEVELOPMENT OF COMPUTER CODE FOR K-M METHOD BASED ON STATE-SPACE ANALYSIS APPROACH

The computer code is developed using MATLAB programming as it is more convenient for carrying out computations of repetitive nature as involved in the K-M method.

The various steps involved in MATLAB programming are as follows:

Step 1: To proceed, a computation time-interval Δt is chosen. Using moment matching method, (Subramanya, 2006) we try to estimate the most suitable value of number of reservoirs n and the value of storage coefficient K . For non-integer number of reservoirs the fractional part of numbers of reservoirs x is obtained using eq.(4.1).

$$x = [n - \text{int}(n)]. \quad (4.1)$$

Step 2: Now after estimation of value of x , use the values k (i. e. K^{-1}) and x in the below given equation to form the state transition matrix (STM) $\Phi_t(\Delta t)$. The order of the matrix

will be $n^* \times n^*$ where $n^* = (\text{int } n) + 1$.

$$\underline{\Phi}(t) = e^{Et} = \begin{bmatrix} e^{-kt} & 0 & 0 & \dots & 0 \\ kte^{-kt} & e^{-kt} & \dots & \dots & 0 \\ \frac{(kt)^2 e^{-kt}}{2} & kte^{-kt} & e^{-kt} & \dots & 0 \\ \vdots & \ddots & \ddots & \ddots & \vdots \\ \frac{(kt)^{n-1} e^{-kt}}{(n-1)} & \frac{(kt)^{n-2} e^{-kt}}{(n-2)} & \ddots & \ddots & e^{-kt} \end{bmatrix} \quad (4.2)$$

While the last element of the STM is estimated as

$$\Phi_{n^*-1} = \frac{k(k\tau)^{n^*-2} e^{-k_x t}}{(n^*-2)!(k_x - k)} \left(e^{(k_x - k)t} + \left\{ [(k - k_x)t]^{2-n^*} [(n^* - 2)\Gamma(n^* - 2, (k - k_x)t) - (n^* - 2)!] \right\} \right) \quad (4.3)$$

Step 3: Similarly Γ is estimated as

$$\underline{\Gamma}_t(\Delta t) = \begin{bmatrix} (1 - e^{-k\Delta t}) / k \\ (1 - e^{-k\Delta t}(1 + k\Delta t)) / k \\ \vdots \\ 1 - e^{-k\Delta t} \sum_{j=0}^{n-1} \frac{(k\Delta t)^j}{j!} / k \end{bmatrix} \quad (4.4)$$

And the last element of this matrix for fractional reservoir is expressed as

$$\Gamma_{n^*}(\Delta t) = \frac{1 - e^{-k_x \Delta t}}{k_x} - e^{-k_x \Delta t} \times \sum_{j=0}^{n^*-2} \left\{ \frac{(k\Delta t)^j}{(k_x - k)^j j!} \left(e^{(k_x - k)\Delta t} + \left[\frac{j\Gamma(j, (k - k_x)\Delta t) - j!}{[(k - k_x)\Delta t]^j} \right] \right) \right\} \quad (4.5)$$

Where, $n^* \geq 2; k_x \neq k$

Step 4: Assuming the initial storage in the reservoirs zero at time t , computation of storage for the next time interval $t + \Delta t$, is made for the known value of input $u(t)$ as

$$x_{t+\Delta t} = \underline{\Phi}_t(\Delta t)x_t + \underline{\Gamma}_t(\Delta t)u_t \quad (4.6)$$

Step 5: Now for each storage vector computation, the corresponding output of the system, is computed as

$$y(t) = \underline{H}x(t) \quad (4.7)$$

where \underline{H} is the row vector, as shown below:

Note that in the case of non-integer number of reservoirs the H row vector would be

$$H = [0 \ 0 \ 0 \ \dots \ k_x] \quad (4.8)$$

$$\text{where, } k_x = \frac{k}{x}$$

4.2.1 Computation Procedure

Using state space analysis approach, the flood hydrograph is routed for different combinations of inflow hydrograph shape factor, roughness coefficient, bed slope and bed width. The shape of the channel is considered as uniform rectangular in all the cases studied.

To illustrate the above described algorithm, a typical simulation event is considered herein.

A given inflow hydrograph of the following characteristics is routed in a rectangular channel reach having the following geometrical elements of the routing reach:

Routing reach length $L = 40 \text{ km.}$

Number of sub-reaches = 40 (only for VPMD and HEC-RAS)

Peak inflow $I_p = 1600 \text{ m}^3/\text{sec.}$

Initial flow $I_0 = 100 \text{ m}^3/\text{sec.}$

Time to peak $t_p = 10 \text{ hours}$

Bed width B = 50 m

Roughness coefficient n = 0.04

Bed slope S₀ = 0.0004

Shape factor of inflow hydrograph γ = 1.25.

Using the developed MATLAB program, the inflow hydrograph with the above characteristic is routed to arrive at the outflow hydrograph at 40 km., as shown below in Figure 4.1.

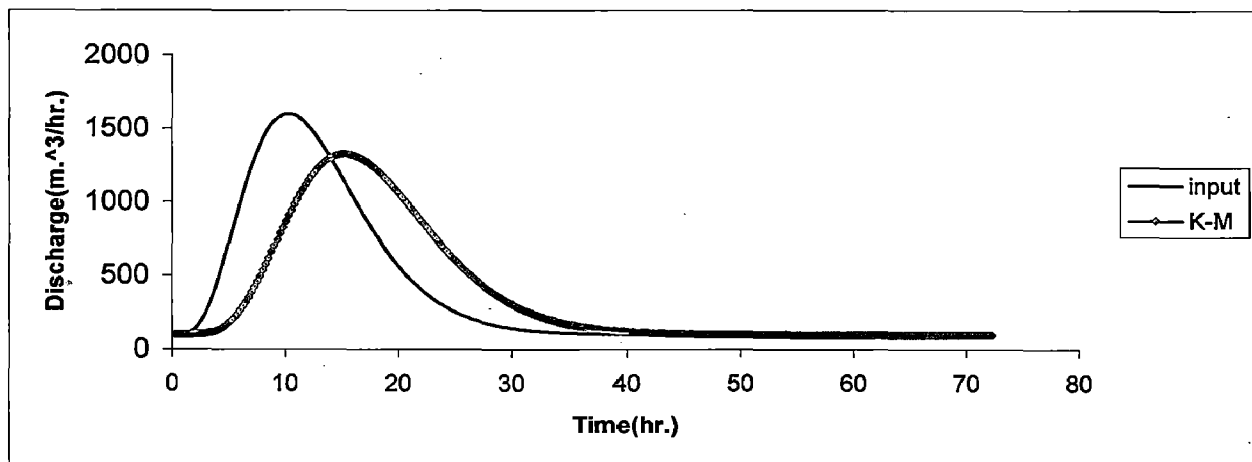


Figure 4.1 Typical Routing Results using the K-M method

4.3 VARIABLE PARAMETER MUSKINGUM DISCHARGE ROUTING METHOD

The VPMD method proposed by Perumal [1994a, 1994b] is directly derived from the Saint-Venant equations using various assumptions, including the assumption of approximate linear variation of water surface at any instant of time over the routing space step Δx .

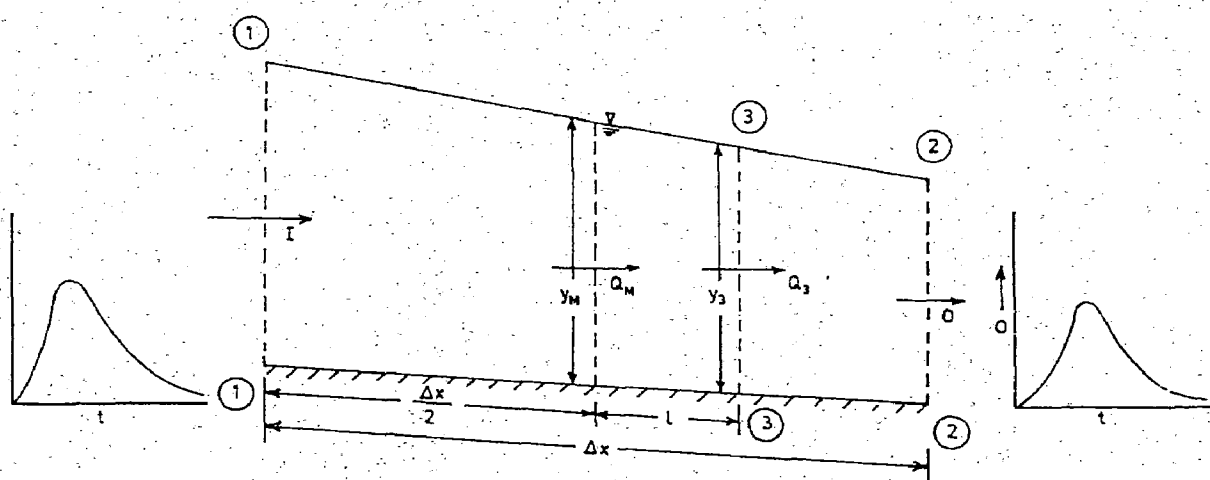


Figure 4.2 Definition Sketch of the Muskingum Reach

Different steps involved in the flood routing procedure using the VPMD method are described below briefly:

The unrefined discharge $Q_{d,j+1}$ for the current routing time interval is computed using the values of K and θ , estimated at the previous time step and, subsequently, using this estimate and $Q_{u,j+1}$, the flow at the middle of the reach is estimated as

$$Q_M = 0.5(Q_{u,j+1} + Q_{d,j+1}) \quad (4.9)$$

The initial values of the routing parameters K and θ are estimated using the initial steady flow in the reach. The normal discharge at section 3 of Figure 4.2 is computed as

$$Q_3 = \theta Q_{u,j+1} + (1-\theta) Q_{d,j+1} \quad (4.10)$$

Using Q_3 , the stage y_m at the midsection is estimated using the Newton-Raphson method, by solving the following equations.

$$Q_3 = \frac{A_M}{n} \left(\frac{A_M}{P_M} \right)^{\frac{2}{3}} \sqrt{S_0} \quad (4.11)$$

where A_M is evaluated at the midsection of the reach.

Using the values of Q_3 , c_3 , and $(\partial Q / \partial y)_3$, the refined values of K and θ are estimated.

Then using equation

$$K = \frac{\Delta x}{c_3} \text{ and} \quad (4.12)$$

$$\theta = \frac{1}{2} - \frac{Q_3}{2S_0 \left(\frac{\partial A}{\partial y} \right) c_3 \Delta x} = \frac{1}{2} - \frac{Q_3}{2S_0 \left(\frac{\partial Q}{\partial y} \right) \Delta x} \quad (4.13)$$

respectively, at the current routing time interval, which are, subsequently, used to estimate the refined discharge hydrograph estimate using equations

$$Q_{d,j+1} = C_1 Q_{u,j+1} + C_2 Q_{u,j} + C_3 Q_{d,j} \quad (4.14)$$

$$C_1 = \frac{-K\theta + 0.5\Delta t}{K(1-\theta) + 0.5\Delta t} \quad (4.15a)$$

$$C_2 = \frac{K\theta + 0.5\Delta t}{K(1-\theta) + 0.5\Delta t} \quad (4.15b)$$

$$C_3 = \frac{K(1-\theta) - 0.5\Delta t}{K(1-\theta) + 0.5\Delta t} \quad (4.15c)$$

4.3.1 COMPUTATION PROCEDURE

The plot of the inflow and routed hydrographs arrived by the program are shown below. For testing the VPMD method, same set of inflow-outflow hydrograph data used for testing the K-M method was used.

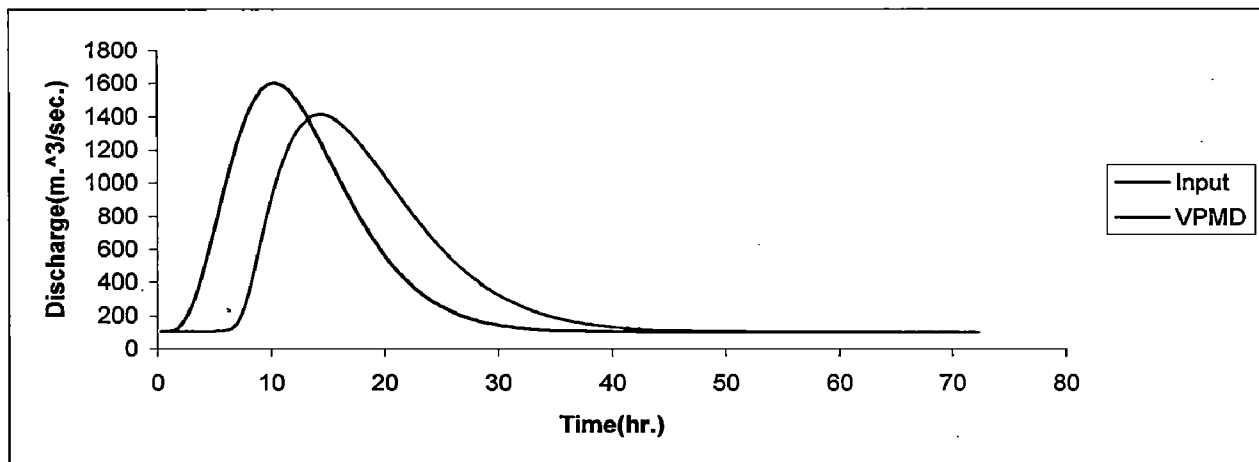


Figure 4.3 Typical Routing results using the VPMD method

4.4 ROUTING USING THE HEC-RAS MODEL

Various steps involved in the flood routing using HEC-RAS model are described below briefly:

Step1

The first step in developing a hydraulic model with HEC-RAS is to establish which directory to work in and to enter a title for the new project. To start a new project, open the File Menu on the main HEC-RAS window and select New Project. This will bring up a New Project window as shown in Figure 4.4. Now from the window, first select the drive and path to work with, and then enter a project title and file name. The project filename must have the extension “.prj”.

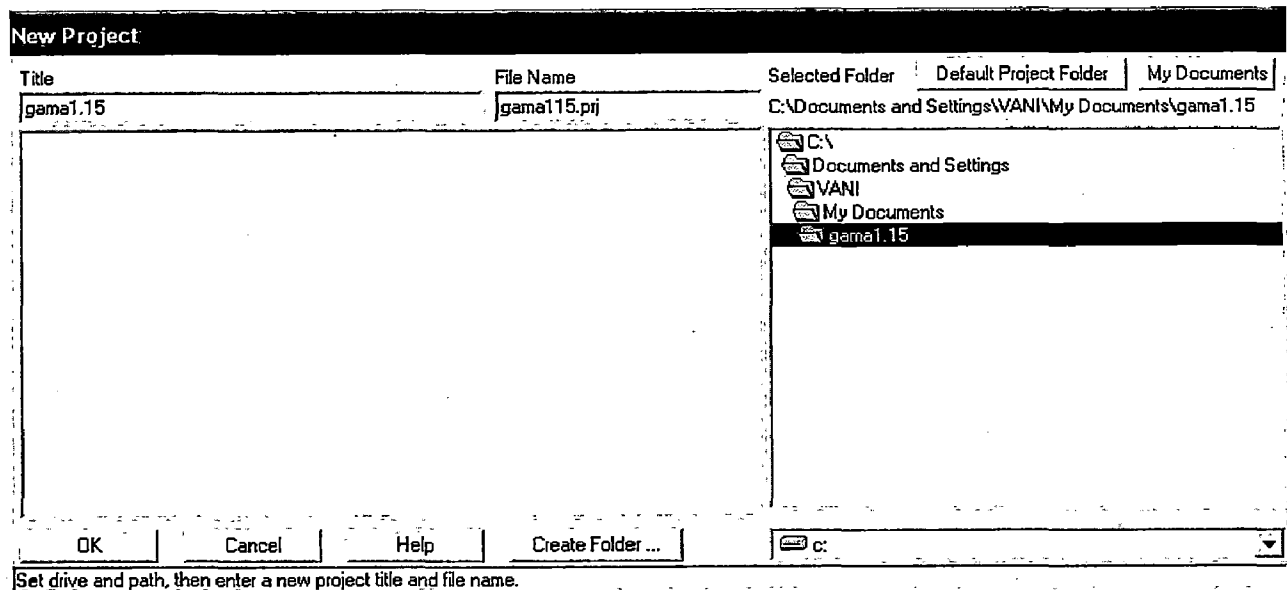


Figure 4.4 New Project Window

Step 2

The next step is to enter the necessary geometric data, which consist of connectivity information for the stream system (River System Schematic), cross section data, and hydraulic structure data. Geometric data are entered by selecting Geometric Data from the Edit menu on the main HEC-RAS window. Once this option is selected, the geometric data window will appear as shown in Figure 4.5. The geometric data is developed by first drawing in the river system schematic. This is accomplished, on a reach-by-reach basis and starting in a reach from upstream to downstream (in the positive flow direction). After the reach is drawn, it is prompted to enter a "River" and a "Reach" identifier.

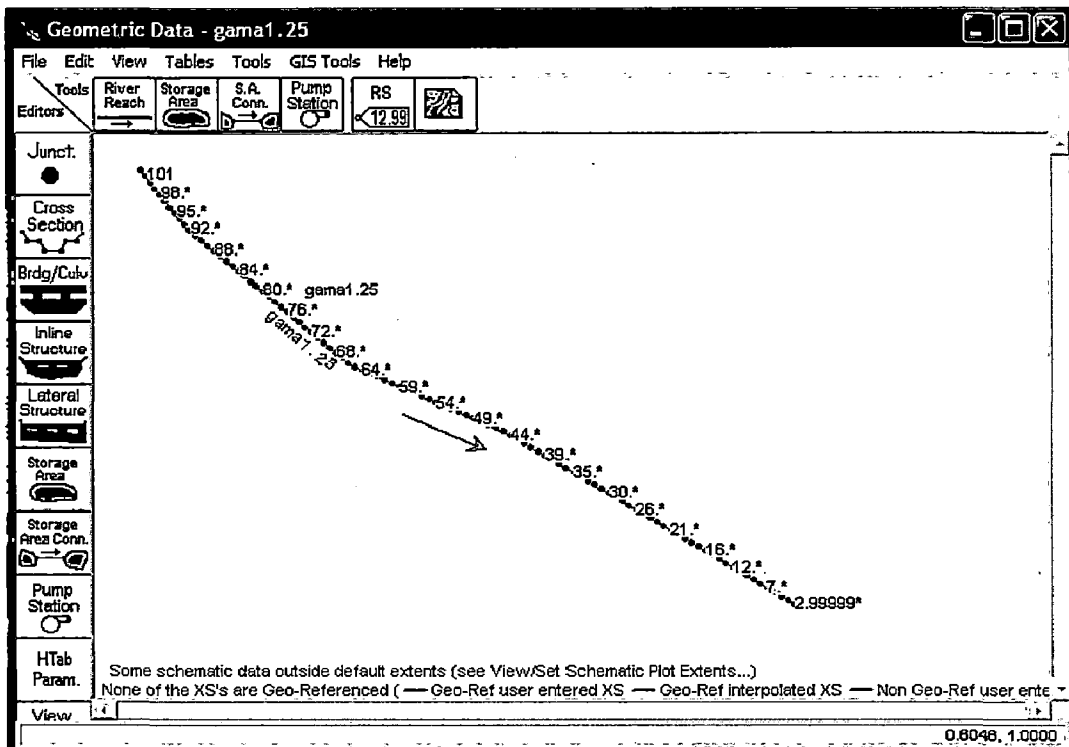


Figure 4.5 Geometric Data Window

After the river system schematic is drawn, the cross section and the hydraulic data are to be entered. This editor is shown in Figure 4.6. As shown, each cross section has a River name, Reach name, River Station, and a Description. The River, Reach and River Station identifiers are used to describe where the cross section is located in the river system. The “River Station” identifier does not have to be the actual river station (miles or kilometers) at which the cross section is located on the stream. Numeric values are used to place cross sections in the appropriate order within a reach, starting from the highest river station upstream to the lowest river station downstream. The basic data required for each cross section are shown on the Cross Section Data editor in Figure 4.6. Additional cross section features are available under options from the menu bar. These options include: adding, copying, renaming and deleting cross sections; adjusting cross section elevations, stations, and Manning’s n or resistance number k-values; skew cross section; ineffective

flow areas; levees; blocked obstructions; adding a lid to a cross section; adding ice cover; adding a rating curve; horizontal variation of Manning's n or resistance number k-values; and vertical variation of n values. Here as we have taken into account a prismatic channel so the value of contraction coefficient and expansion coefficient has been taken as zero.

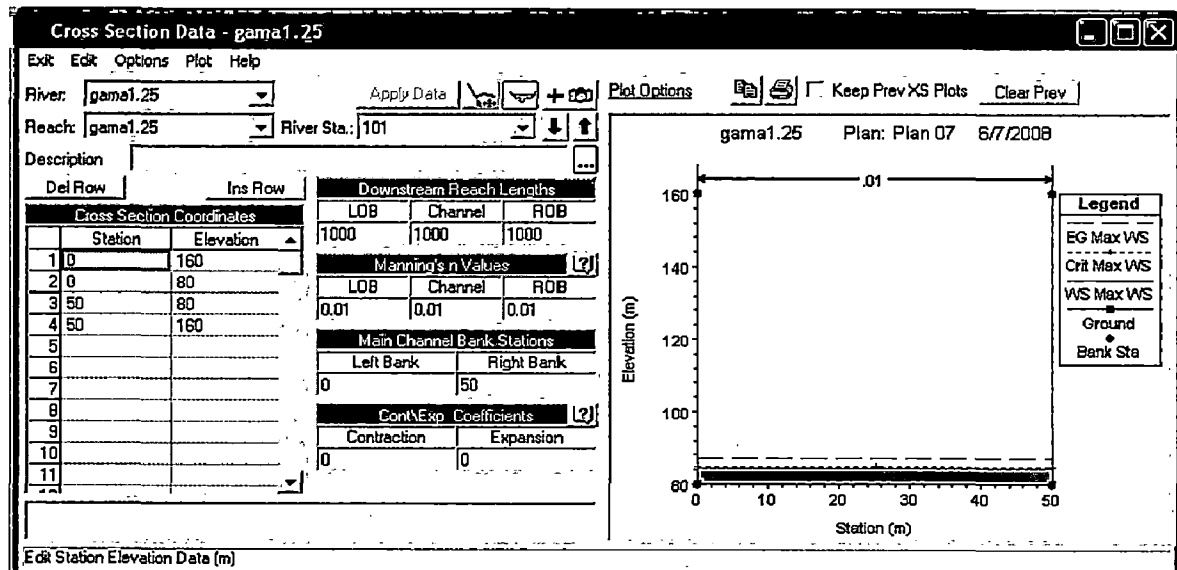


Figure 4.6 Cross-Section Data Window

Step 3. Entering Flow Data and Boundary Conditions

Once the geometric data are entered, the unsteady flow data are to be entered. The type of flow data entered depends upon the type of analyses to be performed. For the flood-routing computation, unsteady flow analysis is to be performed. The data entry form for unsteady flow data is available under the Edit menu bar option on the HEC-RAS main window shown in Figure 4.7. First we have to enter boundary conditions at all of the external boundaries of the system, as well as any desired internal locations, and set the initial flow and storage area conditions at the beginning of the simulation.

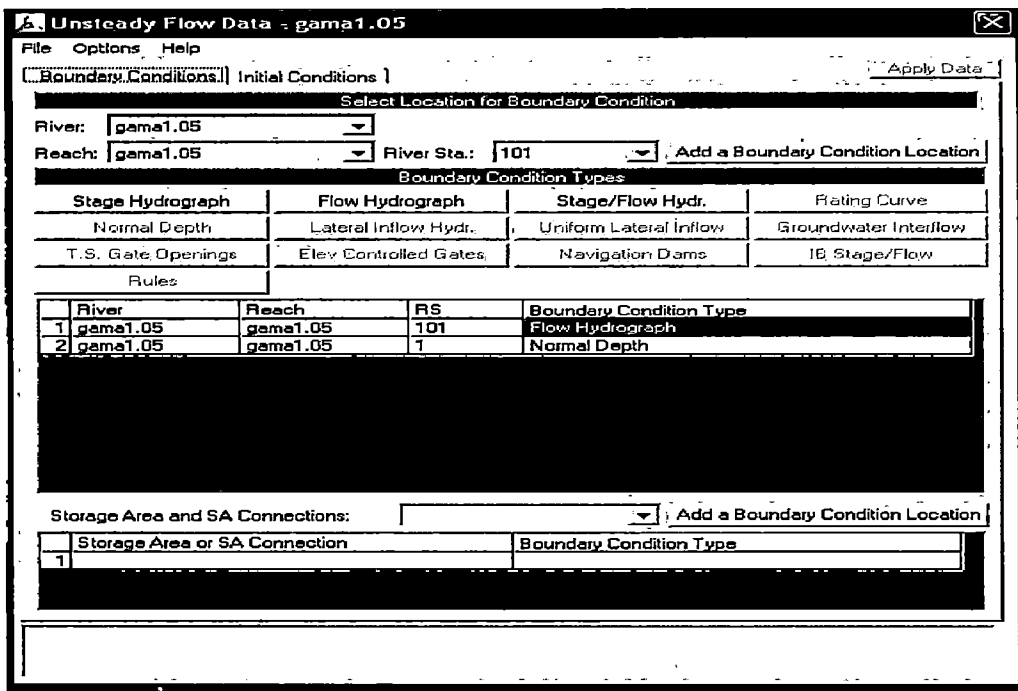


Figure 4.7 Unsteady Flow Data Window

Boundary conditions are entered by first selecting the Boundary Conditions tab from the Unsteady Flow Data editor. River, Reach and River Station locations of the external bounds of the system automatically get entered into the table. Boundary conditions are entered by first selecting a cell in the table for a particular location, then selecting the boundary condition type that is desired at the location.

There are several different types of boundary conditions available, which are listed below:

- Stage and Flow Hydrograph
- Stage Hydrograph
- Rating Curve
- Normal Depth
- Lateral Inflow Hydrograph
- Uniform Lateral Inflow Hydrograph
- Ground Water Inflow

- Time Series of Gate Openings
- Elevation Controlled Gates
- Navigation Dam
- Internal Observed Stage and Flow Hydrograph

Here we enter the flow hydrograph as shown in the Figure 4.8. If any other boundary condition is chosen then it can be given by pressing corresponding boundary condition tab. Also we have to enter the downstream boundary condition. In this steady flow vs. normal depth is given as the downstream boundary condition.

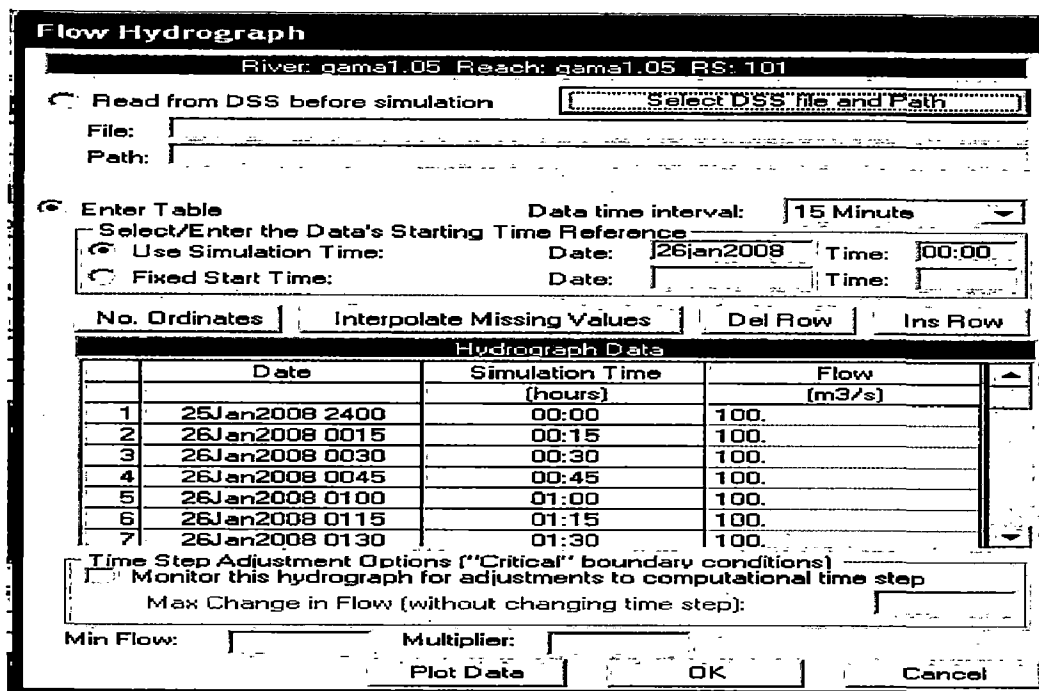


Figure 4.8 Flow Hydrograph Window (for boundary condition)

Step 4:

In addition to the boundary conditions, the initial conditions of the system at the beginning of the unsteady flow simulation should also be given. The next step is to enter the initial condition, and the initial flow value is entered.(Figure 4.9)

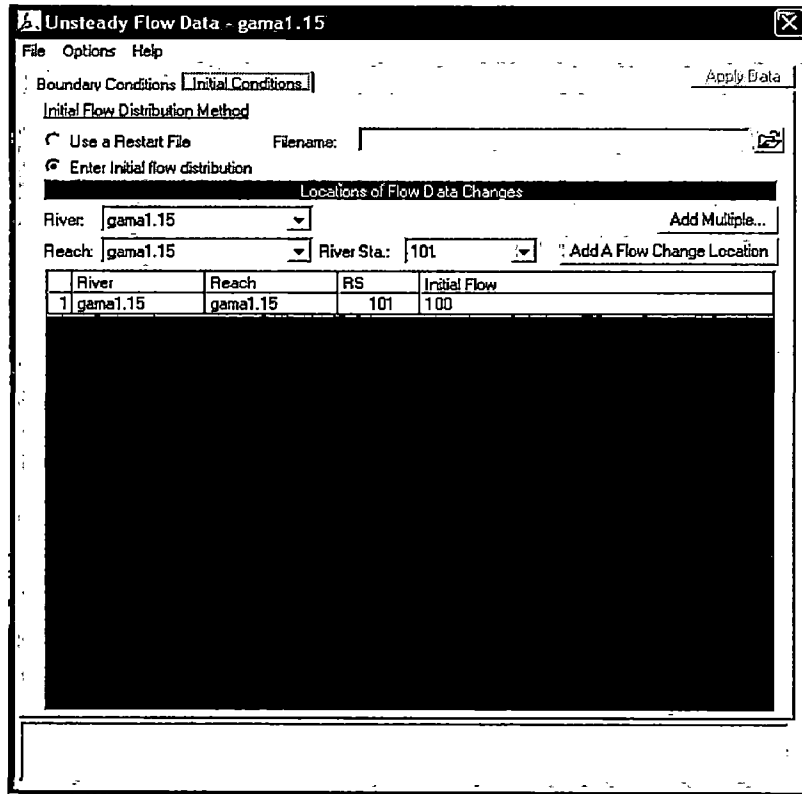


Figure 4.9 Unsteady Flow Data Window (Initial Condition)

Step 5:

Once all of the geometry and unsteady flow data have been entered, we can begin performing the unsteady flow calculations. To run the simulation, we go to the HEC-RAS main window and select Unsteady Flow Analysis from the Run menu.(Figure 4.10)

After defining the plan, locations of stage and flow hydrograph we select geometric data pre-processor, the unsteady flow simulator, and an output post-processor. After pressing the tab COMPUTE the calculation get started.

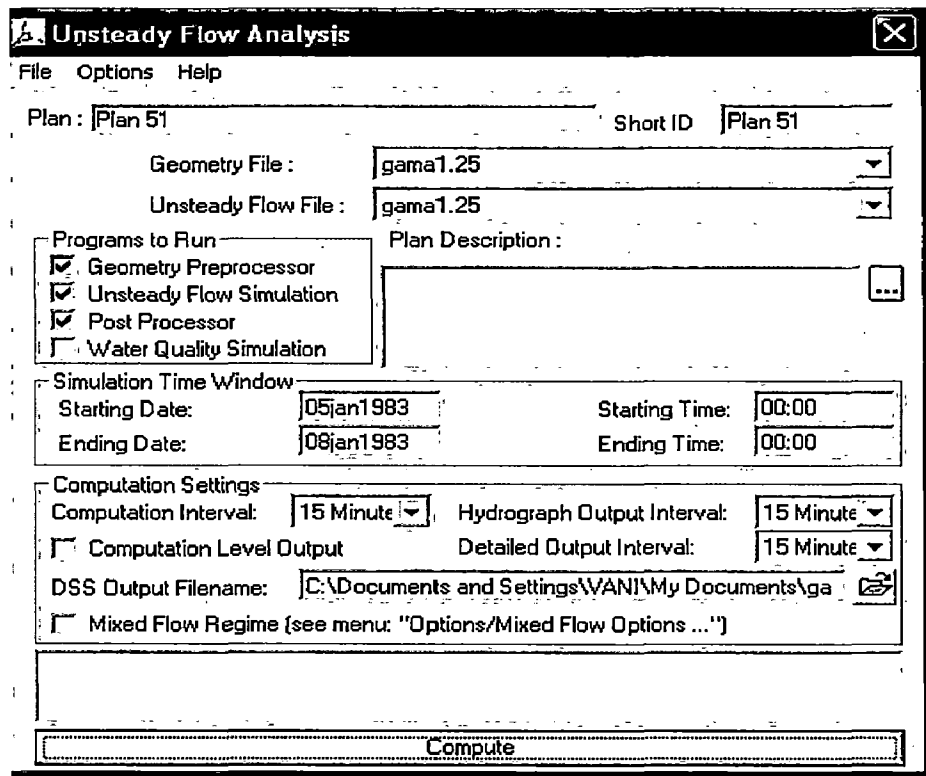


Figure 4.10 Unsteady Flow Analysis Window

Taking the above mentioned flood routing data we route the flood hydrograph, using HEC-RAS. The inflow and the HEC-RAS model routed hydrograph are shown in Figure 4.11.

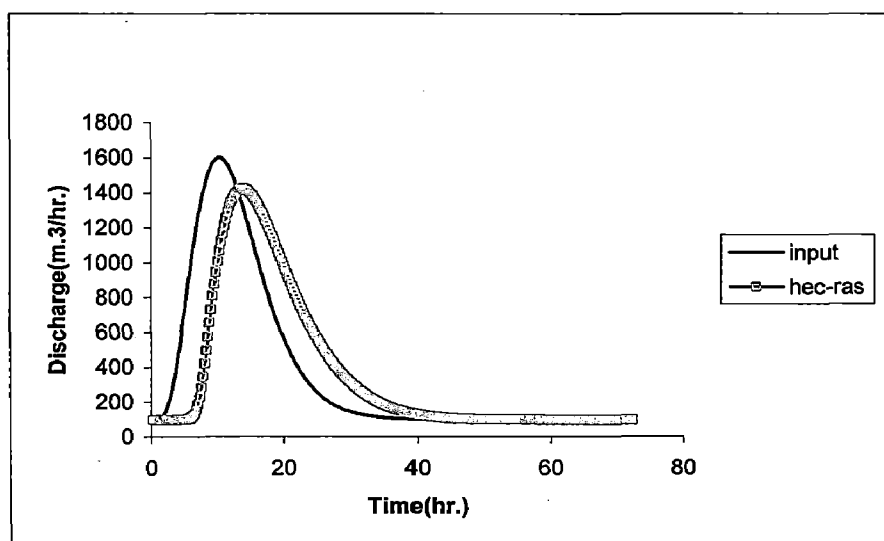


Figure 4.11 Flood Routing using HEC-RAS model

4.5 COMARISON OF HEC-RAS RESULT WITH BOTH OF THE METHODS

As we have got the results using State Space analysis as well as VPMD. Now we can compare the results of these methods using HEC-RAS results. The comparison curve is shown below. On the observation of graph, we can see that the HEC-RAS results and VPMD results are more or less same, as both curves are coinciding while in the case of S.S. curve there is an early rise and the peak is under-estimated. But in the recession limb all the results are coinciding very well.

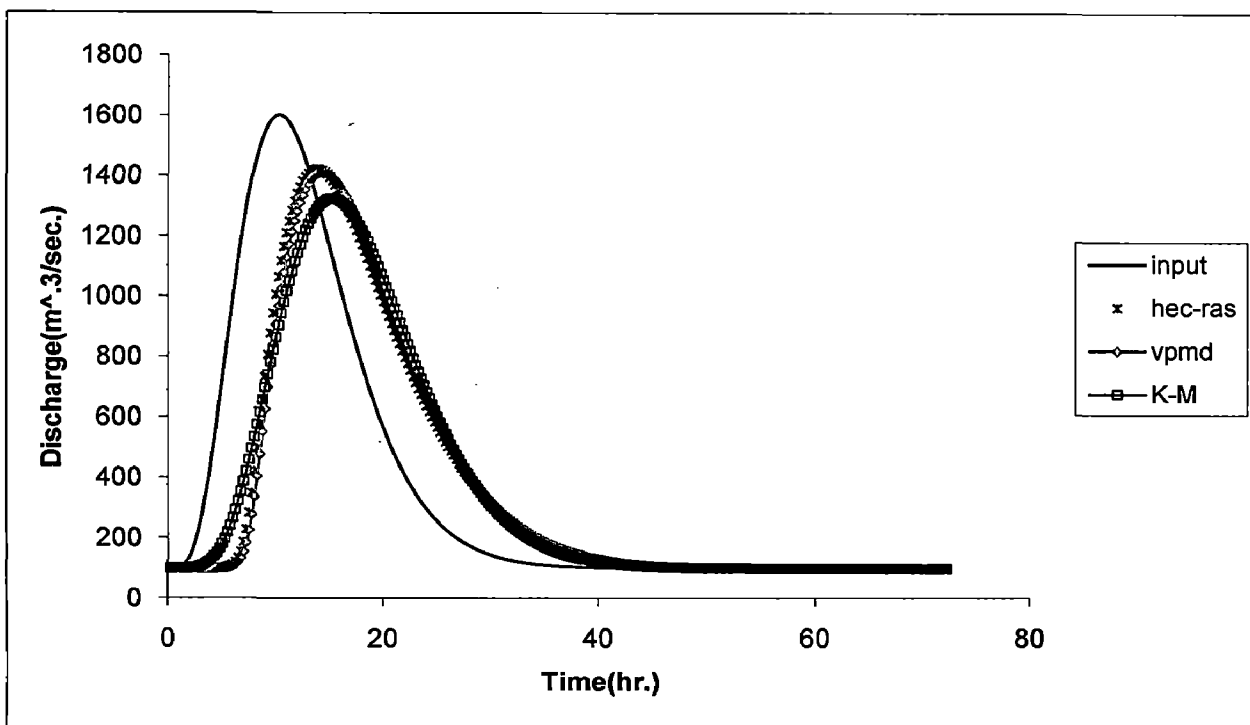


Figure 4.12 Comparison of both of the methods using HEC-RAS

4.6 EVALUATION CRITERIA

The following evaluation criteria were adopted for verifying the efficiency of the K-M method as well as the VPMD method in simulating the corresponding benchmark solutions:

4.6.1 Variance Explained Criterion

The closeness with which both K-M method and VPMD method reproduces the benchmark solution, including the closeness of shape and size of the hydrograph, can be measured using the criterion of variance explained advocated by Nash and Sutcliffe (1970), popularly known as Nash-Sutcliffe criterion. It is expressed in percentage as:

$$\eta_k (\%) = \frac{(Total variance - Remaining variance)}{Total variance} \times 100\% \quad (4.16)$$

where,

$$Total variance = \frac{1}{N} \sum_{i=1}^N (Q_{oi} - \bar{Q}_{oi})^2 \quad (4.17)$$

$$Remaining variance = \frac{1}{N} \sum_{i=1}^N (Q_{oi} - Q_{ci})^2 \quad (4.18)$$

In which, Q_{oi} = the i^{th} ordinate of the discharge-hydrograph at the outlet; \bar{Q}_{oi} = mean of the observed discharge-hydrograph at the outlet; Q_{ci} = the i^{th} ordinate of the computed discharge-hydrograph using the K-M and VPMD methods; N = the total number of discharge-hydrograph ordinates to be simulated.

4.6.2 Reproduction of Routed Hydrograph Peak Criterion

Relative error in peak of the routed discharge hydrograph is given as:

$$Q_{pe} = \frac{(Q_{pc} - Q_{po})}{Q_{po}} \times 100 \quad (4.19)$$

where Q_{pe} = the computed peak of the discharge-hydrograph at the outlet, and

Q_{po} = the observed peak of the discharge-hydrograph at the outlet.

A positive value of Q_{pe} indicates overestimation of the peak from the observed value, and a negative value of Q_{pe} indicates the underestimation.

4.6.3 Reproduction of Time of Peak Criterion

Error in time to peak discharge (hours) is given as:

$$t_{pQer}(h) = t(Q_{pe}) - t(Q_{po}) \quad (4.20)$$

where $t(Q_{pe})$ = time corresponding to computed peak discharge at the outlet, and

$t(Q_{po})$ = time corresponding to observed peak stage at the outlet.

4.6.4 Volume Error Criterion

The relative error in the flow volume is expressed as

$$EVOL(\text{in\%}) = \frac{\sum_{i=1}^N Q_{ci} - \sum_{i=1}^N I_i}{\sum_{i=1}^N I_i} \times 100 \quad (4.21)$$

where Q_{ci} is the i^{th} ordinate of the calculated discharge hydrograph; and I_i is the i^{th} ordinate of the inflow discharge hydrograph.

A negative value of EVOL indicates loss of mass and positive value of EVOL indicates gain of mass. A value close to zero indicates mass conservation ability of the method.

4.7 CONCLUSION

This chapter describes the strategy adopted in the evaluation if the routing capability of the K-M method based on state-space formulation reproducing the benchmark solutions given by the HEC-RAS model. Steps involved in the computation of the hydrographs using the Kalinin-Miliyukov method based on state-space analysis and the VPMD methods were described. Besides the steps involved in arriving at the routing solutions using the HEC-RAS model were presented along with typical routing results. Further the criteria adopted for making comparative evaluations of the results of the K-M method and the VPMD method with the corresponding benchmark solutions given by the HEC-RAS model were described.

CHAPTER 5

RESULTS AND DISCUSSION

5.1 GENERAL

Following the strategy described in Chapter-4 for the evaluation of the two simplified hydraulic routing methods considered in this study, viz., the K-M method in state-space formulation and the VPMD method, a total of 120 test runs of channel routing were made for each of these two methods. For each of these test runs, the corresponding benchmark solutions have been obtained using the HEC-RAS model. These results are presented herein and they are analyzed to arrive at an appropriate conclusion about the efficacy of these two methods based on their ability to reproduce the benchmark solutions.

5.2 RESULTS OBTAINED

Table 5.1 shows the details of five sets of input data used in the study for conducting 120 test runs. Each set of input data is characterized by varying inflow hydrograph characteristics, defined by its shape factor (γ), time to peak (t_p), initial flow in the channel (I_0) and inflow hydrograph peak (I_p).

It is seen from Table 5.1, the shape factor of inflow hydrograph varies from 1.05 to 1.5 and that of its peak flow varies from $500 \text{ m}^3/\text{sec}$. to $2000 \text{ m}^3/\text{sec}$. Table 5.2 gives the test runs details with each test run made for each of the input data set considered in Table 5.1 and for each input set there are 24 unique combinations of channel configurations, each characterized by a set of Manning's roughness coefficient (n), channel bed slope (S_0) and bed width (B) of uniform rectangular channel. Manning's roughness values vary from 0.01 to 0.06 and the channel bed slope varies from 0.0001 to

0.001. Two different widths (50 m. and 100 m.) of uniform rectangular channels were used. Thus, corresponding to five sets of input data , a total of 120 runs were formulated each for routing using the K-M method and the VPMD

Table 5.1: Pertinent Inflow Hydrograph Characteristics

Input set	Shape factor	Time to peak t_p	Initial flow Q_0	Peak flow Q_p
1	1.05	10	100	1600
2	1.05	10	100	500
3	1.15	10	100	1600
4	1.25	10	100	1600
5	1.5	10	100	2000

methods, and for obtaining the corresponding benchmark solution using the HEC-RAS model. Table 5.3 presents the summary of results showing the pertinent characteristics of the benchmark solutions, such as magnitude of peak outflow and it's time to peak and the ability to reproduce the same by the K-M and the VPMD methods. Apart from the reproduction of these pertinent characteristics, the ability of these two methods in reproducing the overall shape of the benchmark solutions are measured by the criteria of variance explained estimated by the Nash-Sutcliff criterion and the volume error. These details are also shown for each of these runs estimated.

Figure: 5.1 to 5.6 show the visual description of some of the typical test runs presented in Table 5.3. In all these test runs , the given inflow hydrograph was routed using the VPMD method for a distance of 40 km. Considering the spatial resolution of $\Delta x = 1$ km., except in some cases corresponding to test runs characterized by a small channel bed slope or a high Manning's n or the combination of both. In such cases either the solution by the VPMD method could not be obtained due to the failure of the method in routing the inflow hydrograph or the solution could be obtained considering the entire

40 km. reach as a single reach. No such problem was encountered in any of the test runs while routing using the K-M method. Unless otherwise indicated in Table 5.3, all the benchmark routing solutions were obtained by the HEC-RAS model. A routing interval

Table 5.2: Test Run details

Channel type	Manning's n	Bed slope, S_0	Bed Width	Input set
1*	0.01	0.0001	50	1
2*	0.01	0.0002	50	1
3*	0.01	0.0004	50	1
4*	0.01	0.0005	50	1
5*	0.01	0.0008	50	1
6*	0.01	0.001	50	1
7*	0.02	0.0001	50	1
8*	0.02	0.0002	50	1
9*	0.02	0.0004	50	1
10*	0.02	0.0005	50	1
11*	0.02	0.0008	50	1
12*	0.02	0.001	50	1
13*	0.04	0.0001	50	1
14*	0.04	0.0002	50	1
15*	0.04	0.0004	50	1
16*	0.04	0.0005	50	1
17*	0.04	0.0008	50	1
18*	0.04	0.001	50	1
19*	0.06	0.0001	50	1
20*	0.06	0.0002	50	1
21*	0.06	0.0004	50	1
22*	0.06	0.0005	50	1
23*	0.06	0.0008	50	1
24*	0.06	0.001	50	1
25*	0.01	0.0001	100	2
26*	0.01	0.0002	100	2
27*	0.01	0.0004	100	2
28*	0.01	0.0005	100	2
29*	0.01	0.0008	100	2
30*	0.01	0.001	100	2
31*	0.02	0.0001	100	2
32*	0.02	0.0002	100	2
33*	0.02	0.0004	100	2
34*	0.02	0.0005	100	2
35*	0.02	0.0008	100	2
36*	0.02	0.001	100	2
37*	0.04	0.0001	100	2
38*	0.04	0.0002	100	2

Channel type	Manning's n	Bed slope, S_0	Bed Width	Input set
39*	0.04	0.0004	100	2
40*	0.04	0.0005	100	2
41*	0.04	0.0008	100	2
42*	0.04	0.001	100	2
43*	0.06	0.0001	100	2
44*	0.06	0.0002	100	2
45*	0.06	0.0004	100	2
46*	0.06	0.0005	100	2
47*	0.06	0.0008	100	2
48*	0.06	0.001	100	2
49**	0.01	0.0001	50	3
50	0.01	0.0002	50	3
51	0.01	0.0004	50	3
52	0.01	0.0005	50	3
53	0.01	0.0008	50	3
54	0.01	0.001	50	3
55	0.02	0.0001	50	3
56	0.02	0.0002	50	3
57	0.02	0.0004	50	3
58	0.02	0.0005	50	3
59	0.02	0.0008	50	3
60	0.02	0.001	50	3
61	0.04	0.0001	50	3
62	0.04	0.0002	50	3
63	0.04	0.0004	50	3
64	0.04	0.0005	50	3
65	0.04	0.0008	50	3
66	0.04	0.001	50	3
67	0.06	0.0001	50	3
68	0.06	0.0002	50	3
69	0.06	0.0004	50	3
70	0.06	0.0005	50	3
71	0.06	0.0008	50	3
72	0.06	0.001	50	3
73**	0.01	0.0001	50	4
74	0.01	0.0002	50	4
75	0.01	0.0004	50	4
76	0.01	0.0005	50	4
77	0.01	0.0008	50	4
78	0.01	0.001	50	4
79	0.02	0.0001	50	4
80	0.02	0.0002	50	4
81	0.02	0.0004	50	4
82	0.02	0.0005	50	4
83	0.02	0.0008	50	4
84	0.02	0.001	50	4

Channel type	Manning's n	Bed slope, S_0	Bed Width	Input set
85	0.04	0.0001	50	4
86	0.04	0.0002	50	4
87	0.04	0.0004	50	4
88	0.04	0.0005	50	4
89	0.04	0.0008	50	4
90	0.04	0.001	50	4
91	0.06	0.0001	50	4
92	0.06	0.0002	50	4
93	0.06	0.0004	50	4
94	0.06	0.0005	50	4
95	0.06	0.0008	50	4
96	0.06	0.001	50	4
97**	0.01	0.0001	100	5
98	0.01	0.0002	100	5
99	0.01	0.0004	100	5
100	0.01	0.0005	100	5
101	0.01	0.0008	100	5
102	0.01	0.001	100	5
103	0.02	0.0001	100	5
104	0.02	0.0002	100	5
105	0.02	0.0004	100	5
106	0.02	0.0005	100	5
107	0.02	0.0008	100	5
108	0.02	0.001	100	5
109	0.04	0.0001	100	5
110	0.04	0.0002	100	5
111	0.04	0.0004	100	5
112	0.04	0.0005	100	5
113	0.04	0.0008	100	5
114	0.04	0.001	100	5
115	0.06	0.0001	100	5
116	0.06	0.0002	100	5
117	0.06	0.0004	100	5
118	0.06	0.0005	100	5
119	0.06	0.0008	100	5
120	0.06	0.001	100	5

* → Explicit solutions

** → MIKE-11 solutions

of $\Delta t = 900$ sec. was used in obtaining the routing solutions of the K-M method and VPMD methods.

5.3 DISCUSSION OF RESULTS

It is seen from Table 5.3 that in general the VPMD method is able to reproduce the benchmark solutions more closely than the K-M method, except for those cases for which the VPMD solutions could not be obtained. Failure of the VPMD method to route the given inflow hydrograph in a given channel reach may be attributed to the inapplicability of the method due to the magnitude of $(1/S_0) \partial y / \partial x \geq 0.43$ (Perumal and Sahoo, 2007), where $\partial y / \partial x$ is the longitudinal gradient of the water surface estimated at the inlet of the routing reach. Such cases mostly pertain to routing of inflow hydrographs in channels characterized by very small slope $S_0=0.0001$ and Manning's n ranging from 0.02 to 0.06, and in few cases with $S_0= 0.0002$ and with n = 0.06. The combination of such small bed slopes and high roughness values invariably result in higher $(1/S_0) \partial y / \partial x$ values exceeding the applicability limit of the VPMD method (Perumal and Sahoo, 2007). However, for such cases the K-M method also performs poorly as seen from Table 5.3. As far as the measure of volume conservation is concerned, the K-M method scores better than the VPMD method for almost all the runs with nearly zero volume error. Such a result is expected when using the K-M method as the parameters remain constant in the entire routing. However, the VPMD estimates less than 1% volume error nearly for all the runs except in the cases of routing in very small slopes channels with moderate roughness values (ranging from 0.04 to 0.06). Out of all the successful runs of the VPMD method only in four cases the volume error exceeded > 1% and among these only in one case the volume error estimated was > 2% (i.e. 2.13%). Therefore, for all practical purposes it may be concluded that the VPMD method also conserves mass fully. Unlike in the K-M method, wherein the parameters remain constant, the parameters of the

VPMD method varies at every routing time level and even then the volume error estimated for all the runs may be considered as nearly zero. This feature of the VPMD method suggests that the VPMD method is capable of reproducing the Saint-Venant's solutions closely.

As far as the reproduction of the peak of the benchmark solutions are concerned, the VPMD method demonstrates it's better ability to reproduce these peaks closely from the consideration of it's magnitude and it's timing better than that of the K-M method. It is desirable that the basic model used for flood forecasting should be able to reproduce this feature in off-line mode as close as possible to that of the benchmark model. It is expected that the model which possesses this characteristic may be considered as more suitable to be employed in a flood forecasting model for achieving accurate forecast.

Table 5.3 amply demonstrates the better performance of the VPMD model over that of the K-M method in this regard. Figures 5.1 to 5.6 show the graphical results of some of the typical test runs demonstrating the capability of the VPMD method over that of the K-M method in reproducing the benchmark solutions closely from the consideration of overall reproduction of the benchmark solutions and its peak. It is inferred from the results given in Table 5.3 and shown in Figure 5.1 to 5.6 that the K-M method always underestimates the peak flow of the benchmark model. One of the plausible reasons for the overestimation of the attenuation may be due to early rise of the outflow hydrograph estimated by the K-M method owing to the use of constant parameter values for the entire routing process. The constant parameters of the K-M method imply the use of average reference discharge for their estimation. Therefore, when the magnitude inflow hydrograph ordinates less than that corresponding to average reference discharge are

routed, they arrive at the outlet point earlier than anticipated. To preserve the volume conservation of the K-M method solution, the estimated peak value of the outflow hydrograph needs to be smaller than that of the peak of the benchmark solution.

In some of the test runs (Test run nos. 1-48, 49, 73, 97) the benchmark solutions could not be obtained using the HEC-RAS model due to numerical problems encountered in the solutions. One such a case is shown in Figure 5.6. In such cases either the explicit method or the MIKE-11 model was used to arrive at the error free solutions.

Table 5.3 Results Obtained

Channel type	Explicit solutions		K-M Method		VPMD		K-M Method		VPMD		K-M Method		VPMD	
	Q_p (m ³ /sec.)	t_p (h)	Q_p (m ³ /sec.)	t_p (h)	Q_p (m ³ /sec.)	t_p (h)	Q_p (%)	t_p (h)	Q_p (%)	t_p (h)	Q_p Variance explained	t_p (h)	Q_p Variance explained	t_p (h)
1	1305.550	11.750	1173.100	12.500	1215.019	11.750	-10.145	0.750	-6.934	0.000	97.320	-0.002	98.498	0.749
2	1440.080	11.500	1321.600	12.250	1422.779	12.000	-8.227	0.750	-1.201	0.500	98.365	-0.001	98.756	0.556
3	1565.240	11.250	1429.700	11.750	1552.691	11.500	-8.659	0.500	-0.802	0.250	98.783	0.000	99.086	0.652
4	1578.760	11.250	1451.300	11.750	1571.607	11.500	-8.073	0.500	-0.453	0.250	98.878	-0.001	99.136	0.639
5	1586.670	11.000	1474.900	11.500	1590.953	11.250	-7.044	0.500	0.270	0.250	98.061	0.000	99.200	0.578
6	1590.710	14.750	1403.000	11.750	1594.894	11.250	-11.800	-3.000	0.263	-3.500	91.584	0.000	99.399	0.544
7	1116.560	12.250	881.415	12.750			-21.060	0.500		12.250	94.413	-0.001		
8	1228.380	12.250	1086.300	13.250	1192.645	12.500	-11.566	1.000	-2.909	0.250	96.702	-0.001	98.352	0.270
9	1426.140	12.000	1279.400	12.750	1406.247	12.500	-10.289	0.750	-1.395	0.500	97.865	0.000	98.729	0.697
10	1471.050	12.000	1318.200	12.750	1468.389	12.250	-10.391	0.750	-0.181	0.250	98.012	0.000	98.846	0.771
11	1560.470	11.750	1394.700	12.250	1547.054	12.000	-10.623	0.500	-0.860	0.250	98.262	-0.001	99.006	0.817
12	1560.700	11.500	1412.300	12.250	1566.741	11.750	-9.509	0.750	0.387	0.250	98.351	0.000	99.058	0.798
13	908.600	13.250	661.210	13.250			-27.228	0.000		13.250	89.842	-0.086		
14	995.550	13.250	817.524	14.750	863.743	13.000	-17.882	1.500	-13.240	-0.250	93.722	0.000	97.981	0.035
15	1190.510	13.250	1040.500	14.500	1186.314	13.250	-12.600	1.250	-0.352	0.000	96.419	-0.002	98.076	0.167
16	1210.410	13.000	1107.100	14.250	1188.030	13.750	-8.535	1.250	-1.849	0.750	96.940	-0.001	98.182	0.603
17	1388.480	12.750	1287.600	13.000	1389.588	13.250	-7.265	0.250	0.080	0.500	95.582	0.000	98.616	0.883
18	1489.340	12.750	1278.500	13.500	1456.488	13.000	-14.157	0.750	-2.206	0.250	97.365	0.000	98.703	0.982
19	787.370	13.750	581.335	13.750			-26.168	0.000		13.750	88.394	-0.309		
20	853.320	14.000	671.729	15.750			-21.281	1.750		14.000	91.912	-0.013		
21	989.370	14.000	868.852	15.750	1000.401	13.750	-12.181	1.750	-1.115	-0.250	95.179	0.000	93.088	-0.475
22	1109.560	14.000	1051.700	13.500	1091.543	14.250	-5.215	-0.500	-1.624	0.250	86.383	-0.001	94.539	-0.085
23	1206.690	13.750	1599.800	10.000	1203.407	14.250	32.578	-3.750	-0.272	0.500	92.288	0.000	98.225	0.685
24	1302.800	13.500	1166.900	14.500	1307.804	14.000	-10.431	1.000	0.384	0.500	96.885	-0.001	98.416	0.875

Channel type	Explicit solutions		K-M Method		VPMD		K-M Method		VPMD		K-M Method		VPMD	
	Q_p (m ³ /sec.)	$t_b(h)$	Q_p (m ³ /sec.)	$t_p(h)$	Q_p (m ³ /sec.)	$t_b(h)$	Q_p (%)	$t_b(h)$	Q_p (%)	$t_b(h)$	Q_p Variance explained	EVOL (%)	Q_p Variance explained	EVOL (%)
25	398.064	13	384.8867	13	375.3746	14.25	-3.3103	0	-5.7	1.25	83.6147	-1.06E-06	98.0122	0.3629
26	455.0071	12.75	401.9445	14	454.2383	13.5	-11.662	1.25	-0.169	0.75	97.9786	-1.77E-06	98.5339	0.5424
27	487.9199	12.25	445.265	12.75	488.3743	12.75	-8.7422	0.5	0.0931	0.5	95.3847	3.53E-07	98.7289	0.5323
28	492.8193	12	449.3113	13.25	492.9839	12.5	-8.8284	1.25	0.0334	0.5	96.109	6.06E-07	96.8189	0.4342
29	497.6334	11.75	456.5391	12	497.6235	12.25	-8.2579	0.25	-0.002	0.5	92.868	-2.12E-06	98.894	0.4422
30	498.803	11.5	446.2038	12.25	498.7444	12	-10.546	0.75	-0.013	0.5	97.5115	7.07E-07	98.9924	0.4118
31	322.3891	14.75	331.981	14	375.3746	14.25	2.9753	-0.75	16.435	-0.5	70.4868	-9.76E-04	78.2316	0.3629
32	386.8347	14.5	370.6162	14.75	374.219	15.5	-4.1926	0.25	-3.261	1	91.1446	-3.53E-07	98.1574	0.4623
33	452.8677	13.75	406.4399	14.25	454.0324	14.25	-10.252	0.5	0.2572	0.5	94.5324	3.53E-07	98.3153	0.6754
34	468.1943	13.25	421.7037	14.25	469.0694	13.75	-9.9298	1	0.1869	0.5	96.0849	1.41E-06	98.2914	0.6919
35	487.7389	12.75	431.0862	13.5	487.9469	13	-11.615	0.75	0.0426	-0.25	94.6802	3.53E-07	99.1388	0.664
36	492.4197	12.5	426.5251	13.75	492.3771	13	-13.382	1.25	-0.009	0.5	96.1134	-1.41E-06	98.5223	0.6324
37	253.2919	16.75	286.5159	14.5	198.4877	18.5	13.117	-2.25	-21.64	1.75	36.3045	-0.0603	85.3073	-1.2081
38	302.8938	16.75	295.6741	16.5	277.7507	18.25	-2.3836	-0.25	-8.301	1.5	82.9445	-0.0026	97.5818	0.1117
39	379.7302	16	353.8201	16.75	376.0649	16.5	-6.8233	0.75	-0.965	0.5	94.5522	-3.02E-06	98.5134	0.5832
40	405.8267	15.5	365.9545	16.25	405.1302	16.25	-9.8249	0.75	-0.172	0.75	94.4105	-6.04E-07	98.0673	0.7244
41	452.3537	14.75	399.3686	15.75	454.5009	15.25	-11.713	1	0.4747	0.5	96.2724	-9.06E-07	97.8293	0.8684
42	468.544	14.25	405.7649	15.25	463.7971	14.75	-13.399	1	-1.013	0.5	95.7589	-1.51E-06	98.0272	0.8262
43	220.9582	18	252.0027	16	315.1274	19	14.05	-2	42.619	1	71.3618	-0.1397	74.9468	0.4481
44	257.7348	18.5	261.8399	17.75	225.2119	21	1.5928	-0.75	-12.62	2.5	75.3144	-0.0445	93.3332	-0.132
45	326.7196	17.75	307.6998	18.25	315.1274	19	-5.8214	0.5	-3.548	1.25	90.0768	-3.36E-04	97.8308	0.4481
46	353.9019	17.25	331.2009	18.25	348.2933	18.25	-6.4145	1	-1.585	1	94.0601	-1.34E-05	97.9919	0.604
47	411.7773	16.25	364.1478	17.25	413.5505	17	-11.567	1	0.4306	0.75	95.1441	-3.53E-07	97.9098	0.753
48	435.8874	15.75	379.2578	17	438.7498	16.25	-12.992	1.25	0.6567	1	96.4513	-1.51E-06	97.5698	0.9691

Channel type	HEC-RAS solutions			K-M Method			VPMD			K-M Method			VPMD			K-M Method			VPMD		
	Q _p (m ³ /sec.)	t _b (h)	Q _p (m ³ /sec.)	t _b (h)	Q _p (m ³ /sec.)	t _b (h)	Q _p (%)														
49	1436.58	11.75	1340	13	1383.8054	12.25	-6.7229	1.25	-3.674	0.5	98.5575	-0.0011	99.1839	0.1309							
50	1517.62	11.75	1457.7	12.75	1529.8688	12	-3.9483	1	0.8071	0.25	99.0639	-1.6E-14	99.5995	0.2552							
51	1566.68	11.25	1503.9	12.75	1583.5892	11.5	-4.0072	1.5	1.0793	0.25	99.244	1.14E-04	99.6952	0.3077							
52	1574.9	11.25	1515.3	12	1590.2855	11.5	-3.7844	0.75	0.9769	0.25	99.3168	-2.28E-04	99.7054	0.2985							
53	1583.42	11	1529.4	11.75	1596.9415	11.25	-3.4116	0.75	0.8539	0.25	99.4527	3.41E-04	99.7168	0.2669							
54	1588.11	11	1516.2	12.25	1598.2534	11.25	-5.1254	1.25	0.009	0.25	93.3756	-6.83E-04	99.2708	0.2504							
55	1269.48	12.5	1122.7	14			-13.604	1.5	-100	-12.5	96.5159	-0.0014									
56	1398.49	12.5	1318.4	14	1356.7139	13	-5.7269	1.5	-2.987	0.5	98.0576	-9.10E-04	99.2122	0.085							
57	1503.14	12.25	1418.8	13.25	1523.0812	12.5	-5.6109	1	1.3266	0.25	98.6228	-6.83E-04	99.594	0.341							
58	1527.76	12	1442	13	1550.5944	12.25	-5.6134	1	1.4946	0.25	98.7001	-1.6E-14	99.6352	0.378							
59	1560.38	11.75	1476.3	12.75	1581.4735	12	-5.3884	1	1.3518	0.25	98.8458	-3.41E-04	99.6809	0.387							
60	1568.72	11.5	1482.1	12.5	1588.6113	11.75	-5.5217	1	1.268	0.25	98.8883	3.31E-14	99.6918	0.3733							
61	1133.98	13.5	902.6274	15			-20.402	1.5	-100	-13.5	92.4904	-0.0841									
62	1221.74	13.5	1095.5	15.5	1108.6975	13.5	-10.333	2	-9.253	0	96.0877	-1.14E-04	97.9407	0.4056							
63	1356.74	13.5	1269.1	15	1329.2648	14	-6.4596	1.5	-2.025	0.5	97.6457	1.14E-04	99.206	0.0991							
64	1403.93	13.25	1321.9	14.75	1406.0679	13.75	-5.8429	1.5	0.1523	0.5	97.8583	-7.97E-04	99.3967	0.2404							
65	1487.38	12.75	1389.1	14.25	1515.6625	13.25	-6.6076	1.5	1.9015	0.5	98.0471	-6.83E-04	99.5656	0.449							
66	1515.94	12.75	1412.1	14	1545.6217	12.75	-6.8499	1.25	1.958	0	98.0848	1.14E-04	99.6024	0.4892							
67	1028.26	14.25	801.2654	15.75			-22.076	1.5	-100	-14.25	90.4614	-0.3443									
68	1101.7	14.25	937.714	16.5			-14.885	2.25	-100	-14.25	94.4103	-0.0339									
69	1233.25	14.25	1122.4	16.25	1203.1866	14.25	-8.9884	2	-2.438	0	96.6384		98.2085	-0.1601							
70	1286.16	14.25	1199.7	16.25	1234.9213	14.75	-6.7223	2	-3.984	0.5	97.0081	-2.28E-04	98.9032	8.28E-04							
71	1399.11	13.75	1302.3	15.25	1415.3475	14.25	-6.9194	1.5	1.1606	0.5	97.5849	-5.6E-04	99.4066	0.3338							
72	1445.65	14	1346.3	15	1474.6891	14.5	-6.8723	1	2.0087	0.5	97.6724	-1.66E-14	99.4896	0.4568							

Channel type	HEC-RAS solutions		K-M Method		VPMD		K-M Method		VPMD		K-M Method		VPMD	
	Q _p (m ³ /sec.)	t _p (h)	Q _p (m ³ /sec.)	t _p (h)	Q _p (m ³ /sec.)	t _p (h)	Q _p (%)	t _p (h)	Q _p (%)	t _p (h)	Q _p Variance explained	EVOL (%)	Q _p Variance explained	EVOL (%)
73	1477.85	11.25	1387.8	12.25	1446.9674	11.5	-6.0933	1	-2.09	0.25	98.7857	-6.62E-04	98.5029	0.2245
74	1545.04	12	1526.7	13.25	1595.4213	12.5	-1.1187	1.25	3.2608	0.5	98.9521	-6.89E-14	99.7443	0.1791
75	1579.45	11.75	1518.5	12	1590.0872	11.75	-3.8589	0.25	0.6735	0	99.3347	-6.62E-04	99.7984	0.2245
76	1584.71	11.25	1526.7	12	1555.6925	12	-3.6606	0.75	-1.831	0.75	99.5297	0.2843	99.8035	0.218
77	1589.9	11	1527.1	11.75	1598.6495	11.5	-3.9499	0.75	0.5503	0.5	99.4287	9.46E-05	99.8065	0.195
78	1598.89	11	1545.9	12.5	1598.9734	11.25	-3.3142	1.5	0.0052	0.25	94.1723	-5.68E-04	99.8408	0.1828
79	1360.81	12.75	1215.2	14.5	1249.4503	13	-10.7	1.75	-8.183	0.25	97.0193	0.0023	98.4397	1.2096
80	1450.92	12.75	1383.5	14	1428.9918	13	-4.6667	1.25	-1.511	0.25	98.5431	6.62E-04	99.5143	-0.0413
81	1536.4	12.25	1461.4	13.5	1551.4775	12.5	-4.8815	1.25	0.9814	0.25	98.8098	-9.46E-05	99.7414	0.2448
82	1553.94	12	1477.6	13.25	1569.4318	12.25	-4.9127	1.25	0.9969	0.25	98.8669	-3.79E-04	99.7651	0.275
83	1575.8	11.75	1504.4	12.75	1588.7791	12	-4.531	1	0.8237	0.25	99.024	-3.79E-04	99.79	0.2834
84	1580.93	11.5	1512.1	12.5	1593.1497	11.75	-4.3538	1	0.7729	0.25	99.1024	9.46E-05	99.7956	0.2736
85	1214.67	13.75	1004	16		-0.75	-17.344	2.25	-100	-14.5	92.8265	-0.1148		
86	1299.16	14	1184.2	16	1204.9352	14	-8.8488	2	-7.253	0	96.7704	0.0032	98.6911	-0.1268
87	1422.38	13.5	1325.5	15.25	1410.2649	14	-6.8111	1.75	-0.852	0.5	97.9246	-9.64E-14	99.5075	0.002
88	1461.49	13.5	1367.4	15	1469.285	13.75	-6.438	1.5	0.5334	0.25	98.1178	-3.79E-04	99.6216	0.1503
89	1526.77	13	1430.6	14.25	1546.7968	13.25	-6.2889	1.25	1.3117	0.25	98.2947	-5.68E-04	99.7252	0.3273
90	1546.79	12.75	1447.1	14	1566.3173	12.75	-6.445	1.25	1.2624	0	98.3166	-1.89E-04	99.7464	0.3586
91	1118.99	14.5	2884.8	17		-0.75	157.8	2.5	-100	-15.25	94.2537	-5.63E-04		
92	1192.7	14.75	1046.5	16.75		-0.75	-12.258	2	-100	-15.5	95.5233	-0.0569		
93	1317.19	14.5	1205.8	16.75	1247.4371	15.25	-8.4566	2.25	-5.296	0.75	96.9818	-9.46E-04	98.9305	-0.2877
94	1364.66	14.25	1276.7	16.25	1335.0833	15	-6.4456	2	-2.167	0.75	97.565	-6.62E-04	99.3265	-0.1287
95	1460.41	14	1370.2	15.5	1476.5696	14.25	-6.177	1.5	1.1065	0.25	97.8852	-1.89E-04	99.6279	0.2309
96	1496.62	13.75	1396.2	15.25	1519.0813	14	-6.7098	1.5	1.5008	0.25	97.8669	-1.89E-04	99.6796	0.3322

Channel type	HEC-RAS solutions			K-M Method			VPMD			K-M Method			VPMD			K-M Method			VPMD		
	Q _p (m ³ /sec.)	t _p (h)	Q _p (m ³ /sec.)	t _p (h)	Q _p (m ³ /sec.)	t _p (h)	Q _p (%)	t _p (h)	Q _p Variance explained (%)	EVOL (%)	Q _p Variance explained (%)	EVOL (%)									
97	1904.85	12.5	1782.8	14	1908.5269	12.75	-6.4073	1.5	0.193	0.25	98.2865	-0.0084	99.7056	-0.038							
98	1967.07	12	1844	13.25	1978.0092	12.25	-6.2565	1.25	0.5561	0.25	98.41	-0.0049	99.8389	0.2289							
99	1988.08	11.5	1890.8	12.75	1995.2297	11.75	-4.8932	1.25	0.3596	0.25	98.7606	-0.0034	99.8644	0.2637							
100	1990.3	11.25	1903.7	12.5	1997.0804	11.5	-4.3511	1.25	0.3407	0.25	98.909	-0.0028	99.8647	0.2559							
101	1991.13	11	1924.1	12.25	1998.9261	11.5	-3.3664	1.25	0.3915	0.5	99.1693	-0.0028	99.862	0.2283							
102	2086.6	12.75	1917	12.5	1999.5106	11.25	-8.1281	-0.25	-4.174	-1.5	98.9933	-0.0028	99.0143	0.213							
103	1784.7	13.5	1610.6	15.75	1710.1613	14.25	-9.7551	2.25	-4.177	0.75	96.8538	-0.0395	99.1138	-0.6997							
104	1894.88	13	1755.7	15	1906.5183	13.5	-7.3451	2	0.6142	0.5	97.7663	-0.0112	99.7183	0.0334							
105	1964.31	12.75	1825	14.25	1977.3784	12.5	-7.0921	1.5	0.6653	-0.25	97.834	-0.0076	99.9751	0.3053							
106	1974.58	12.5	1831.3	14	1985.6736	12.75	-7.2562	1.5	0.5618	0.25	97.8785	-0.0067	99.8445	0.3316							
107	1985.61	11.75	1845.7	13.25	1998.9261	11.5	-7.0462	1.5	0.6706	-0.25	97.9941	-0.0056	98.7297	0.2283							
108	1988.55	11.75	1859	13.25	1996.6317	12	-6.5148	1.5	0.4064	0.25	98.1791	-0.005	99.8583	0.3297							
109	1621.06	14.75	1408.3	17.5	1414.2179	15.5	-13.125	2.75	-12.76	0.75	94.3458	-0.2835	96.2234	-0.1256							
110	1747.32	14.75	1612.5	17.25	1691.2604	15.5	-7.7158	2.5	-3.208	0.75	96.5711	-0.041	99.1264	-0.7038							
111	1886.16	14	1724.3	16.25	1905.3225	14.25	-8.5815	2.25	1.016	0.25	96.7179	-0.0157	99.7188	0.1267							
112	1918.97	13.75	1754.1	15.75	1939.5754	13.75	-8.5916	2	1.0738	0	96.8194	-0.0128	99.772	0.2637							
113	1961.59	13	1958.2	11.75	1977.0414	13.25	-0.1728	-1.25	0.7877	0.25	85.5273	-0.0021	99.8199	0.4167							
114	1971.74	12.75	1972.4	11.5	1985.5073	13	0.0335	-1.25	0.6982	0.25	85.4427	-0.0011	99.8297	0.4462							
115	1511.19	15.75	1335.4	19.25	-0.75	-11.633	3.5	-100	-16.5	92.8207	-0.5621										
116	1630.88	15.75	1868.4	13	1483.5491	17	14.564	-2.75	-9.034	1.25	57.6561	-0.0045	97.7088	-1.3668							
117	1794.96	15.25	1972.4	11.5	1796.1703	15.75	9.9855	-3.75	0.0674	0.5	50.507	-0.0011	99.5038	-0.2371							
118	1918.97	13.75	1754.1	15.5	1939.5754	13.5	-8.5916	1.75	1.0738	-0.25	95.9384	-0.0245	99.6442	0.0279							
119	1924.25	14	1873.5	13	1946.7969	14.25	-2.6374	-1	1.1717	0.25	84.8323	-0.0047	99.7714	0.3683							
120	1946.79	13.75	1895	12.75	1966.3855	13.75	-2.6603	-1	1.0066	0	85.5914	-0.0034	99.7948	0.4555							

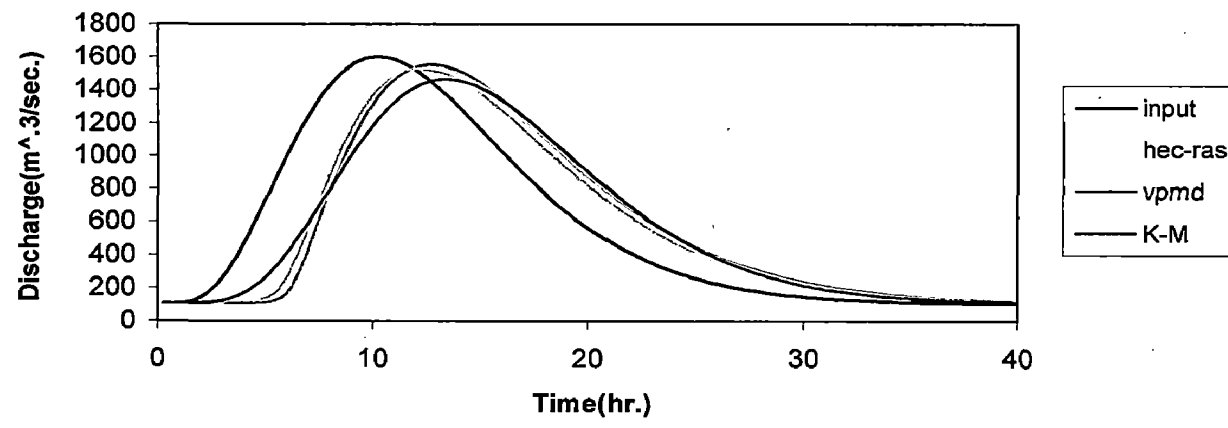


Figure 5.1 Routing Results of Test Run No. 81

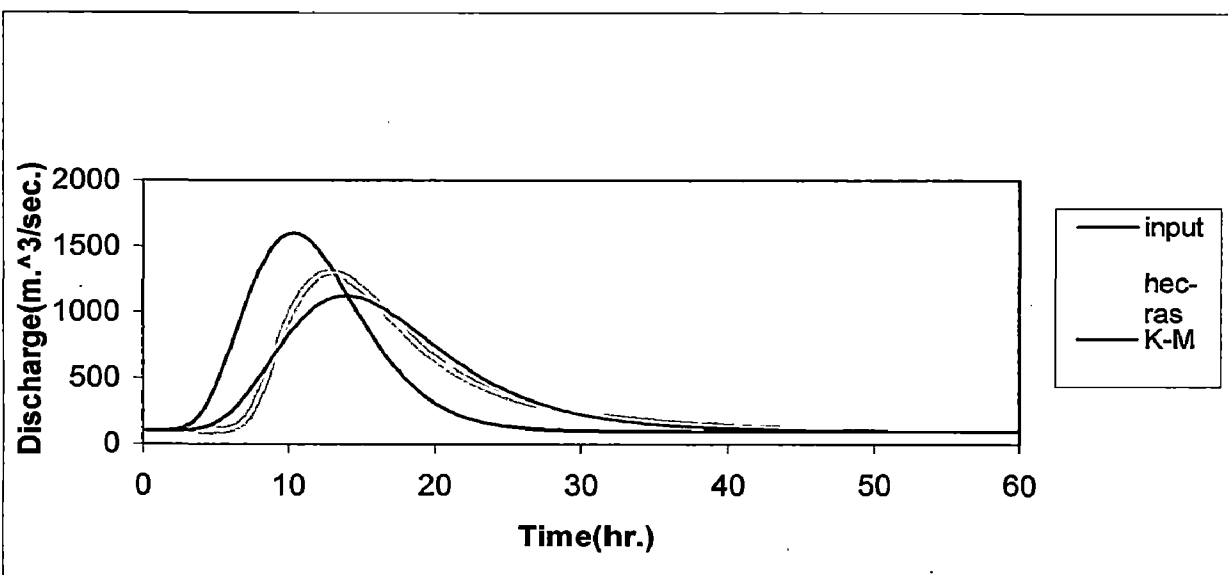


Figure 5.2 Routing Results of Test Run No. 55

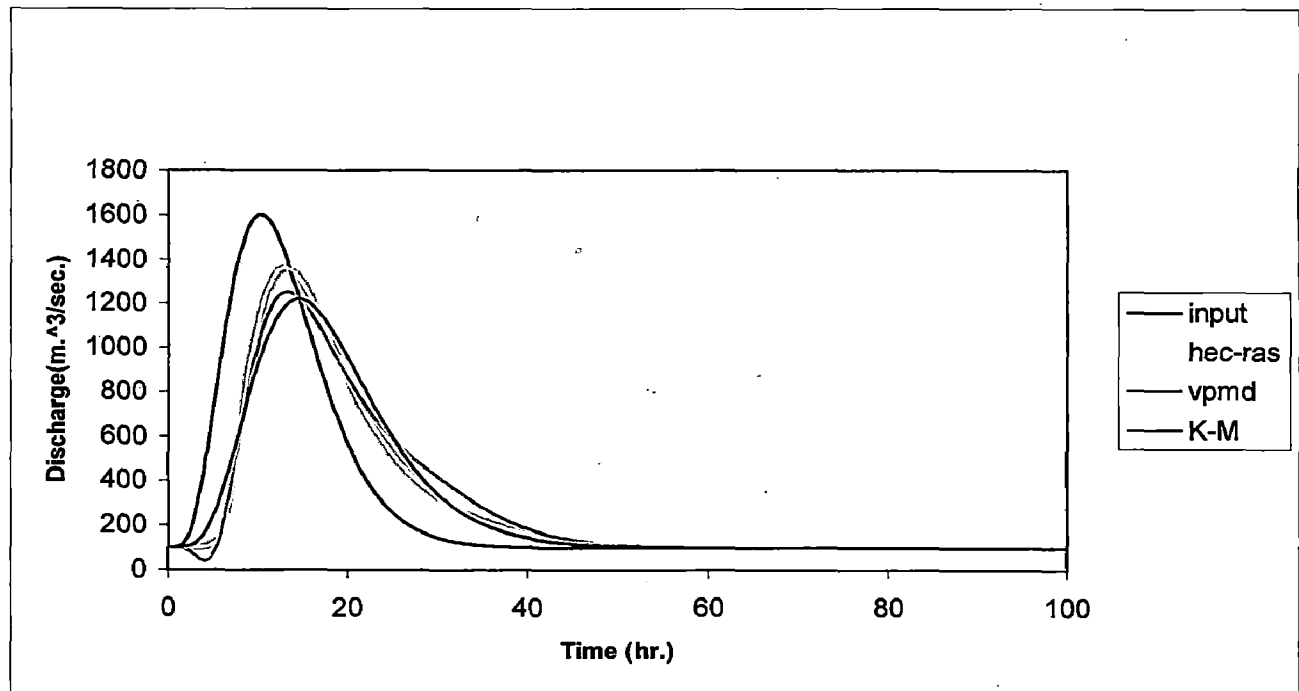


Figure 5.3 Routing Results of Test Run No. 79

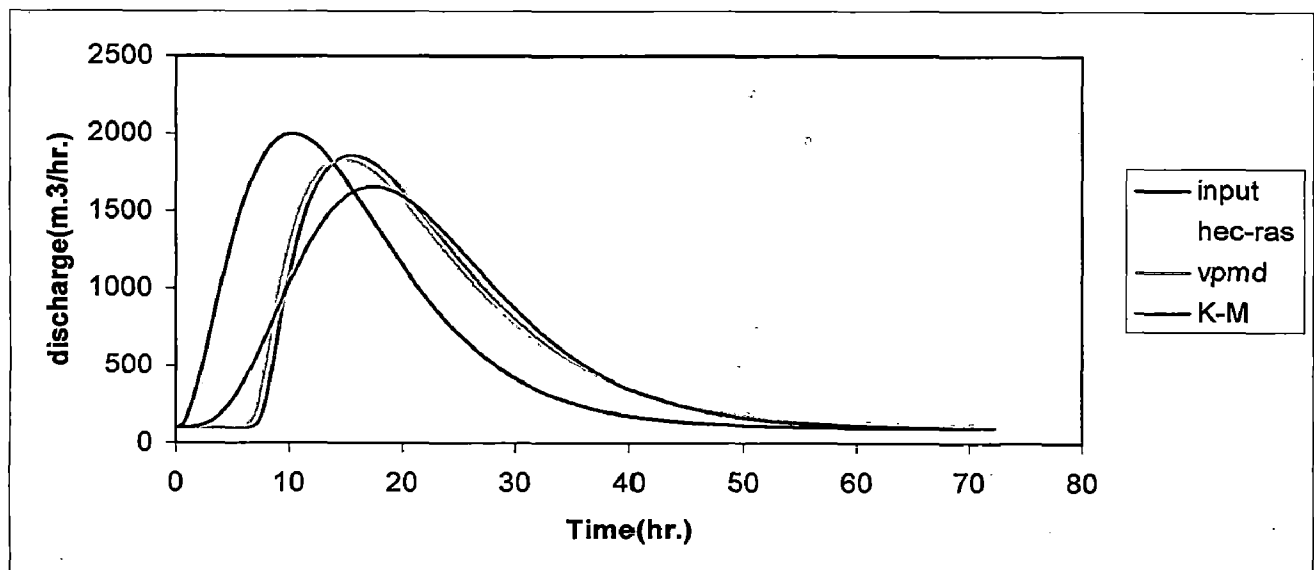


Figure 5.4 Routing Results of Test Run No. 118

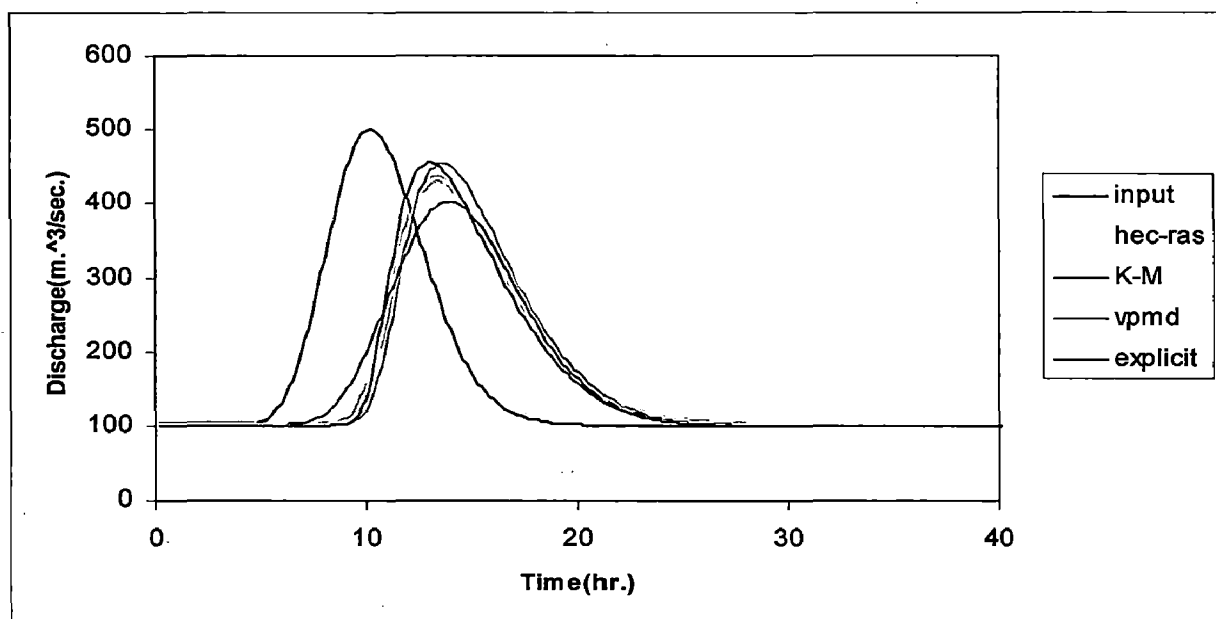


Figure 5.5 Routing Results of Test Run No. 25

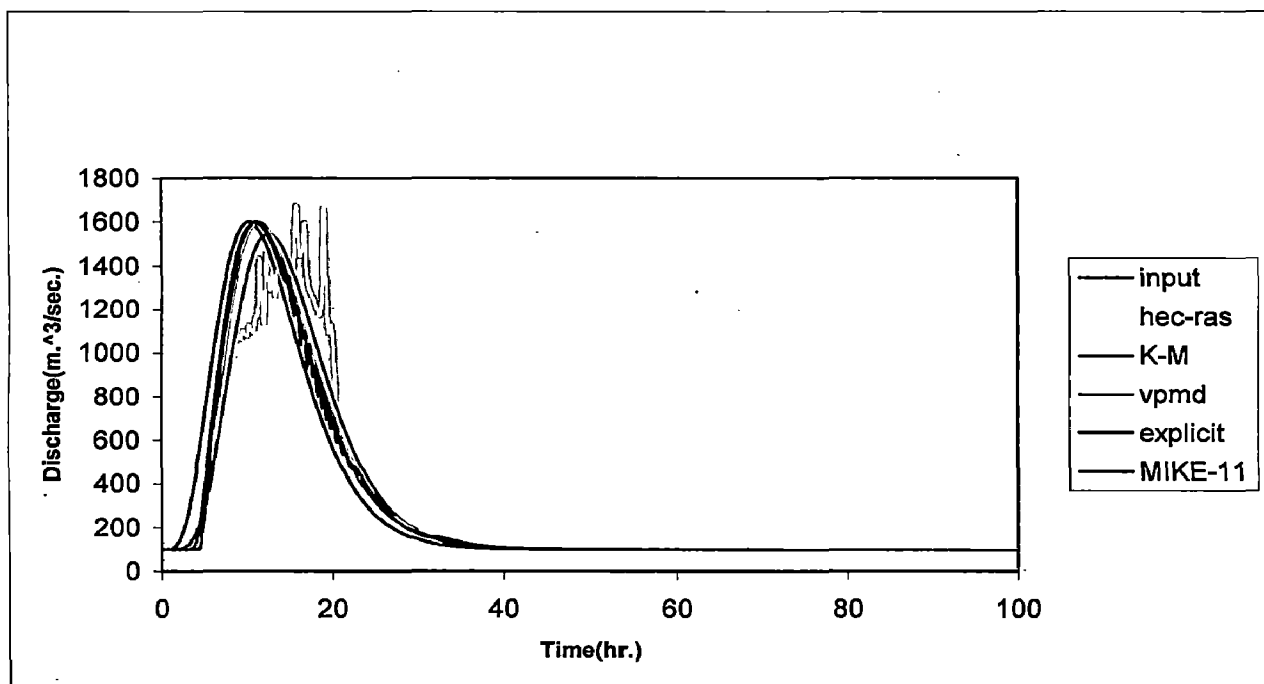


Figure 5.6 Routing Results of Test Run No. 78

5.4 CONCLUSION

It may be inferred from the above discussion that in general the Variable Parameter Muskingum Discharge routing method is able to reproduce the benchmark solutions closely, from the perspective of overall reproduction and the peak discharge reproduction better than that of the K-M routing method developed based on the state-space analysis approach. It is surmised that this inference may also holds good when these models are used in real-time operation mode when applied for practical flood forecasting problems.

CHAPTER 6

CONCLUSIONS

6.1 GENERAL

The study was taken up on the premise that in any real-time flood forecasting model it is desirable to employ a physically based basic model to describe the physical behavior of the system from the remaining part which describe the structure of the residuals; and the parameter of the "physical" part of the model should be estimated independently of those of the residual component in order to reduce the domination of the residual component model over the basic model. While this concept is difficult to introduce in a flood forecasting model dealing with rainfall-runoff transformation process; it is amenable for incorporating in hydrometric data based flood forecasting models, mainly dealing with flood routing process only.

Accordingly the emphasis of the study was on the use of such a physically based routing model *viz.* the VPMD method (Perumal, 1994a) as a replacement of the well known linear theory based routing model *viz.*, the Kalinin-Miliyukov method in state-space formulation, as advocated by Szollosi-Nagy (1976 and 1982). It is considered logical that among these two methods, the one which is capable of closely reproducing the past observed flood hydrograph at the point of forecast interest, routing the corresponding recorded inflow hydrograph in off-line mode may be considered as the best model to be employed in a forecasting model; on this consideration a strategy was formulated for evaluating the performance of the two methods by routing hypothetical inflow hydrographs in hypothetical uniform rectangular channel reaches for a routing reach length of 40 km and the solutions obtained by these routing methods were

compared with the corresponding solutions of a benchmark model to evaluate their ability to closely reproduce these benchmark solutions.

6.2 CONCLUSIONS

Accordingly a total of 120 hypothetical test runs were made in simulating the HEC-RAS model routed solutions (benchmark solutions) by these two routing methods. Based on these simulations results, the following conclusions may be arrived at:

1. The Variable Parameter Muskingum Discharge routing method is able to reproduce the benchmark solutions more closely than the Kalini-Miliyukov method based on state-space analysis approach in all aspects of reproduction such as variance explained, peak discharge reproduction and time to peak discharge reproduction, and
2. While the VPMD failed in some cases of routing due to the inapplicability of the method in small slope channel reaches or in channel reaches with high Manning's roughness or in channel with combination of these characteristics, the K-M method did not fail, though it resulted in poor reproduction of the benchmark solutions. This implies that the use of simplified flood routing models under such channel conditions may be inappropriate to use, and one needs to use an improved routing models instead.

6.3 RECOMMENDATION FOR FURTHER STUDY

It needs to be tested whether one may arrive at the same conclusion when these two methods are used in online mode, i.e. when they are applied for real-time forecasting purpose. Further study may be taken up to test this aspect.

REFERENCES

1. Abebe, A. J., and R. K. Price (2004), Information theory and neural networks for managing model uncertainty in flood routing, *J. Computing in Civil Engineering, ASCE*, 18(4), 373–380.
2. Akan, A. O., and B. C. Yen (1977), A nonlinear diffusion-wave model for unsteady
3. Apollov, B. A., G. P. Kalinin, and V. D. Komarov (1964), Hydrological forecasting, translated from Russian, Israel Program for Scientific Translations, Jerusalem.
4. Arnold, J. G., and N. Fohrer (2005), SWAT2000: current capabilities and research opportunities in applied watershed modeling, *Hydrol. Process.*, 19, 563–572.
5. Barré de Saint-Venant, A. J. C. (1871a), Théorie du Mouvement Non Permanent des Eaux, avec Application aux Crues de Rivières et à l'Introduction des Marées dans leur Lit, *Comptes Rendus des séances de l'Académie des Sciences, Paris, France*, 73(4), 237-240 (in French).
6. Barré de Saint-Venant, A. J. C. (1871b), Théorie et Equations Générales du Mouvement Non Permanent des Eaux Courantes, *Comptes Rendus des séances de l'Académie des Sciences, Paris, France, Séance*, 73(17 July), 147–154 (in French).
7. Bates, B. C., and D. H. Pilgrim (1983), Investigation of storage-discharge relations for river reaches and runoff routing models, *Civ. Eng. Trans., 25, Inst. Engrs., Australia*, 153–161.

8. Bates, B. C., and M. Sivapalan (1990), A generalized diffusion wave flood routing model, in *Hydraulic Engineering*, Vol. I, Proceedings 1990 National Conference on Hydraulic Engineering, H. H. Chang, and J. C. Hill (Eds.), Am. Soc. Civ. Engrs., New York, 545–550.
9. Bazartseren, B., G. Hildebrandt, and K. -P. Holz (2003), Short-term water level prediction using neural networks and neuro-fuzzy approach, *Neurocomputing*, 55(3–4), 439–450.
10. Birikundavyi, S., R. Labib, H. T. Trung, and J. Rousselle (2002), Performance of neural networks in daily streamflow forecasting, *J. Hydrol. Eng., ASCE*, 7(5), 392–398.
11. Chang, F., and Y. Chen (2003), Estuary water-stage forecasting by using radial basis function neural network, *J. Hydrol.*, 270, 158–166.
12. Chau, K. W. (2002), Calibration of flow and water quality modeling using genetic algorithms, *Lecture Notes in Artificial Intelligence*, Vol. 2557, 720–720.
13. Chau, K. W., and C. T. Cheng (2002), Real-time prediction of water stage with artificial neural network approach, *Lecture Notes in Artificial Intelligence*, Vol. 2557, 720–720.
14. Chow, V. T. (1959), *Open Channel Hydraulics*, McGraw Hill, New York, USA.
15. Cunge, J. A. (1969), On the subject of a flood propagation method (Muskingum Method), *J. Hydraul. Res., IAHR*, 7(2), 205–230.
16. Cunge, J. A., F. M. Holly, Jr., and A. Verwey (1980), *Practical Aspects of Computational River Hydraulics*, Pitman Publishing Limited, London,
ISBN:0273084429.

17. Dawson, C. W., and R. Wilby (1998), An artificial neural network approach to rainfall-runoff modeling, *Hydrol. Sci. J.*, 43(1), 47–66.
18. Diskin, M. H. (1967), On the solution of the Muskingum flood routing equation, *J. Hydrol.*, 5, 286–289.
19. Dooge, J. C. I., W. G. Strupczewski, and J. J. Napiorkowski (1982), Hydrodynamic derivation of storage parameters of the Muskingum model, *J. Hydrol.*, 54(4), 371–387.
20. Dooge, J. C. I. (1973), Linear theory of hydrologic systems, USDA, *Agric. Res. Serv., Tech. Bull., No. 1468*.
21. Dooge, J. C. I. (1980), Flood routing in channels, Post Graduate Lecture Notes, Department of Civil Engineering, University College Dublin, Dublin, Ireland.
22. Dooge, J. C. I. (1986), Theory of flood routing, in *River Flow Modeling and Forecasting*, D. A. Kraijenhoff and J. R. Moll (Eds.), D. Reidel Publishing Company, Kluwer Academic Publishers, USA.
23. Dooge, J. C. I., and B. M. Harley (1967), Linear routing in uniform open channel, in *Proc. Int. Hydrol. Symp.* (6–8 September, 1967), Fort Collins, Colorado, USA, Vol. 1, 57–63.
24. Dooge, J. C. I., and J. J. Napiorkowski (1987), Applicability of diffusion analogy in flood routing, *Acta Geophysica Polonica*, 35(1), 66–75.
25. Fernando, D. A. K., and A. W. Jayawardena (1998), Runoff forecasting using RBF networks with OLS algorithm, *J. Hydrol. Eng.*, 3(3), 203–209.
26. Ferrick, M. G. (1985), Analysis of river wave types, *Water Resour. Res.*, 21(2), 209–220.
27. Ferrick, M. G., and Goodman (1998), N. J., Analysis of linear and monoclonal river wave solutions, *J. Hydrol. Eng., ASCE*, 124(7), 728–741.

28. Ferrick, M. G., J. Bilmes, and S. E. Long (1984), Modeling rapidly varied flow in tailwaters, *Water Resour. Res.*, 20(2), 271–289.
29. Fread, D. L. (1975), Computation of stage-discharge relationships affected by unsteady flow, *Water Resour. Bull.*, 11(2), 213–218.
30. Fread, D. L. (1981), Flood routing: a synopsis of past, present, and future capability, in *Proc. Int. Symp. Rainfall-Runoff Modeling*, V. P. Singh (Ed.), Mississippi, USA, 521–541.
31. Fread, D. L. (1985), Applicability criteria for kinematic and diffusion routing models, Laboratory of Hydrology, National Weather Service, NOAA, U.S. Dept. of Commerce, Silver Spring, Md.
32. Fread, D. L. (1990), *DAMBRK: The NWS Dam-Break Flood Forecasting model*, National Weather Service, Office of Hydrology, Silver Spring, Maryland, USA.
33. Gassman, P. W., M. R. Reyes, C. H. Green, and J. G. Arnold (2007), The Soil and Water Assessment Tool (SWAT): Historical development, applications, and future research directions, *Working Paper 07-WP 443*, Center for Agricultural and Rural Development, Iowa State University, Ames, Iowa. < www.card.iastate.edu >
34. Gopakumar, R. and P. P. Mujumdar (2007), A fuzzy dynamic wave routing model, *Hydrological Processes, Wiley InterScience*, (In Print), [M. S. No. HYP-06-0368].
35. Hayami, S. (1951), On the propagation of flood waves, *Bull. Disaster Prevention Research Institute*, Kyoto Univ., Japan, 1(1), 1–16.
36. Henderson, F. M. (1966), *Open Channel Flow*, The Macmillan Co., New York.

37. Iwagaki, Y. (1955), Fundamental studies on the runoff analysis by characteristics, *Bulletin 10*, Disaster Prevention Research Institute, Kyoto University, Kyoto, Japan, 25 p.
38. Jolly, J. P., and V. Yevjevich (1971), Amplification criterion of gradually varied, single peaked waves, *Hydrol. Pap. No. 51*, Colorado State University, Fort Collins, USA.
39. Kalinin, G. P., and P. I. Milyukov (1958), Priblizhennyi raschet neutstanovivshegosya dvizheniya vodnykh mass (Approximate computation of unsteady flow of water masses), *Trudy TSIP*, 66.
40. Katapodes, N. D. (1982), On zero-inertia and kinematic waves, *J. Hydraul. Div. ASCE*, 108(11), 1380–1387.
41. Keefer, T. N., and R. S. McQuivey (1974), Multiple linearization flow routing model, *J. Hydraul. Div., ASCE*, 100(HY7), 1031–1046.
42. Klemeš, V. (1982), Stochastic models of rainfall-runoff relationship, in: statistical analysis of rainfall and runoff, V. P. Singh (Ed.), *Water Resour. Publications*, Littleton, Colorado.
43. Klemeš, V. (1986), Dilettantism in hydrology: transition or destiny?, *Water Resour. Res.*, 22(9), 177S–188S.
44. Klemeš, V. (1988), A hydrological perspective, *J. Hydrol.*, 100(1), 3–28.
45. Koussis, A. D. (1975), Improved method for approximate flood routing computations (in German), *Techn. Bericht Nr. 15*, Inst. Fuer Hydraulik and Hydrologie, TH Darmstadt, Germany.
46. Koussis, A. D. (1976), An approximate dynamic flood routing method, *Proc. Int. Symp. On Unsteady Flow in Open Channels*, Paper L1, Newcastle-Upon Tyne, U.K.

47. Koussis, A. D. (1978), Theoretical estimation of flood routing parameters, *J. Hydraul. Div., ASCE*, 104 (HY1), 109–115.
48. Koussis, A. D. (1980), Comparison of Muskingum method difference schemes, *J. Hydraul. Div., ASCE*, 106, (HY5), 925–929.
49. Koussis, A. D. (1983), Unified theory for flood and pollution routing, *J. Hydraul. Eng., ASCE*, 109(HY12), 1652–1664.
50. Koussis, A. D., and B. J. Osborne (1986), A Note on Nonlinear Storage Routing, *Water Resour. Res.*, 22(13), 2111–2113.
51. Kuchment, L. S. (1972), *Mathematical Modeling of Streamflow* (in Russian). Hydrometeorological Publishing House, Leningrad.
52. Kulandaiswamy, V. C. (1964), A basic study of the rainfall excess-surface runoff relationship in a basin system, Ph. D. Thesis, University of Illinois, Urbana, Illinois, USA.
53. Kulandaiswamy, V. C., and C. V. Subramanian (1967), A nonlinear approach to runoff studies, *Proc. Int. Hydrol. Symp.*, Fort Collins, USA, 1, 72–79.
54. Kundzewicz, Z. W. (1986), Physically based hydrological flood routing method, *Hydrol. Sci. J., IAHS*, 31(2), 237–261.
55. Lai, C. (1986), Numerical modeling of unsteady open channel flow, *Advances in Hydroscience*, 14, Academic Press, USA, 161–333.
56. Langbein, W. B. (1942), Storage in relation to flood waves, *Hydrology*, O. E. Meinzer (Ed.), Dover Publication, New York, USA.
57. Laurenson, E. M. (1962), Hydrograph synthesis by runoff routing, *Water Research Laboratory, University of New South Wales Report No. 66*.
58. Laurenson, E. M. (1964), A basin storage model for runoff routing, *J. Hydrol.*, 2, 141–163.

59. Lighthill, M. J., and G. B. Whitham (1955), On kinematic waves: 1. Flood movement in long rivers, *Proc. Roy. Soc. of London*, A229, 281–316.
60. Linsley, R. K., M. A. Kohler, and J. L. H. Paulhus (1949), *Applied Hydrology*, McGraw-Hill, New York, 689 p.
61. Liong, Y. S., W. H. Lim, and G. N. Paudyal (2000), River stage forecasting in Bangladesh: neural networks approach, *J. Computing in Civil. Eng., ASCE*, 14(1), 1–8.
62. McCarthy, G. T. (1938), The unit hydrograph and flood routing, *Conf. North Atlantic Division*, U.S. Army Corps of Engineers, New London, Conn.
63. Mein, R. G., E. M. Laurenson, and T. A. McMahon (1974), Simple nonlinear method for flood estimation, *J. Hydraul. Div., ASCE*, 100(HY11), 1507–1518.
64. Miller, W. A., and Cunge, J. A. (1975), Simplified equations of unsteady flow, in: *Unsteady Flow in Open Channels*, Vol. I, K. Mahmood and V. Yevjevich (Eds.), Water Resour. Publ., Highlands Ranch, Colo., 183–249.
65. Mohan, S. (1997), Parameter estimation of nonlinear Muskingum models using genetic algorithm, *J. Hydraul. Eng., ASCE*, 123(2), 137–142.
66. Moramarco T., and V. P. Singh (2001), Simple method for relating local stage and remote discharge, *J. Hydrol. Eng., ASCE*, 6(1), 78–81.
67. Moramarco, T., and V. P. Singh (2000), A practical method for analysis of river waves and for kinematic wave routing in natural channel networks, *Hydrol. Process.*, 14, 51–62.288
68. Muttiah, R. S., R. Srinivasan, and P. M. Allen (1997), Prediction of the two-year peak stream discharges using neural networks, *J. American Water Resour. Assoc.*, 33(3), 625–630.

69. Napiorkowski, J. J., and Z. W. Kundzewicz (1986), A discrete conceptualization of a Volterra series model for surface runoff, *Water Resour. Res.*, 22(10), 1413–1421.
70. Nash, J. E. (1959), Systematic determination of unit hydrograph parameters, *J. Geophys. Res.*, 64(1), 111–115.
71. Nash, J. E. (1960), A unit hydrograph study with particular reference to British catchments, *Proc. Inst. Civ. Eng.*, 17, 249–282.
72. Natural Environment Research Council (NERC) (1975), Flood Routing Studies, in *Flood Studies Report*, Vol. III, Institute of Hydrology, Wallingford, UK.
73. Neitsch, S. L., J.G. Arnold, J. R. Kiniry, R. Srinivasan, and J. R. Williams (2005), *Soil and Water Assessment Tool Theoretical Documentation* (version 2005), Temple, TX: Grassland, Soil and Water Research Laboratory, Agricultural Research Service, USA. <<http://www.brc.tamus.edu/swat/doc.html>>
74. Perumal, M. (1989), Unification of Muskingum difference schemes, *J. Hydraul. Eng., ASCE*, 115(4), 536–543.
75. Perumal, M. (1992a), Discussion on the kinematic wave controversy, *J. Hydraul. Eng., ASCE*, 118(9), 1335–1337.
76. Perumal, M. (1992c), The cause of negative initial outflow with the Muskingum method, *Hydrological Sci. J.*, 37(4), 391–401.
77. Perumal, M. (1993b), The cause of negative initial outflow with the Muskingum method—Closure, *Hydrol. Sci. J.*, 38, 153–154.
78. Perumal, M. (1994a), Hydrodynamic derivation of a variable parameter Muskingum method: 1. Theory and solution procedure, *Hydrological Sci. J.*, 39(5), 431–442.

79. Perumal, M. (1994b), Hydrodynamic derivation of a variable parameter Muskingum method: 2. Verification. *Hydrological Sci. J.*, 39(5), 443–458.
80. Perumal, M. (1995), Variable parameter flood routing using hydrodynamic principles, Ph. D. Thesis, Department of Civil Engineering, University of Roorkee, India, 226 p.
81. Perumal, M., and K. G. Ranga Raju (1999), Approximate convection diffusion equations, *J. Hydrol. Eng., ASCE*, 4(2), 161–164.
82. Perumal, M., P. E. O'Connell, and K. G. Ranga Raju (2001), Field applications of a variable-parameter Muskingum method, *J. Hydrol. Eng.*, 6(3), 196–207.
83. Pilgrim, D. H. (1986), Bridging the gap between flood research and design practice, *Water Resour. Res.*, 22(9), Supplement, 165S–176S.
84. Ponce, V. M. (1991), Kinematic wave controversy, *J. Hydraul. Eng., ASCE*, 117(4), 511–525.
85. Ponce, V. M. (1992), Kinematic wave modeling: where do we go from here?, *Proc. Int. Symposium on Hydrology of Mountainous Areas*, Shimla (India), May 28–30, 485–495.
86. Ponce, V. M., and D. B. Simons (1977) Shallow wave propagation in open channel flow, *J. Hydraul. Div., ASCE*, 103(HY12), 1461–1476.
87. Price, R. K. (1973), Flood routing methods for British rivers, *Proc. Inst. Civ. Engrs.*, 55(12), 913–930.
88. Ranga Raju, K. G., G. L. Asawa, P. D. Porey, M. Perumal, and U. C. Kothiyari (1993), Dam-break study for Jamrani dam, U. P., *Report of Hydraulic Engineering Section*, Department of Civil Engineering, University of Roorkee (currently Indian Institute of Technology Roorkee), Roorkee, India.

89. Rockwood, D. M. (1958), Columbia basin streamflow routing by computer, *J. Waterways and Harbors Division, ASCE*, Vol. 84, Part 1, Paper No. 1874(December),(Also published in *ASCE Transactions*, 1961, Paper No. 3119).
90. Sahoo, G. B., and C. Ray (2006), Flow forecasting for a Hawaii stream using rating curves and neural networks, *J. Hydrol.*, 317(1), 63–80.
91. Seddon, J. A. (1900), River hydraulics, *Trans. Am. Soc. Civ. Eng.*, 43, 179–229.
92. Singh, V. P. (1988), *Hydrologic Systems: Rainfall-Runoff Modeling*, Vol. I, Prentice Hall, Englewood Cliffs, New Jersey.
93. Singh, V. P. (1998), The use of entropy in hydrology and water resources, *Hydrol. Process.*, 11, 587–626.
94. Singh, V. P. (2002), Is hydrology kinematic?, *Hydrol. Process.*, 16, 667-716, doi: 10.1002/hyp.306., 667–716.
95. Singh, V. P., and D. A. Woolhiser (1976), Sensitivity of linear and nonlinear surface runoff models to input errors, *J. Hydrol.*, 29, 243–249.
96. Singh, V. P., and P. D. Scarlatos (1987), Analysis of the nonlinear Muskingum-flood routing, *J. Hydraul. Eng., ASCE*, 113(1), 61–79.
97. Singh, V. P., and V. Aravamuthan (1997), Accuracy of kinematic wave and diffusion wave approximations for time-independent flow with momentum exchange included, *Hydrol. Process.*, 11, 511–532.
98. Singh, V. P., G. T. Wang, and D. D. Adrian (1997), Flood routing based on diffusion wave equation, *Hydrol. Process.*, 14(11), 1881–1894.
99. Singh, V. P., G. T. Wang, and D. D. Adrian (2000), Flood routing based on diffusion wave equation using mixing cell method, in *High Resolution Flow Modeling in Hydrology and Geomorphology*, P. D. Bates and S. N. Lane (Eds.), John Wiley and Sons, New York, 167–180.

100. Sivapalan, M., B. C. Bates, and J. E. Larsen (1997), A generalized, non-linear, diffusion wave equation: theoretical development and application, *J. Hydrol.*, 192(1–4), 1–16.
101. Stoker, J. J. (1957), *Water waves*, Interscience, New York, USA.
102. Strupczewski, W. G., and Z. W. kundzewicz (1980), Muskingum method revisited, *J. Hydrol.*, 48, 327–342.
103. Szilagyi J. (2003), State-Space Discretization of the Kalinin-Miliyukov Nash Cascade in Sample-Data System Framework
104. Szilagyi, J. (2006), Discrete state-space approximation of the continuous Kaninin-Milyukov-Nash cascade of noninteger storage elements, *J. Hydrol.*, 328(1–2), 132–140.
105. Szollosi-Nagy, A. (1976), An Adaptive Identification and Prediction Algorithm for the Real-time Forecasting of Hydrological Time Series, *Hydrological Sciences-Bulletin-des Sciences Hydrologiques*, 21, 13/1976, P(163-176).
106. Szollosi-Nagy, A. (1982), The discretization of the continuous linear cascade by means of state space analysis, *J. Hydrol.*, 58(3–4), 223–236.
107. Tayfur, G., T. Moramarco, and V. P. Singh (2007), Predicting and forecasting flow discharge at sites receiving significant lateral inflow, *Hydrol. Process.*, 21(14), doi: 10.1002/hyp.6320, 1848–1859.
108. Thirumalaiah, K., and M. C. Deo (1998a), Real time flood forecasting using artificial neural networks, *J. Computer-aided Civil and Infrastructural Engineering*, Blackwell Publishers, Oxford, UK, 13, 101–111.

109. Thomas, I. E., and P. R. Wormleaton (1970), Flood routing using a convective diffusion model, *Civil Eng. and Public Works Review*, 65, 257–259.
110. Thomas, I. E., and P. R. Wormleaton (1971), Finite difference solution of the flood diffusion equation, *J. Hydrol.*, 12, 211–221.
111. Tung, Y. K. (1984), River flood routing by nonlinear Muskingum method, *J. Hydraul.Div., ASCE*, 111(12), 1447–1460.
112. U.S. Army Corps of Engineers (1960), Routing of floods through river channels, EM1110-2-1408.
113. U.S. Army Corps of Engineers (USACE) (2006a), HEC-RAS river analysis system user's manual (version 4.0 beta), Rep. CPD-68, Hydrol. Eng., Cent., Davis, Calif.
114. Weinmann, P. E., and E. M. Laurenson (1979), Approximate flood routing methods: a review, *J. Hydraul. Div., ASCE*, 105(12), 1521–1526.
115. Wong, T. H. F. (1984), Improved parameters and procedures for flood routing in rivers, Ph. D. Thesis, Monash University, Victoria, Australia.
116. Wong, T. H. F., and E. M. Laurenson (1983), Wave speed-discharge relation in natural channels, *Water Resour. Res.*, 19(3), 701–706.
117. Wong, T. H. F., and E. M. Laurenson (1984), A model of flood wave speed-discharge characteristics of rivers, *Water Resour. Res.*, 20(12), 1883–1890.
118. Woolhiser, D. A., and J. A. Liggett (1967), Unsteady one-dimensional flow over a plane: the rising hydrograph, *Water Resour. Res.*, 3(3), 753–771.
119. Xiong, L., Y. Asaad, Y. Shamseldin, and K. M. O'Connor (2001), A nonlinear combination of the forecast of rainfall-runoff models by first order Takagi-Sugeno fuzzy system, *J. Hydrol.*, 254(1–4), 196–217.

120. Yeou-Koung Tung, (1985), River Flood Routing by Nonlinear Muskingum Method, *J. Hydraulic Eng.*, 111, (1447-1460)
121. Yoon, J., and G. Padmanabhan (1993), Parameter estimation of linear and nonlinear Muskingum models, *J. Water Resour. Plann. Manag. Div., ASCE*, 119(5), 600-610.
122. Yu, P. S., and S. T. Chen (2005), Updating real-time flood forecasting using a fuzzy rule-based model, *Hydrol. Sci. J., IAHS*, 50(2), 265-278.
123. Yu, P. S., and T. C. Yang (2000) Fuzzy multi-objective function for rainfall-runoff model calibration, *J. Hydrol.*, 238(1-2), 1-14.
124. Zoch, R. T. (1934), On the relation between rainfall and stream flow, *Mon. Weather Rev.*, 62, 315-322.
125. Zoppou, C., and I. C. O'Neill (1982), Criteria for the choice of flood routing methods in natural channels, in *Proc. Hydrology and Water Resources Symposium*, Melbourne, Inst. of Eng., Barton, A.C.T., 75-81.

APPENDIX- 1

FORTRAN PROGRAM USED FOR VPMD METHOD

```
C*****
C PROGRAM VPMQ - VARIABLE PARAMETER MUSKINGUM DISCHARGE ROUTING
METHOD * *
C PROGRAM FOR DISCHARGE HYDROGRAPH ROUTING IN RECTANGULAR CHANNELS.
*
C NO BACKWATER EFFECT CONSIDERED. *
C COMPUTES ALSO THE UPSTREAM AND DOWNSTREAM STAGE HYDROGRAPHS *
C CORRESPONDING TO THE GIVEN INFLOW AND COMPUTED OUTFLOW *
C HYDROGRAPHS: *
C COMPUTES ALSO THE WATER SURFACE SLOPE AT THE INLET OF THE REACH. *
C TO CHECK THE SUITABILITY OF THE METHOD FOR THE GIVEN PROBLEM, *
C COMPUTED HYDROGRAPH IS COMPARED WITH THE ST.VENANT'S SOLUTION BASED
ON *. *
C THE NASH-SUTCLIFFE CRITERION AND ERROR IN VOLUME CRITERION. *
C *
C DESCRIPTION OF VARIABLES USED IN THE PROGRAM. *
C *
C AI - INFLOW HYDROGRAPH ORDINATE AT THE INLET OF EACH SUB-REACH.* *
C QOBS - OBSERVED OUTFLOW HYDROGRAPH ORDINATE. *
C QCOM - COMPUTED OUTFLOW HYDROGRAPH ORDINATE. *
C YM - COMPUTED STAGE AT THE MIDDLE OF THE SUB-REACH. *
C YOBS - OBSERVED STAGE AT THE OUTLET OF THE REACH. *
C YCOM - COMPUTED STAGE AT THE OUTLET OF THE REACH. *
C AIN1 - ORDINATE OF THE GIVEN INFLOW HYDROGRAPH. *
C Y1 - COMPUTED STAGE CORRESPONDING TO AI. *
C YCOM1 - INTERPOLATED STAGE AT ANY LOCATION WITHIN A SUB-REACH * *
C - USING Y1 AND YCOM. *
C QCOM1 - INTERPOLATED DISCHARGE AT ANY LOCATION WITHIN A SUB-REACH *
C - USING AI AND QCOM. *
C SIN - STAGE CORRESPONDING TO GIVEN INFLOW AIN1. *
C DYDXUP - NON-DIMENSIONALISED WATER SURFACE SLOPE COMPUTED AT THE *
C - INLET OF THE REACH. *
C DYDX1 - NON-DIMENSIONALISED WATER SURFACE SLOPE GIVEN AT THE *
C - INLET OF THE REACH (COMPUTED USING ST.VENANT'S EQNS.). *
C*****
C
DIMENSION AI(800),QOBS(800),QCOM(800),FUNC(100),YM(100),YOBS(800)
DIMENSION YCOM(800),YOUT(100),RJ(100),FSQ1(100),SF(100),FUNC2(100)
DIMENSION AIN1(800),Y1(800),YCOM1(800),QCOM1(800),SIN(800)
DIMENSION DYDXUP(800),DYDX1(800),aift(800)
C
C FILE 'dybydx.dat' IS AN OUTPUT FILE AND IT DISPLAYS GIVEN INFLOW, ,CORRES-
C PONDING COMPUTED AND ST.VENANT'S SOLUTION NON-DIMENSIONALISED WATER
C SURFACE SLOPES.
C
C OPEN(UNIT=1,FILE='dybydx.dat')
C
C FILE 'muskn.dat' IS AN INPUT FILE AND IT STORES GIVEN INFLOW AND OUTFLOW,
```

```

C CORRESPONDING STAGE HYDROGRAPHS,INITIAL INFLOW AND OUTFLOW,AND THE
C CORRE
C SPONDING STAGE VALUES . BESIDES IT ALSO STORES THE VALUES OF N,DT,YIN,
C B,G,SO,AN,TTL,NREACH,JUMP AND REQLEN,THE DESCRIPTION OF WHICH ARE MADE
C WITHIN NEXT FEW LINES.
      OPEN(UNIT=2,FILE='muskn.dat')
C
C FILE 'muskn.out' IS AN OUTPUT FILE AND IT DISPLAYS GIVEN INPUT VALUES
C OF N,DT,YIN,B,G,SO,AN,TTL,NREACH,JUMP,REQLEN. BESIDES IT ALSO DISPLAYS
C GIVEN INFLOW AND OUTFLOW,AND THE CORRESPONDING COMPUTED INFLOW AND
C OUTFLOW AND THE COMPUTED AND OBSERVED OUTFLOW STAGE HYDROGRAPHS. SUM
C OF
C INFLOW ,SUM OF OUTFLOW AND SUM OF COMPUTED OUTFLOW ALONG WITH
C MEASURES
C FOR VARIANCE EXPLAINED AND ERROR IN VOLUME ARE DISPLAYED.
C
      OPEN(UNIT=4,FILE='muskn.out')
C FILE 'akth.out' IS AN OUTPUT FILE WHICH DISPLAYS THE LAST SUBREACH
C INFLOW AND THE CORRESPONDING COMPUTED MUSKINGUM WEIGHTING
C PARAMETER.
C
      OPEN(UNIT=8,FILE='akth.out')
C
C FILE 'dydx.dat' IS AN INPUT FILE WHICH STORES NON-DIMENSIONALISED
C WATER SURFACE SLOPE COMPUTED USING ST.VENANT'S SOLUTION AT THE
C INLET OF THE REACH.
      OPEN(UNIT=7,FILE='dydx.dat')
C
C DESCRIPTION OF INPUT DATA
C N - TOTAL NUMBER OF INFLOW AND OUTFLOW VARIABLE.
C DT - ROUTING TIME INTERVAL.
C YIN - INITIAL STAGE.
C B - WIDTH OF THE CHANNEL.
C G - ACCELERATION DUE TO GRAVITY (9.81 M/SEC)
C SO - BED SLOPE.
C AN - MANNING'S ROUGHNESS COEFFICIENT.
C TTL - TOTAL LENGTH OF THE REACH.
C NREACH - NUMBER OF SUB-REACHES USED IN THE GIVEN ROUTING REACH.
C JUMP - NUMBER OF ROUTING INTERVALS TO BE SKIPPED FOR MAKING
C THE ROUTING INTERVAL MORE THAN 15 MINUTES. MINIMUM
C VALUE OF 'JUMP ' IS 15 MIN.
C REQLEN - DESIRED LENGTH OF REACH AT WHICH ROUTING RESULTS ARE
C TO BE OBTAINED.
      READ(2,*) N,DT,YIN,B,G,SO,AN,TTL,NREACH,JUMP,REQLEN
      WRITE(4,99) N,DT,YIN,B,G,SO,AN,TTL,NREACH,JUMP
99 FORMAT(20X,'NO.OF ORDINATES=',I6/20X,'ROUTING TIME INTERVAL(IN SECS.)
1=!,F8.2/20X,'INITIAL DEPTH(IN MTS)=',F8.2/20X,'CHANNEL WIDTH (IN MTS
2.=!,F8.2/20X,'ACCN.DUE TO GRAVITY(IN MTS./SEC/SEC)=',F5.2/20X,
3'BED SLOPE (IN MTS./MTS.)=',F6.4/20X,'MANNINGS ROUGHNESS COEFF.=',
4F5.3/20X,'TOTAL LENGTH OF THE REACH(IN MTS.)=',F10.0/20X,'NUMBER OF
5'SUB-REACHES=',I5/20X,'JUMP=',I4)
      WRITE(4,98)REQLEN
98 FORMAT(20X,'REQUIRED ROUTING REACH LENGTH=',F12.0)
      READ(2,*) AI(1),YOBS(1),QOBS(1),SIN(1)

```

I=2

C

```
1000 READ(2,*) AI(I),QOBS(I),YOBS(I),SIN(I)
      write(6,*)I,AI(I),QOBS(I),YOBS(I),SIN(I)
      I=I+1
      IF(I.LE.(N+1)) GO TO 1000
      WRITE(*,*)"CHAL GAYA"
```

C

```
c      READ(7,890)(DYDX1(I),I=2,(N+1))
```

```
890 FORMAT(10F8.5)
```

```
C   OPERATION FOR SKIPPING THE READING OF INPUT DATA AS PER THE VALUE OF JUMP
      N=N+1
```

```
N=(N-1)/JUMP+1
```

```
DO 2 J=2,N
```

```
    AI(J)=AI((J-1)*JUMP+1)
```

```
    aift(j)=ai(j)*35.31
```

```
    QOBS(J)=QOBS((J-1)*JUMP+1)
```

```
2   YOBS(J)=YOBS((J-1)*JUMP+1)
```

```
      write(2,188) (aift(j),j=1,n)
```

```
188 format(8f10.0)
```

```
C   STORING OF ORIGINAL AI VALUES IN AIN1 ARRAY.
```

```
DO 6 I=1,N
```

```
6   AIN1(I)=AI(I)
```

```
C   DX - LENGTH OF EQUAL SUB-REACH.
```

```
DX=TTL/NREACH
```

```
DX1=0.
```

```
C   DX1 - LENGTH OF CUMULATIVE ROUTED REACH
```

```
7   DX1=DX1+DX
```

```
      WRITE(4,95) DX
```

```
C   WRITE(4,199).
```

```
199 FORMAT(3X,'J',9X,'Q3',9X,'YRID',10X,'QMRD',11X,'DYDX')
```

```
95 FORMAT(25X,'REACH LENGTH=',F12.0)
```

```
QIN=AI(1)
```

```
C   AK - TRAVEL TIME ( DX/CEL )
```

```
AK=DX/((5./3.-4./3.*(YIN/(B+YIN)))*QIN/(B*YIN))
```

```
C   FSQ - SQUARE OF FROUDE NUMBER.
```

```
C   R - HYDRAULIC RADIUS.
```

```
C   THETA - WEIGHTING PARAMETER.
```

```
C   THETAN - NUMERATOR OF THE WEIGHTING PARAMETER.
```

```
C   THETAD - DENOMINATOR OF THE WEIGHTING PARAMETER.
```

```
FSQ=QIN*QIN*B/(G*(B*YIN)**3)
```

```
R=YIN/(B+2.*YIN)
```

```
THETAN=YIN*(1.+4./9.*FSQ*(-1.+4.*R-4.*R*R))
```

```
THETAD=2.*SO*(5./3.-4./3.*R)*DX
```

```
THETA=0.5-THETAN/THETAD
```

```
CONST=(1./AN)*B**((5./3.)*SQRT(SO))
```

```
QCOM(1)=QIN
```

```
QCOM1(1)=QIN
```

```
YCOM1(1)=YIN
```

```
Y1(1)=YIN
```

```
YCOM(1)=YIN
```

```
J=1
```

```

YMIN=YIN
C COUNTER M IS USED FOR UPDATING THE PARAMETERS AT ANY TIME.
5 M=0
J=J+1
9 CDIN=AK*(1.-THETA)+DT/2.
C C1,C2 AND C3 ARE THE COEFFICIENTS OF THE MUSKINGUM ROUTING EQUATION.
C C1=(-AK*THETA+DT/2.)/CDIN
C C2=(AK*THETA+DT/2.)/CDIN
C C3=(AK*(1.-THETA)-DT/2.)/CDIN
M=M+1
C COMPUTATION OF OUTFLOW.
QCOM(J)=C1*AI(J)+C2*AI(J-1)+C3*QCOM(J-1)
C COMPUTATION OF WEIGHTED OUTFLOW.
Q3=QCOM(J)+THETA*(AI(J)-QCOM(J))
I=1
YM(I)=YMIN
C FINDING THE STAGE AT THE MIDDLE OF THE REACH.
FUNC(I)=Q3-CONST*YM(I)**(5./3.)/(B+2.*YM(I))**(2./3.)
I=2
YM(I)=YMIN+0.2*YMIN
10 FUNC(I)=Q3-CONST*YM(I)**(5./3.)/(B+2.*YM(I))**(2./3.)
DYM=-FUNC(I)*(YM(I)-YM(I-1))/(FUNC(I)-FUNC(I-1))
YM(I+1)=YM(I)+DYM
IF(ABS((YM(I+1)-YM(I))/YM(I+1)).LT.0.01) GO TO 30
I=I+1
GO TO 10
30 YMID=YM(I+1)
C COMPUTATION OF DISCHARGE AT THE MIDDLE OF THE REACH.
QMID=(AI(J)+QCOM(J))/2.
C COMPUTATION OF THE SQUARE OF FROUDE NUMBER.
FSQ=(QMID*QMID*B)/(G*(B*YMIN)**3)
C COMPUTATION OF THE STAGE AT THE OUTFLOW SECTION.
YCOM(J)=YMIN+(QCOM(J)-QMID)
1((5./3.-4./3.*YMIN/(B+2.*YMIN))*QMID/YMIN)
C COMPUTATION OF STAGE AT THE WEIGHTED OUTFLOW SECTION.
Y3=YMIN+(Q3-QMID)
1((5./3.-4./3.*YMIN/(B+2.*YMIN))*QMID/YMIN)
C COMPUTATION OF VELOCITY AT THE WEIGHTED OUTFLOW SECTION.
V3=Q3/(B*Y3)
C COMPUTATION OF WAVE CELERITY OF THE REACH.
CEL=(5./3.-(4./3.)*Y3/(B+2.*Y3))*V3
C COMPUTATION OF PARAMETERS AK AND THETA.
AK=DX/CEL
R=YMIN/(B+2.*YMIN)
THETAN=Y3*(1.+4./9.*FSQ*(-1.+4.*R-4.*R*R))
THETAD=SO*(5./3.-4./3.*R)*DX
GM=(QCOM(J)-AI(J))*THETAN/(THETAD*Q3)
GM=0.
THETA=0.5-(THETAN/THETAD)*(0.5+0.125*GM+(1./16.)*GM*GM
1 +(5./128.)*GM**3+(7./256.)*GM**4)
C COMPUTATION OF STAGE AT THE INLET OF THE REACH.
IF(DX1.EQ.DX) Y1(J)=2.*YMIN-YCOM(J)
IF(DX1.EQ.DX) Y1(J)=YMIN+(AI(J)-QMID)/
1((5./3.-4./3.*YMIN/(B+2.*YMIN))*QMID/YMIN)
IF(M.LE.1)GO TO 9
C COMPUTATION OF NON-DIMENSIONALISED WATER SURFACE SLOPE

```

```

C. AT THE INLET OF THE REACH.
    VELUP=AI(J)/(B*Y1(J))
    CELUP=(5./3.-4./3.)*Y1(J)/(B+Y1(J))*VELUP
    DYDXUP(J)=-(AI(J)-AI(J-1))/(SO*DT*B*CELUP**2)
C. CONVERTING AK INTO HOURS.
    IF(DX1.EQ.TTL)AK1=AK/3600.
C. WRITING INFLOW OF THE LAST REACH AND THE CORRESPONDING AK OR
C. THETA.
    IF(DX1.EQ.TTL)WRITE(8,*) J, AI(J), THETA
C. COMPUTATION OF STAGE AND DISCHARGE AT ANY LOCATION OF THE LAST
C. SUB-REACH.
    DYDX=(Y.COM(J)-Y1(J))/DX
    YCOM1(J)=Y1(J)+REQLEN*DYDX
    QCOM1(J)=AI(J)-REQLEN*(AI(J)-QCOM(J))/DX
    DYDX=DYDX/SO
    WRITE(4,198)J,Q3,YMID,QMID,DYDX
198 FORMAT(1X,I3,2X,F10.0,2X,F10.5,2X,F10.0,8X,F10.8)
    IF(J.LT.N)GO TO 5
C. WRITING INFLOW AND THE CORRESPONDING NON-DIMENSIONALISED
C. WATER SURFACE SLOPE OF THE ST.VENANT'S SOLUTION AND THE
C. PRESENT SOLUTION.
    IF(DX1.eq.DX)WRITE(1,222)(J,AIN1(J),DYDXUP(J),DYDX1(J),J=2,N)
222 FORMAT(5X,I3,F8.0,2X,F10.6,5X,F10.6)
C. OUTFLOW AND STAGE FROM THE SUB-REACH BECOMES INFLOW TO THE
C. NEXT SUB-REACH.
    DO 28 I=1,N
    y1(i)=ycom(i)
28  AI(I)=QCOM(I)
    REQLEN=REQLEN-DX
C. CHECKING FOR THE COMPLETION OF THE ROUTING FOR THE LAST SUB-REACH.
    IF(DX1.LT.TTL) GO TO 7
    DO 51 J=1,N
    YCOM(J)=YCOM1(J)
51  QCOM(J)=QCOM1(J)
C. WRITING THE INFLOW, AND OBSERVED AND COMPUTED OUTFLOW AND STAGE.
    WRITE(4,101)((J-1),AIN1(J),QCOM(J),QOBS(J),YCOM(J),YOBS(J),J=1,N)
101 FORMAT(I4,3F10.4,F8.3,5X,F8.3)
C. COMPUTATION OF SUM OF INFLOW,OBSERVED OUTFLOW,COMPUTED OUTFLOW,
C. NASH-SUTCLIFFE CRITERION AND ERROR IN VOLUME.
    SUMAI1=0.
    SUMQC=0.
    SUMQO=0.
    DO 22 J=1,N
    SUMAI1=SUMAI1+AIN1(J)
    SUMQC=SUMQC+QCOM(J)
22  SUMQO=SUMQO+QOBS(J)
    AVEAI=SUMAI1/N
    AVEQC=SUMQC/N
    AVEQO=SUMQO/N
    DO 32 J=1,N
    TOTVAR=TOTVAR+(QOBS(J)-AVEQO)*(QOBS(J)-AVEQO)
32  RESVAR=RESVAR+(QOBS(J)-QCOM(J))*(QOBS(J)-QCOM(J))
    VAREXP=(TOTVAR-RESVAR)/TOTVAR*100.
    EVOL=(SUMQC-SUMAI1)/SUMAI1*100.
    WRITE(4,102) SUMAI1,SUMQC,SUMQO
    WRITE(4,104)VAREXP,EVOL

```

```
104 FORMAT(20X,'VAREXP=',F8.2,5X,'EVOL=',F8.2)
102 FORMAT(20X,'SUMAI=',F10.0,4X,'SUMQC=',F10.0,4X,'SUMQO=',F10.0)
STOP
END
```

APPENDIX- 2

MATLAB PROGRAM DEVELOPED FOR MOMENT-MATCHING METHOD

```
clc
close all
clear all

no=240;
dt=1;
qi=100;
sum1=0;
sum2=0;

t=[1:1:289];
a=load ('in_veri.m');
q=load ('out_veri.m');
% in_veri is input hydrograph file
% out_veri is output hydrograph file
% no is the number of ordinates
% qi is the initial flow
% latflow is the lateral flow
% exvol is the excess volume
% a(i) is the ith input ordinate.
% q(i) is the ith output ordinate

i=1;
while(i<=no)
    sum1=sum1+a(i);
    sum2=sum2+q(i);
    latflow(i)=0;
    i=i+1;
end
exvol=((sum2-sum1)/sum1)*100;
disp(sum1');
disp(sum2');
disp(exvol');
i=1;
while(i<=no)
    a(i)=a(i)-qi;
    q(i)=q(i)-qi;
    i=i+1;
end
sum1=0;
sum2=0;
aim1=0;
aim2=0;
qm1=0;
qm2=0;
i=2;
% aim1 first moment of the input hydrograph
% aim2 is the second moment of the input hydrograph
```

```

% qm1 is the first moment of the output hydrograph
% qm2 is the second moment of the hydrograph
% n is number of reservoirs
% ak is the storage coefficient
% dt is the time interval

while(i<=no)
    sum1=sum1+((a(i)+a(i-1))/2)*dt;
    sum2=sum2+((q(i)+q(i-1))/2)*dt;
    aim1=aim1+((a(i)+a(i-1))/2)*dt*(i-0.5)*dt;
    aim2=aim2+((a(i)+a(i-1))/2)*dt*((i-0.5)*dt)^2;
    qm1=qm1+((q(i)+q(i-1))/2)*dt*(i-0.5)*dt;
    qm2=qm2+((q(i)+q(i-1))/2)*dt*((i-0.5)*dt)^2;
    i=i+1;
end
aim1=aim1/sum1
aim2=aim2/sum1
qm1=qm1/sum2
qm2=qm2/sum2
i=1;
while(i<=no)
    a(i)=a(i)+qi;
    q(i)=q(i)+qi;
    i=i+1;
end
taunk=qm1-aim1;
ank2=qm2-aim2-qm1*qm1+aim1*aim1;
ak=ank2/taunk
n=taunk/ak

```

APPENDIX-3

MATLAB PROGRAM DEVELOPED FOR K-M METHOD

```
clc
close all
clear all
% this example is for three reservoirs.
% k is 0.316 and kx is 0.604
% initialveri is the input file of input hydrograph deducted base flow
from each ordinate.
% A system storage matrix
% y(i) is the output ordinates.
%no is number of ordinates.
A=[-0.316 0 0;0.316 -0.316 0;0 0.316 -0.604];
C=[0 0.0.604];
G=[1 0 0]';
x=zeros(3,1);
I=eye(size(A));
% TAYLOR SERIES TO FIND EXP(A)
E=zeros(size(A));
F=eye(size(A));
K=1;
while norm(E+F-E,1)>0
    E=E+F;
    F=A*F/K;
    K=K+1;
end
E2=E
% E2 is state transition matrix
% gama function calculation
gama=(E2-I)*inv(A)*G;

no=289;
u=load('initialveri.m');
x=[0;0;0];
i=1;
while(i<=no)
    x1=E2*x+gama*u(i);
    y(i)=x1(3,1)*0.604;
    y(i)=y(i)+100;
    x=x1;
    i=i+1;
end
disp(y')
```

APPENDIX- 4

MATLAB PROGRAM DEVELOPED FOR NASH-SUTCLIFFE CRITERIA

```
close all
clear all
ai=load('inputstate.m');
qc=load('outputstate.m');
qo=load('outputhec.m');
no=241;
j=1;
sumai=0;
sumqo=0;
sumqc=0;
% inputstate is the input file
% outputstate is the routed hydrograph file
% outputhec is the routed benchmark hydrograph
% sumai is the total of input ordinates
% sumqc is the sum of calculated output ordinates.
Sumqo is the sum of observed output ordinates.
while(j<=no)
    sumai=sumai+ai(j);
    sumqc=sumqc+qc(j);
    sumqo=sumqo+qo(j);
    j=j+1;
end
aveai=sumai/no;
veqc=sumqc/no;
aveqo=sumqo/no;
k=1;
totvar=0;
resvar=0;
while(k<=no)
    totvar=totvar+(qo(k)-aveqo)^2;
    resvar=resvar+(qo(k)-qc(k))^2;
    k=k+1;
end
% varexp is variance explained
% evol is the error in volume.
varexp=((totvar-resvar)/totvar)*100
evol=((sumqc-sumai)/sumai)*100
```